


# The medium to long term effects of SARS-CoV-2 infection on multiple organs, exercise capacity, cognition, quality of life and mental health.

---

Thesis submitted for the Degree of Doctor of Philosophy

Hilary Term 2024

---

Dr Mark Philip Cassar. MD (Melit.), MRCP (Lon.), PgCert (Dundee)

St Anne's College

Division of Cardiovascular Medicine, Radcliffe Department of Medicine, University of Oxford.

## Contents

Acknowledgements ..... 1
Declaration ..... 3
Abbreviations ..... 4
Thesis Abstract ..... 6
Chapter 1: General Introduction ..... 9
- Background ..... 9
- Acute COVID-19 ..... 11
  - Transmission ..... 13
  - Clinical Characteristics and Prognosis ..... 14
- Mechanisms of organ injury after SARS-CoV-2 infection ..... 16
  - Reduced ACE2 receptor activity and direct toxicity ..... 16
  - Endothelial cell dysfunction ..... 16
  - Immune dysregulation ..... 17
  - Multiorgan injury ..... 17
- Histopathological features of organ injury ..... 19
- Lessons from previous pandemics ..... 23
- Evidence gap ..... 26

Chapter 2: Methods ..... 27
- Study design ..... 27
- Recruitment ..... 29
- Data collection ..... 29
- Study visit overview ..... 29
- Admission details ..... 29
- Vital signs ..... 29
- Laboratory analysis ..... 30
- Electrocardiogram ..... 30
- MRI protocol ..... 30
  - Brain MRI ..... 30
  - Lung MRI ..... 31
  - Cardiac MRI ..... 33
  - Abdominal MRI ..... 34
- Lung function assessment ..... 35
- Cardiopulmonary exercise testing ..... 35
- Questionnaires ..... 35
- Statistical methods ..... 35

Chapter 3: Long-term impact of COVID-19 on Cardiopulmonary Health and Exercise Capacity ..... 37
- Abstract ..... 37
- Introduction ..... 39
- Methods ..... 40
  - MRI Protocol ..... 40
  - MRI image analysis ..... 40
  - Spirometry, Gas Transfer and Total Lung Capacity assessment ..... 41

Lung function analysis....43
Cardiopulmonary Exercise Testing....45
Data acquired....46
Statistical Analyses and Definitions....47
Results....49
Study Population and demographics....49
Blood markers of cardiac health....52
Electrocardiography....52
Serial Cardiac Imaging....53
Respiratory Imaging....59
Respiratory Function Assessment....62
Cardiopulmonary Exercise Testing....67
Discussion....72
Clinical Implications....78
Study limitations....78
Conclusions....79

Chapter 4 – Long-term impact of COVID-19 on hepatic and renal health post COVID-19 hospitalization....80
Abstract....80
Introduction....82
Methods....83
MRI Protocol....83
Data acquired....84
Statistical Analyses and Definitions....84
Results....87
Renal and hepatic dysfunction during admission....87
Hepatic health....89
Renal Health....94
Discussion....104
Clinical Implications....109
Study limitations....109
Conclusion....110

Chapter 5 –Impact of COVID-19 on cerebral function, cognition, mental health and quality of life....111
Abstract....111
Introduction....113
Methods....114
Brain MRI protocol....114
Brain MRI image analysis....114
Questionnaires....116
Data acquired....117
Statistical Analyses and Definitions....118
Results....120
Cerebral injury during admission....120
Findings from brain imaging....120
Cognitive assessment....122
Mental health....126
Quality of life....131
Symptoms....133

Discussion ..... 140
Clinical Implications ..... 143
Study limitations ..... 144
Conclusion ..... 144

Chapter 6: General Conclusions ..... 145

References ..... 148

Scientific Papers ..... 161

Conference Abstracts ..... 163

## Acknowledgements

To my supervisor Professor Betty Raman: Thank you for always believing in me and redefining the limits of what I can achieve. You have taught me that, with hard work and resolve, I can achieve anything I put my mind to. Undertaking a DPhil during an unprecedented lockdown was a daunting, lonely, and at times, overwhelming experience. For the numerous phone calls you answered, the multitude of e-mails you responded to, and the knowledge you shared with me, I thank you.

To my supervisor Professor Neubauer: Thank you for your direction throughout my time as a student within the department. Your kindness, insightful comments and continuous belief in my project and abilities have been essential to my success.

To my supervisor Dr Nicholas Talbot: Thank you for being patient with me throughout our numerous conversations on respiratory and exercise physiology, and for taking the time to catch up with me within and outside working hours. Your ability to translate research into clinical relevance is inspiring.

I would like to thank Professor Oliver Rider, who encouraged me to join the Radcliffe Department of Medicine for a DPhil. Without you, this may not have been possible.

To Dr Elizabeth Tunnicliffe, Dr Ferenc Mozes, Dr Cheng Xie and Dr Godwin Ogbole: Thank you for your significant contributions to this work.

To Dr Zakariye Ashkir, Dr Azlan Abd Samat and Dr Lucy Finnigan: We formed a fantastic team and worked together to achieve incredible things. Above all, we will always be friends. Thank you for your company and friendship.

Thank you to all the radiographers at OCMR, in particular, Ms Rebecca Mills and Ms Joana Pelado – without your stellar training and supervision, this work would not have been possible.

Thank you to my parents, Mario and Rita, and my sister Stephanie: you have always believed in my abilities and were incredible sources of comfort during times of stress.

Thank you to my wife, Marta, who has been an incredible partner throughout my time as a student. For all the early mornings and late evenings, for all the delayed vacations, for all the care and love you showed me, and last but not least, for your unwavering belief that I could do this – thank you.

I am extremely grateful to the National Institute for Health Research, Oxford Biomedical Research Centre for funding the work outlined in this thesis.

Last but not least, I thank every participant who decided to take part in this project. Your stories and experiences of COVID-19 will stay with me forever.

## Declaration

I declare that the work presented in this thesis is my own. For the blinded analysis of data, Professor Betty Raman helped with processing of late gadolinium enhancement quantification, Dr Cheng Xie provided qualitative readouts of lung imaging, and Dr Godwin Ogbole provided qualitative readouts of brain acquisitions. Dr David Holdsworth acted as an expert second observer for challenging CPET cases. Dr Elizabeth Tunnicliffe provided expert guidance on the interpretation of renal T1 maps. Dr Ferenc Mozes performed the final step in the processing of hepatic MRI values. I recruited all the participants to this study and imaged the majority of participants in this work with the invaluable assistance of the Clinical Magnetic Resonance Research (OCMR) research nurses (who assisted by delivering some questionnaires, performing blood tests and acquiring ECGs), OCMR radiographers and Professor Raman. I interpreted the data and carried out statistical analysis under the supervision of Professor Raman. This work was funded by the National Institute for Health and Research, Oxford Biomedical Research Centre.

## Abbreviations

| Abbreviation | Full Text |
|---|---|
| ALT | Alanine aminotransferase |
| ASL | Arterial spin labelling |
| AST | Aspartate aminotransferase |
| AT | Anaerobic threshold |
| BAME | Black/Asian and minority ethnic groups |
| CMR | Cardiac magnetic resonance imaging |
| COPD | Chronic obstructive pulmonary disease |
| COVID-19 | Coronavirus disease |
| CPET | Cardiopulmonary exercise test |
| CRP | C-reactive protein |
| CT | Computed tomography |
| DLco | Diffusion capacity for carbon monoxide |
| DWI | Diffusion-weighted imaging |
| ECG | Electrocardiogram |
| ECMO | Extracorporeal membrane oxygenation |
| ECV | Extracellular volume |
| EDTA | Ethylenediaminetetraacetic acid |
| EDV | End-diastolic volume |
| EF | Ejection fraction |
| ESV | End systolic volume |
| $FEV_1$ | Forced expiratory volume in 1 second |
| FLAIR | Fluid attenuated inversion recovery |
| FSS | Fatigue severity scale |
| FVC | Forced vital capacity |
| GGT | Gamma-glutamyltransferase |
| HASTE | Half-fourier-acquisition single-shot turbo spin-echo |
| HFOT | High flow oxygen therapy |
| HLA | Horizontal long axis |
| IDEAL | Iterative decomposition of water and fat with echo asymmetry and least-squares estimation |
| IQR | Interquartile range |
| LGE | Late gadolinium enhancement |
| LV | Left ventricle |

| | |
|---|---|
| LVEF | Left ventricular ejection fraction |
| LVOT | Left ventricular outflow tract |
| MRC | Medical research council |
| MRI | Magnetic resonance imaging |
| NIV | Non-invasive ventilation |
| NT-proBNP | N-terminal pro-brain natriuretic peptide |
| $O_2$ | Oxygen |
| PDFF | Proton density fat fraction |
| PHQ-15 | Patient health questionnaire-15 |
| PSIR | Phase-sensitive inversion recovery |
| RAAS | Renin-angiotensin-aldosterone system |
| RRT | Renal replacement therapy |
| RV | Right ventricle |
| RVEF | Right ventricular ejection fraction |
| SARS-CoV-2 | Severe acute respiratory syndrome coronavirus-2 |
| ShMOLLI | Shortened modified look locker |
| SSFP | Steady-state free precession |
| SWI | Susceptibility-weighted imaging |
| ULN | Upper limit of normal |
| TR | Repetition time |
| TE | Echo time |
| TI | Inversion time |
| Va | Alveolar volume |
| $\dot{V}E/\dot{V}CO_2$ | Ventilatory equivalent for carbon dioxide |
| VLA | Vertical long axis |
| $\dot{V}O_2$ | Oxygen consumption |

## Thesis Abstract

Since the initial outbreak of COVID-19, over 775 million infections have been documented and over 7 million deaths confirmed. Initially thought to exclusively target the respiratory system, physician accounts of the disease trajectory revealed that extra-pulmonary manifestations were common, with reports of neurological, cardiac, renal, hepatic and muscle involvement. At the start of this project, very little was known about the long-term impact of COVID-19 on multiorgan health, exercise capacity, cognition, mental health and quality of life.

Method: In this thesis, the impact of moderate to severe COVID-19 on multi-organ health was examined using blood and urine tests, ECG, state of the art MRI imaging of the heart, lungs, liver, kidneys and brain, spirometry, gas transfer and total lung capacity assessment, cardiopulmonary exercise testing and a series of questionnaires. Fifty-eight patients with moderate to severe COVID-19, 2-3 months post infection, and 30 age, sex and comorbidity-matched COVID-19 naïve controls were recruited. Patients were invited for repeat assessment 6 and 18 months post infection.

Result: Elevated native myocardial T1 (a marker of fibrosis, inflammation and/or oedema) was seen in post-COVID-19 participants 2-3 months post-infection which resolved with time. Of note, none had evidence of acute myocarditis according to the Modified Lake Louise Criteria. Biventricular size and function were comparable to controls throughout assessment. Lung MR imaging revealed a high burden of lung abnormalities in post-COVID-19 participants, which improved but did not completely resolve with time. Lung function impairment using spirometry was mild and transient, but abnormal gas transfer findings were seen in 1/4$^{th}$ of participants 18 months post-infection. A high prevalence of exercise impairment was seen shortly after infection (54% having a reduction in their peak oxygen capacity). This improved by 6 months but remained significantly reduced compared with controls. Despite the persistent abnormalities on MR lung imaging and

gas transfer, cardiorespiratory limitations did not account for reduced exercise capacity, but rather were secondary to intrusive symptoms and reduced tissue oxygen extraction.

Separate to cardiorespiratory health, longitudinal assessments of renal and hepatic health were performed. Serial blood testing revealed near-total resolution of COVID-19 associated acute hepatic dysfunction. Transient elevations in iron corrected T1 on MR hepatic imaging was observed in COVID-19 participants during the initial study visit, which resolved by 6 months post-infection. In contrast, serial renal function assessment revealed that participants with COVID-19 associated acute kidney injury continued to have reduced renal function compared to those with stable renal function during infection. Furthermore, a downward trajectory in renal function was observed between the initial and final study visit, which was not predicted using a validated CKD risk prediction score. MR renal imaging revealed elevated renal cortical T1 (a marker of inflammation, fibrosis and/or oedema) in participants 2-3 months post-infection; although this resolved with time, it was not accompanied by an improvement in renal function.

Longitudinal MR imaging of the brain throughout the study did not reveal significant qualitative differences between post-COVID-19 participants and controls. At 2-3 months post infection, COVID-19 participants had lower total MoCA scores compared to controls (median 27 (25 – 29) vs median 28 (27-29)) and higher PHQ-9 and GAD-7 scores (markers of depression and anxiety). By 6 months, COVID-19 participants displayed better cognitive performance and markers of depression and anxiety improved, with all measures becoming comparable to controls.

Quality of life (assessed using the SF-36 questionnaire) was severely diminished shortly after infection. Although significant improvements were seen on longitudinal assessment, COVID-19 participants continued to experience poorer general health compared with controls. Similarly, while symptom burden was reduced by the end of the

follow-up period, limiting breathlessness (dyspnoea while walking briskly on level ground or when walking up a hill) was reported by 40% of COVID-19 participants 18 months post infection, which did not associate with CMR, lung function, ECG or CPET measures.

Conclusion: In the early post-acute phase (2-3 months) of moderate to severe COVID-19 disease, participants had multiorgan tissue abnormalities on MR imaging and evidence of organ dysfunction, reduced exercise capacity, poorer cognition scores and significantly reduced quality of life when compared with controls. Over time, MR tissue abnormalities resolved. Despite this, deficits in lung and renal function, reduced exercise capacity, and reduced quality of life due to limiting breathlessness and poorer general health persisted at 18 months. There was no association between persistent breathlessness and markers of cardiopulmonary health, suggesting that the mechanisms driving persistent symptoms post-COVID-19 disease are not easy to explain using objective clinical measures of multiorgan health.

# Chapter 1: General Introduction

## Background

In December 2019, an outbreak of pneumonia of unknown cause occurred in Wuhan, the capital city of Hubei province,[1] with fever, dry cough, myalgia and fatigue being common in patients at the time of presentation.[2] Dyspnoea was present in 55%, and the need for high-level oxygen support was surprisingly high, with 24% requiring non-invasive ventilation (NIV) or high-flow oxygen therapy (HFOT), and 10% requiring invasive mechanical ventilation +/- extracorporeal membrane oxygenation (ECMO). Lung abnormalities on computerised tomography (CT) imaging were detected in all patients, with 98% having bilateral involvement. Common bacterial and viral causes of pneumonia were absent, leading scientists to investigate the causative agent of this novel disease. On the 7$^{th}$ of January, 2020, deep sequencing analysis from lower respiratory tract samples revealed a novel enveloped ribonucleic acid (RNA) betacoronavirus, named 'Severe Acute Respiratory Syndrome Coronavirus-2 (SARS-CoV-2)'. Two months later, COVID-19 was present in over 100 countries, with over 80,000 laboratory-confirmed cases documented globally. By March 2020, the World Health Organisation (WHO) declared COVID-19 a global pandemic.[3]

As COVID-19 continued to spread across the globe, several studies describing the clinical features of patients infected with SARS-CoV-2 started to surface. In one such report, Zhou and colleagues shared their findings of a retrospective multicentre cohort study investigating the clinical characteristics and outcomes of 191 patients (with a median age of 56 years and predominantly male) admitted to hospital with laboratory proven COVID-19.[4] While severe pulmonary injury was already known to be a hallmark of the disease, with 54% and 31% of the study cohort suffering respiratory failure and acute respiratory distress syndrome (ARDS) respectively, the burden of extrapulmonary organ involvement was alarming; 23% developed heart failure, 17% experienced acute

cardiac injury and 19% demonstrated evidence of acute renal injury (with 5% requiring renal replacement therapy). The list of organ injury continued to propagate, with arrhythmia reported in 17%,[5] acute hepatic injury in 29%,[6] and cerebrovascular accidents in 0.5 – 4.6% (Table 1).[7,8]

**Table 1: Studies reporting extrapulmonary manifestations in patients hospitalised with COVID-19.**

| Study | Zhou et al.[4] | Wang et al.[5] | Yang et al.[6] |
|---|---|---|---|
| Number of patients | 191 | 138 | 52 |
| Treatment setting | Hospital | Hospital | ICU |
| Extrapulmonary manifestations | | | |
| Acute cardiac injury (biochemical) | 17.0% | 7.2% | 23.0% |
| Arrhythmia (Rhythm analysis) | .. | 16.7% | .. |
| Coagulopathy (increased D-Dimer) | 19.0% | .. | .. |
| Acute kidney injury (biochemical) | 15.0% | 3.6% | 29.0% |
| Acute liver injury (biochemical) | .. | .. | 29.0% |

## Acute COVID-19

### SARS-CoV-2 Structure and Cell Entry

By January 2020, genomic sequencing of SARS-CoV-2 was complete following genomic analysis of five hospitalised patient samples (bronchoalveolar lavage fluid, oral swabs and anal swabs), revealing a genomic size of 29.9kb coding for four structural proteins (S – Spike , E - Envelope, M - Membrane and N - Nucleocapsid) and sixteen non-structural proteins (nsp1-16).[9] The structure of SARS-CoV-2 (Figure 1) was found to consist of a single strand positive-sense-RNA associated with numerous nucleocapsid proteins (N), encapsulated by a lipid membrane containing the S (responsible for host cell entry, giving the virus its typical crown appearance for which it is named), E (contribute to virulence)[10] and M proteins (play a major role in the assembly of viral particles).[11]

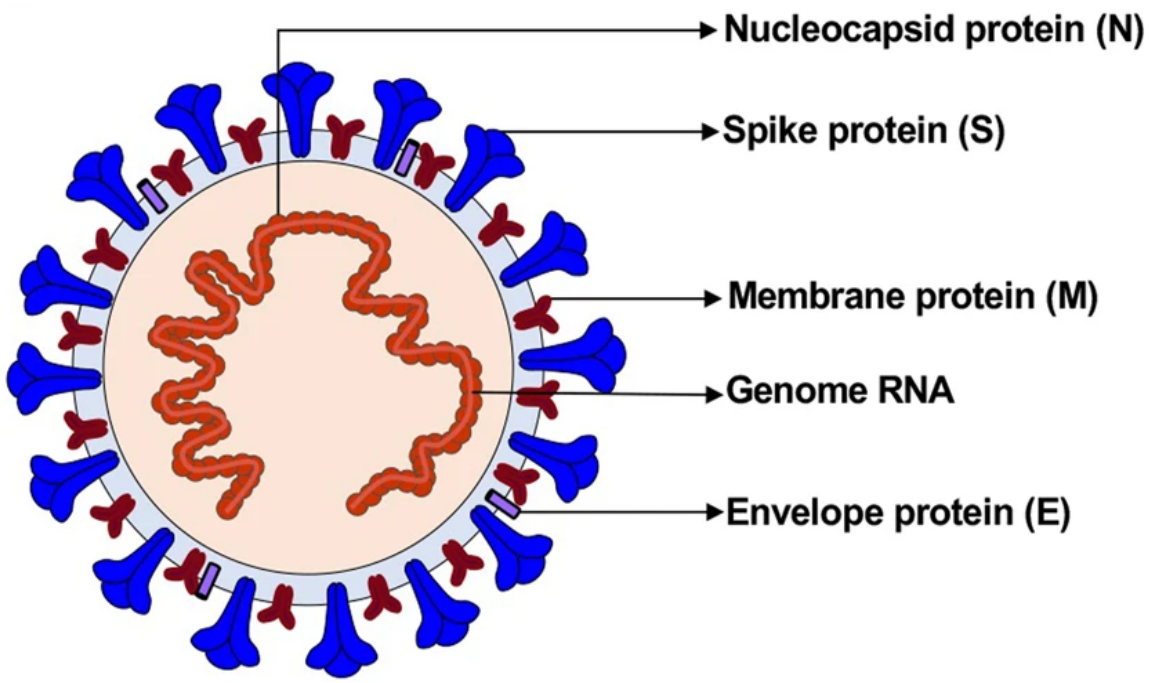


**Figure 1: Structure of SARS-CoV-2. (Reproduced from Zhang, Q., Xiang, R., Huo, S. et al. Molecular mechanism of interaction between SARS-CoV-2 and host cells and interventional therapy. Sig Transduct Target Ther 6, 233 (2021). https://doi.org/10.1038/s41392-021-00653-w). Licensed under CC BY 4.0. https://creativecommons.org/licenses/by/4.0/.**

It soon became clear that the main cellular target of SARS-CoV-2 is the angiotensin-converting-enzyme-2 (ACE2) receptor, although cell entry could occur via two distinct mechanisms:[12]

1) Membrane fusion: This involves cleavage of the S protein by transmembrane protease serine 2 (TMPRSS2), found on the cell surface membrane, succeeded by binding with the ACE2 receptor and membrane fusion.
2) Endosomal entry: In the absence of sufficient TMPRSS2 on the cell membrane, binding of the S protein with the ACE2 receptor may also occur resulting in internalization of the viral particle. Cleavage of the S protein occurs within the lysosome by cathepsin L, resulting in membrane fusion and release of the viral particle contents within the cytoplasm.

## Transmission

It soon became evident that human-to-human transmission could occur through self-inoculation from contaminated fomites (direct contact) or via droplets (particles >5μm in diameter) and aerosols (particles ≤5μm in diameter).[13] In aerosols, SARS-CoV-2 was shown to be viable for three hours, whilst droplets on surfaces (plastic and steel) had detectable virions for up to 3 days.[14] The reproduction number ($R_0$, which represents the average number of secondary infections produced by a typical case) of SARS-CoV-2 was, early in the pandemic, estimated to be between 2 and 2.5.[15]

In a study of 177 cases, the mean time to symptom onset (incubation period) following SARS-CoV-2 infection was seven days.[16] The mean time interval between infection and becoming infectious (latent period) was 36 hours shorter, accounting for the large proportion of transmission observed in asymptomatic individuals (Figure 2).[17]

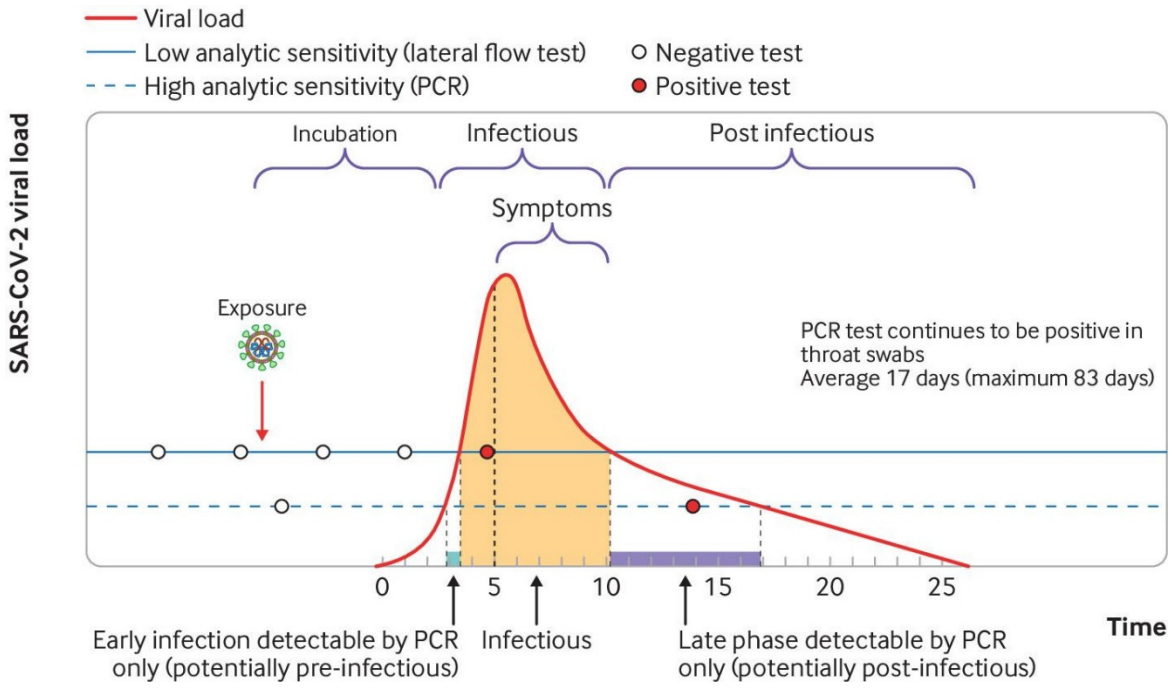


**Figure 2: Dynamics of viral load with time, demonstrating the different phases of SARS-CoV-2 infection and their relationship with high and low sensitivity tests. (Reproduced from Crozier A, Rajan S, Buchan I, McKee M. Put to the test: use of rapid testing technologies for covid-19. BMJ 2021; 372: n208.). Reproduced with permission; licence number 5787000785405.**

## Clinical Characteristics and Prognosis

Early in the pandemic, numerous studies set out to evaluate the prevalence of symptoms.[18-20] Irrespective of the variant, the most common symptoms of COVID-19 are non-specific and include fever, cough, myalgia, sore throat, headache, rigors, and gastrointestinal upset.[21]

Adults with COVID-19 are broadly grouped into five categories:[22]

- Pre-symptomatic or asymptomatic: SARS-CoV-2 is detectable on virological testing in the absence of symptoms.
- Mild illness: Individuals have any of the signs and symptoms of COVID-19, but do not have shortness of breath or abnormal pulmonary imaging.
- Moderate illness: Individuals have evidence of lower respiratory tract disease (clinically or on imaging) but can maintain adequate blood oxygen saturations (SpO2 >94%) without oxygen supplementation.
- Severe illness: Defined by the presence of reduced blood oxygen saturations (SpO2 <94%), a reduced ratio of arterial partial pressure of oxygen ($PaO_2$) to fraction of inspired oxygen ($FiO_2$) ($PaO_2/FiO_2$ < 300 mmHg), a substantial amount of lung infiltrates seen on imaging (>50%), and/or a respiratory rate >30/minute.
- Critical illness: Defined by the presence of respiratory failure, septic shock, and/or multiple organ dysfunction.

In a meta-analysis assessing the proportion of asymptomatic infections, of the 19,884 SARS-CoV-2 individuals, 41% did not experience symptoms.[23] In a separate study which included over 44,000 symptomatic patients, most developed mild to moderate disease, while 14% experienced severe illness, and 5% developed critical illness (Figure 3).

Risk factors for hospitalization and death include increasing age, male gender, obesity, chronic conditions (such as hypertension, diabetes, immunodeficiency, and chronic lung/heart/liver/kidney disease), variant type, vaccination status against SARS-CoV-2, and pregnancy.[24-28] The estimated case fatality ratio (CFR), early in the pandemic, was 2.5%, with significantly higher mortality rates seen in the elderly (15% in individuals 80 years or older).[29]

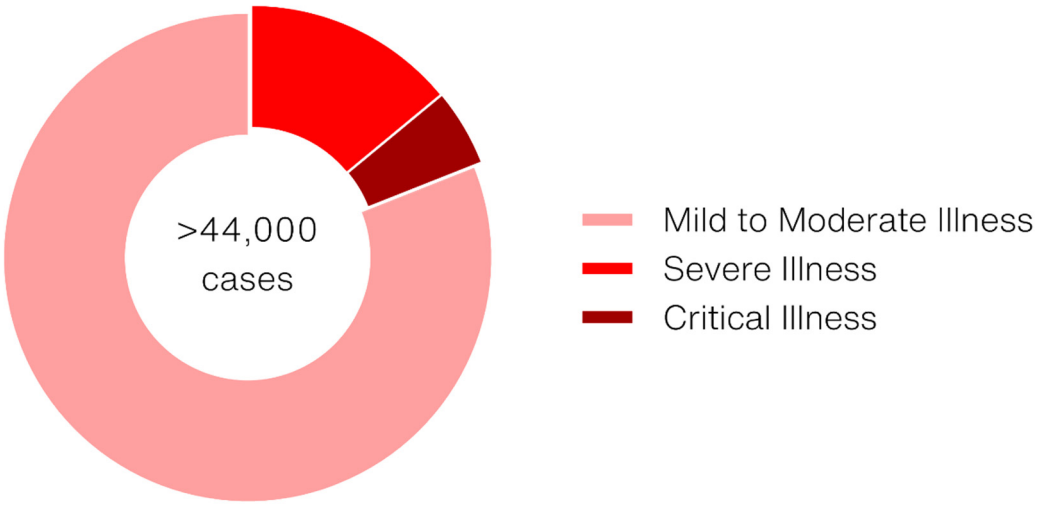


**Figure 3: Illness severity in a Chinese cohort of >44,000 confirmed cases.**

## Mechanisms of organ injury after SARS-CoV-2 infection

### Reduced ACE2 receptor activity and direct toxicity

The process of cell binding and entry *itself* is one of the mechanisms described to contribute to organ injury (**Figure 4**). ACE2 receptors play a critical role in the Renin-Angiotensin-Aldosterone System (RAAS); through the inactivation of angiotensin I and cleavage of angiotensin II into angiotensin 1-7 (which has vasodilatory and antifibrotic effects), ACE2 receptors keep the RAAS in check.[30] In the absence of free ACE2 receptor binding sites (secondary to SARS-CoV-2 binding and cellular down-regulation), levels of angiotensin I and II, which are key mediators of the RAAS, increase, resulting in acute lung injury, adverse cardiac remodelling, excessive vasoconstriction, and increased vascular permeability.[31] ACE2 is expressed throughout the respiratory system, but is highest within the nasal epithelium, which explains why nasal ciliated cells are the primary targets during the initial stage of infection.[32] Despite being primarily a disease of the lungs, higher levels of ACE2 expression are found in extrapulmonary sites, such as the gastrointestinal tract, kidneys, myocardium, and endothelial cells.[33] Following successful cell entry, viral uncoating results in the release of genomic RNA, which then leads to viral gene expression and translation. As the process of viral replication is established, this results in impaired cell function or cell death.[34]

### Endothelial cell dysfunction

Endothelial cell infection following ACE2-mediated SARS-CoV-2 cell entry results in direct cell injury and endothelial inflammation, characterized by the presence of activated neutrophils and macrophages. Endothelial cell dysfunction ushers in a crescendo of inflammatory cytokines and thrombin production, downregulation of fibrinolysis and activation of the complement pathways.[35] The interaction between neutrophils, macrophages and platelets lead to the formation of neutrophil extracellular traps (NETs)

and the generation of microthrombi.[36] Together, these processes lead to a proinflammatory and prothrombotic state.

### Immune dysregulation

T cell lymphopenia (secondary to direct T-cell invasion and delayed release of type 1 interferon, which exerts cellular protective effects in the face of infection and stimulates T-cell maturity and survival),[37] overactivation of innate immunity (via localisation of proinflammatory neutrophils and maturation of monocytes into macrophages through activation of the JAK/STAT pathway),[38] and disruption of interferon signalling (secondary to the release of granulocyte–macrophage colony-stimulating factor (GM-CSF), tumour necrosis factor (TNF), interferon- gamma (IFN) and IL-6)[36] further contribute to a proinflammatory state and prothrombotic environment.[39] In the most severe cases, exaggerated immune activation culminates in a cytokine storm, manifesting clinically as ARDS, multi-organ failure and/or death.[40] Of note, the unravelling of these pathological mechanisms has resulted in the use of JAK/STAT inhibitors and IL-6 inhibitors in the treatment of patients with severe COVID-19.[41]

### Multiorgan injury

The ubiquitous expression of ACE2 receptors and transmembrane serine protease 2 resulting in direct SARS-CoV-2 infection of numerous cell lines, promotion of endothelial cell dysfunction (with endothelial cells present in all vascular beds), systemic impact of RAAS dysregulation and immune response dysregulation all contribute to the occurrence of both pulmonary and extra-pulmonary organ involvement in COVID-19 (**Figure 4**).

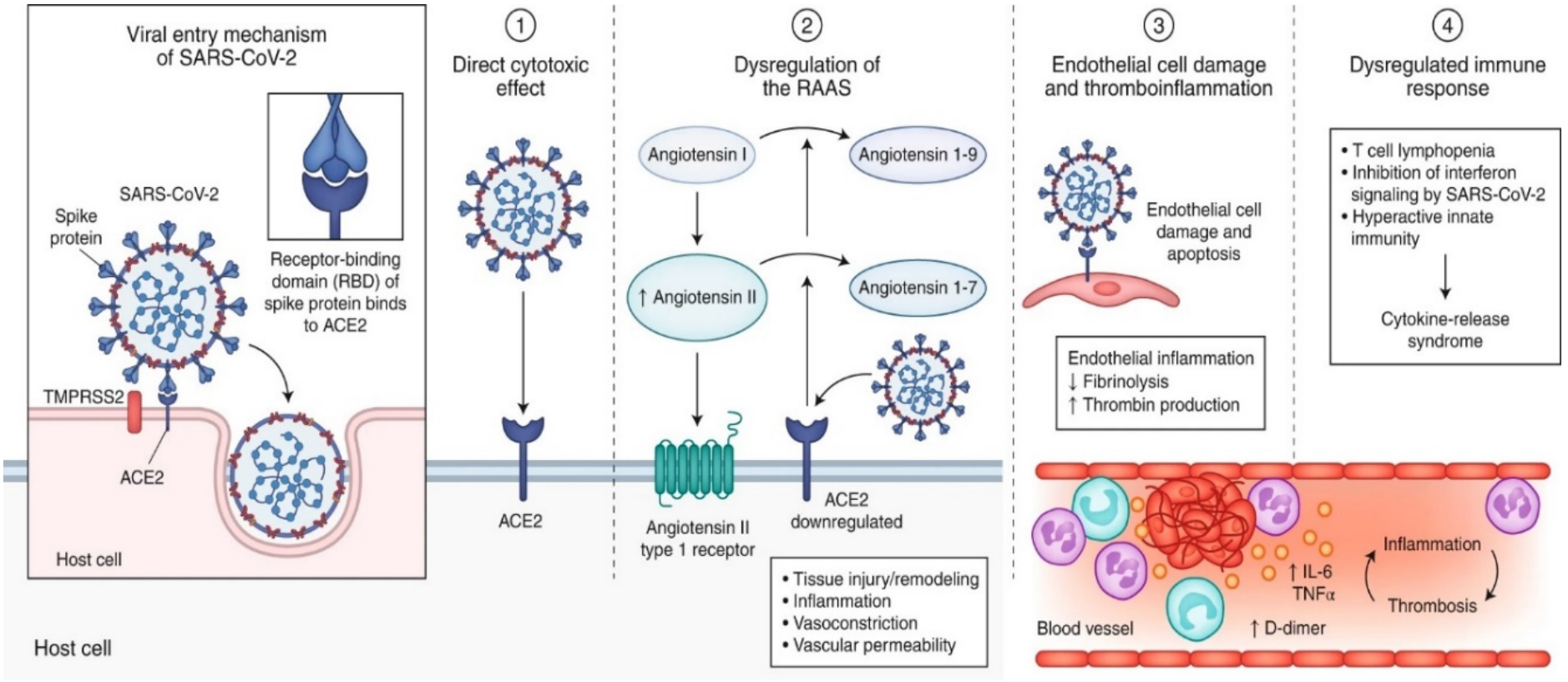


**Figure 4: Mechanisms of injury in COVID-19. (Reproduced from Gupta, A., Madhavan, M.V., Sehgal, K. et al. Extrapulmonary manifestations of COVID-19. Nat Med 26, 1017–1032 (2020). https://doi.org/10.1038/s41591-020-0968-3). Reproduced with permission; Licence number 5787000502674.**

## Histopathological features of organ injury

In February 2020, Xu and colleagues published the first post-mortem findings in a 50-year-old male who died from COVID-19.[42] Features of ARDS (pneumocyte desquamation, hyaline membrane formation and pulmonary oedema) were seen in both lungs, together with mononuclear (predominantly lymphocytic) inflammatory infiltrates. By June 2020, further reports were available. In addition to the histopathological features associated with ARDS, Barnes and colleagues described pulmonary small vessel injury, with features of acute capillaritis seen in areas of alveolar neutrophilic infiltration, with the authors postulating that the observed prothrombotic and proinflammatory environment may lead to the formation of NETs.[43] In a separate report, Menter and colleagues shared post-mortem findings in 21 COVID-19 patients with respiratory failure as the primary cause of death.[44] Hyaline membrane formation, capillary congestion and reactive pneumocyte changes were the most prominent histopathological features observed, typical of diffuse alveolar damage. Of interest, several cases showed alveolar haemorrhage together with pulmonary embolism, and in five patients, microthrombi were found in alveolar capillaries. A high frequency of thrombosis was also reported by Wichmann and colleagues, with massive pulmonary embolism seen in four cases (out of 12), bilateral deep vein thrombi seen in three cases, and microthrombi within alveolar capillaries seen in the majority.[45]

To assess for the presence and characteristics of cardiac injury, Kawakami and colleagues reviewed previously published cases of COVID-19 where post-mortem examination of the heart or endomyocardial biopsy during the acute illness took place; in total, 201 cases were included.[46] In 24 post-mortem examinations, SARS-CoV-2 RNA was detected in cardiac tissue. In situ hybridization (ISH) confirmed that RNA was exclusively present within interstitial cells, and not within the myocytes. Virus-mediated myocyte necrosis was not seen, and the presence of viral RNA was not associated with

increased mononuclear cell infiltration, suggesting that direct viral-mediated myocyte necrosis is unlikely. Of all the cases studied, evidence of myocarditis was only found in 9 (4.5%). In most, analysis for the presence of SARS-CoV-2 within the heart was not performed, and none showed evidence of direct myocyte infection. A low prevalence of myocarditis fulfilling immunohistopathological criteria (≥14 leukocytes/mm$^2$ and ≥7 T lymphocytes/mm$^2$, together with myocyte necrosis)[47] was also reported by Halushka and Vander Heide, who, in a literature review identifying 277 autopsied hearts, estimated the prevalence of myocarditis to be lower than 2% (given the referral bias of autopsy, this is likely an overestimation of the true prevalence within the population).[48] Macrothrombi (occurring anywhere within the vasculature or the heart) were seen in 19%. Single cell myocyte necrosis was seen in 14%, and non-myocarditis inflammation was seen in 13%. Five percent had evidence of acute myocardial infarction. On review of the abnormalities and histopathological findings observed in autopsied hearts, the authors concluded that myocardial injury within the context of COVID-19 is likely secondary to the broader effects of SARS-CoV-2 infection, such as a hyperinflammatory hypercoagulable state, hypoxia, and thrombotic complications, particularly within the lungs.

Histopathological features of other extrapulmonary organs have also been reported. In the first report of renal pathological findings, Su and colleagues describe the renal abnormalities present in 26 autopsies of patients with COVID-19.[49] On light microscopy, severe proximal acute tubule injury was seen, defined by loss of the brush border, dilatation of the tubular lumen with cellular remnants and frank necrosis and detachment of epithelium. In three cases, fibrin thrombus was seen within the glomerular capillary loops, associated with severe endothelial injury. Other cases exhibited peritubular and glomerular capillary obstruction due to erythrocyte stagnation, in the absence of erythrocyte fragmentation, platelets, or fibrin thrombi, features that are often seen in periods of prolonged hypotension. On electron microscopy, SARS-CoV-2 like particles

were found in the two main areas known to express ACE2[50]: the proximal tubular epithelium and podocytes. The presence of SARS-CoV-2 like particles was associated with pedicel effacement and detachment of podocytes from glomerular capillary basement membranes. In summary, COVID-19 mediated renal injury is multifactional, with direct infection of renal tissue and indirect injury secondary to sepsis, dysregulated inflammation and a prothrombotic environment.

While few post-mortem COVID-19 studies have focused on the liver, important insights have been gained from careful prior efforts. Fassan and colleagues describe histopathological findings of three liver biopsies (obtained from living patients with COVID-19 and deranged liver markers) and 25 livers analysed post-mortem.[51] A non-specific pattern of injury was observed, with 1/3$^{rd}$ exhibiting activation of Kuppfer cells (potentially secondary to cytokine storm and/or for the clearance of excess immune complexes) and steatosis (caused either by direct SARS-CoV-2 injury or secondary to the drugs used in the treatment of COVID-19, many of which are known to have hepatotoxic effects).[52] Features of hepatic ischaemia were seen in most autoptic specimens, such as zone 3 sinusoidal ectasia (84%), centrilobular parenchymal atrophy (20%), and sinusoidal fibrosis and/or microthrombi (28%). These findings were attributed to the deranged hypercoagulable state that frequently accompanies COVID-19. Despite the relatively high expression of ACE2 in the liver (predominantly by cholangiocytes)[53], ISH testing for SARS-CoV-2 was negative. Similarly, in three percutaneous liver biopsies obtained from patients with severe COVID-19 requiring mechanical ventilation, despite extensive cholangiocyte injury, both immunohistochemistry and ISH failed to demonstrate direct SARS-CoV-2 infection.

In a report investigating the neuropathological features of COVID-19, Solon and colleagues report their neuropathological findings from 18 autopsies of patients who died due to COVID-19 disease.[54] On microscopic examination, acute hypoxic injury was seen

in the cerebrum and cerebellum of all cases, with loss of neurons in the cerebral cortex, hippocampus and Purkinje cell layer of the cerebellum. No thrombi or features of vasculitis were seen. On quantitative reverse transcriptase polymerase chain reaction (qRT-PCR) testing and immunohistochemical analysis of brain tissue, no convincing evidence of direct viral infection was seen. In contrast, Matschke and colleagues detected SARS-CoV-2 RNA (using qRT-PCR) or proteins (using immunohistochemistry) in the frontal lobe, brain stem and/or the cranial nerves (specifically the glossopharyngeal and vagus nerves) in 21 of the 40 post-mortem brain specimens. In addition, astrogliosis was frequently observed in association with cytotoxic T cell infiltration, predominantly in the brainstem and cerebellum.[55] While small vessel thromboses were absent, six specimens had fresh ischaemic infarctions (with the authors attributing these to a thromboembolic cause). Given the various findings, it is likely that SARS-CoV-2 mediated neurological injury is multifactorial, with both direct SARS-CoV-2 infection and dysregulated inflammation and hypercoagulation all playing a role.

## Lessons from previous pandemics

Severe acute respiratory syndrome coronavirus (SARS-CoV), Middle East respiratory syndrome coronavirus (MERS-CoV) and influenza A are major pathogens that have been responsible for several historical pandemics/outbreaks. Like SARS-CoV-2, their primary target is the human respiratory system.

Influenza A viruses have been the cause of four pandemics, the most deadly occurring in 1918 (termed the "Spanish influenza") and causing an estimated 50 million deaths.[56] A further 2.6 million deaths occurred in the subsequent three pandemics (1957 – "Asian Influenza", 1968 – "Hong Kong flu", and 2009, "swine flu").[57-59] Prior to the fourth influenza pandemic, in 2002, the SARS outbreak resulted in over 8000 infections and 774 deaths in 26 countries.[60] MERS was the last respiratory outbreak prior to COVID-19, with the first case being recorded in June 2012 in Saudi Arabia.[61] As of October 2023 a total of 2608 laboratory-confirmed cases have been documented, with 938 deaths.[62]

SARS-CoV-2, SARS-CoV, MERS-CoV and influenza A share several common features. All have a predilection to infect cells within the lower respiratory tract (in contrast with other human coronaviruses which generally cause mild upper respiratory tract symptoms and are responsible for 15-30% of common colds).[63] Acute infection is characterized by fever, dry cough, shortness of breath and myalgia. Severe illness can be complicated by septic shock, ARDS, cytokine storm and death.[64] Specific to the coronaviruses, all three share similar RNA genomic sequences, with SARS-CoV-2 having a 82.5% point identity (quantitative measurement of the similarity between two sequences) with SARS-CoV and 70% point identity with MERS-CoV (Figure 5).[64]




**Figure 5: The genomes of SARS-CoV, MERS-CoV and SARS-CoV-2. ORF – Open reading frames. S – Spike protein. E – Envelope protein. M – Membrane protein. N – Nucleocapsid protein. ORFs code for non-structural proteins. Reproduced from Li YD, Chi WY, Su JH, Ferrall L, Hung CF, Wu TC. Coronavirus vaccine development: from SARS and MERS to COVID-19. J Biomed Sci 2020; 27(1): 104. Licensed under CC BY 4.0. https://creativecommons.org/licenses/by/4.0/.**

Given that the long-term impact of SARS-CoV-2 was unknown at the beginning of the pandemic, research addressing the outcomes of patients infected with Influenza A, SARS-CoV and MERS provided useful insights into the potential protracted effects of SARS-CoV-2 infection.

Following the SARS global outbreak, several observational studies reported on the outcomes of survivors. In 2007, Su and colleagues published a report investigating the impact of SARS infection on exercise capacity and pulmonary function in 13 previously healthy patients 14 months following infection, and compared their results with 14 individuals who were never infected.[65] While one patient exhibited abnormalities on spirometry (reduced forced expiratory volume in 1 second ($FEV_1$) and forced vital vapacity (FVC)), over half the patients had reduced lung diffusion capacity (assessed using diffusion capacity for carbon monoxide (DLco)). Reduced exercise capacity (maximal oxygen consumption ($\dot{V}O_2max$) <85% predicted) on cardiopulmonary exercise testing (CPET) was seen in eight patients, although this was not different from age matched controls. Interestingly, lung abnormalities did not associate with reductions in exercise capacity, and breathing reserve was preserved in those with impaired exercise tolerance, suggesting a non-pulmonary cause for reduced exercise capacity. In 2009, Hui and

colleagues reported similar findings in a cohort one year following infection with SARS, with 24% having reduced DLco, and overall reduced six-minute walking distance (6MWD) compared to age-matched controls.[66] Patients requiring intensive care (ICU) had worse lung function indices, although this was unrelated to invasive ventilation. The same dissociation between exercise capacity and lung function impairment was noted, with the authors suggesting that exercise limitation may be secondary to extrapulmonary factors such as myopathy (viral, steroid induced, or critical illness related), neuropathy or deconditioning.

Other long term adverse effects have been observed following infection with SARS, MERS and Influenza A. In a cohort of 24 SARS survivors, chronic generalized pain, severe fatigue, depression and sleep disturbance were observed, with two patients fulfilling criteria for post-traumatic stress disorder.[67] The authors described the constellation of symptoms as 'Chronic post-SARS syndrome', which bore a marked resemblance to chronic fatigue syndrome. Similar findings were reported in a larger study of 233 SARS survivors four years following infection, with over 40% having active psychiatric illness, 40% reporting chronic fatigue, and 27% fulfilling criteria for chronic fatigue syndrome.[68] MERS survivors also appear to suffer similar protracted ailments, with 17% having clinically relevant depressive symptoms and 1/3$^{rd}$ experiencing significant fatigue, 18 months following infection.[69] Although formal research during the time of the Spanish flu is lacking, hospitalizations due to influenza related mental disorders increased by seven times in the six years following the pandemic, with survivors also reporting sleep disturbances and depression.[70] The outcomes of other influenza pandemics are more robustly documented, with significant rates of anxiety, depression, fatigue and breathlessness being reported in survivors of Asian flu and Swine flu.[71,72]

## Evidence gap

Early in the pandemic when I embarked upon my research, it was unknown whether multi-organ dysfunction persists or develops beyond the acute stages of COVID-19, as were the underlying mechanisms and clinical implications. I sought to investigate the effects of COVID-19 on the lungs, heart, liver, kidney and brain using state-of-the-art imaging, biochemical analysis, questionnaires and functional tests. I set out to test the following objectives:

1) Examine the prevalence, extent and longitudinal trajectory of lung, heart, liver, kidney and brain injury on MRI in participants following moderate to severe COVID-19 and compare this with matched uninfected controls.
2) Compare serological measures of heart, liver and kidney function on blood tests in participants following moderate to severe COVID-19 with matched uninfected controls.
3) Compare lung function parameters over time in participants with previous COVID-19 and matched controls.
4) Longitudinally evaluate the quality of life of participants following COVID-19.
5) Longitudinally evaluate cognition and the mental health of participants following COVID-19 over time.
6) Assess the impact of COVID-19 on exercise capacity over time.

This DPhil provides insights into the prevalence of organ dysfunction over time and clarifies the mechanisms responsible for pulmonary and extrapulmonary injury following COVID-19.

# Chapter 2: Methods

## Study design

This is a longitudinal observational cohort study. Patients who were previously admitted to the Oxford University Hospitals National Health Service Foundation Trust with moderate-to-severe SARS-CoV-2 infection (defined as requiring admission to hospital for at least 48 hours) were invited to undertake a total of three study visits: at 2-3 months post-infection, 6 months post-infection and finally at 12-24 months post-infection. At the same time, age, sex, body mass index and comorbidity-matched controls with no history of SARS-CoV-2 infection were invited to undergo a single study visit; these controls served as a comparator group.

The inclusion criteria were as follows:

- The participant was willing and able to give informed consent for participation in the study.
- The participant was aged 18 years or above.
- In the case of COVID-19 participants, admission to hospital for a minimum of 48 hours with COVID-19, confirmed by reverse-transcription Polymerase Chain Reaction (RT-PCR), was required.
- In the case of controls, participants must have had a negative SARS-CoV-2 anti-Nucleocapsid IgG test.

The exclusion criteria consisted of:

- Moderate to severe pre-existing neurological, cardiovascular, pulmonary, hepatic or renal disease.
- Active neoplastic disease.
- Any signs of active COVID-19 on the day of the visit.

Moderate to severe disease was defined as any condition that required admission to hospital. Uncontrolled mood disorders, ischaemic or haemorrhagic cerebrovascular accidents (except transient ischaemic attack), uncontrolled epilepsy, progressive autoimmune conditions, systolic heart failure, prior myocardial infarction, prior myocarditis, moderate to severe asthma/COPD[73,74], pre-existing hepatic dysfunction and pre-existing renal dysfunction were deemed exclusionary for the purpose of this study, as were any illnesses that resulted in reduced mobility or impaired exercise capacity.

A total of 58 participants attended a study visit 2-3 months following infection, of which 46 attended for a follow-up visit, 6 months following infection. 23 participants attended a final visit, 18 months following infection (Figure 6). 30 participants with no history of COVID-19 (controls) were recruited and attended a single study visit.

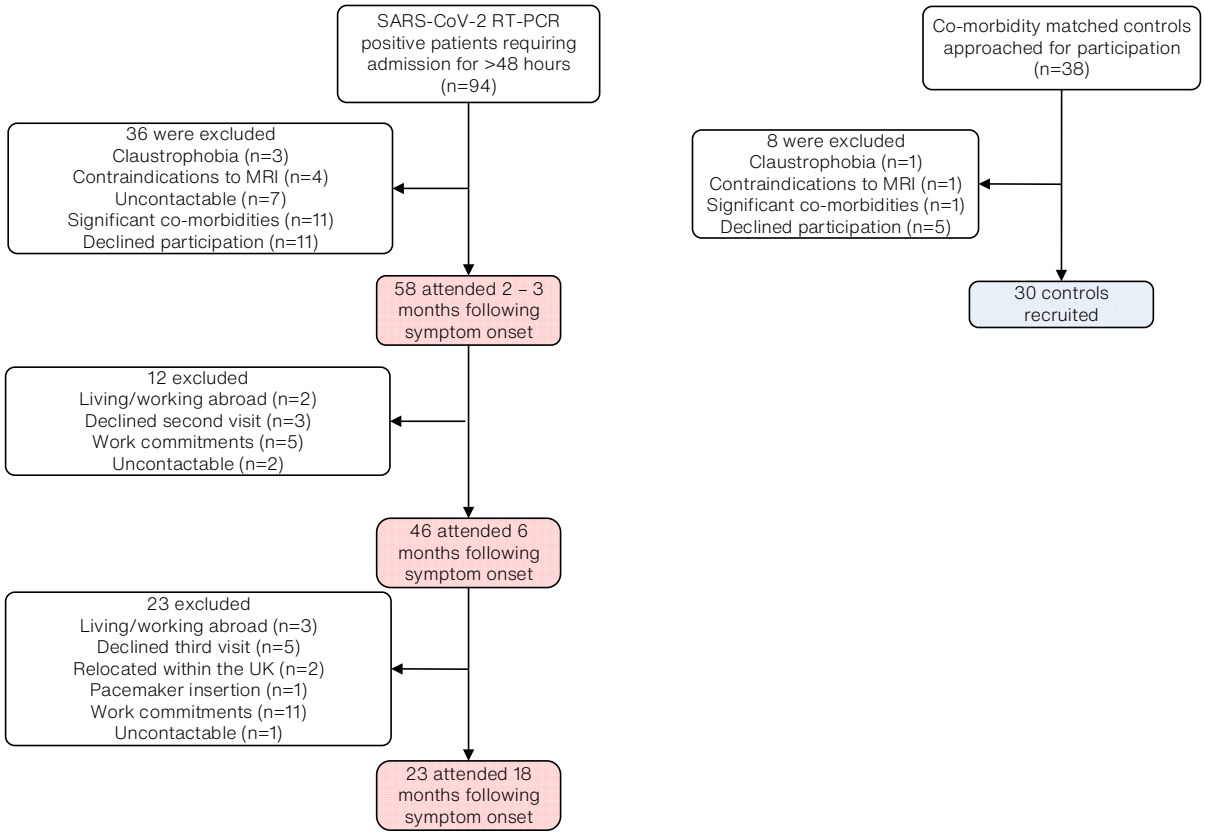


**Figure 6: Flowchart depicting recruitment throughout the study.**

### Recruitment

The COVID-19 participants recruited were admitted to the Oxford University Hospitals National Health Service Foundation Trust between 14th March – 25th May 2020. Uninfected controls from the community were recruited during the same period. Patients were approached by their medical team, at the time of or shortly after discharge, and invited to participate in the study. Comorbidity-matched controls were identified from other studies and by word of mouth.

### Data collection

I designed an electronic case report form using an electronic data capture platform (CASTOR EDC, https://www.castoredc.com). Each participant report incorporates data from multiple visits. No personal identifiable information was stored.

### Study visit overview

Informed consent was obtained at the beginning of each study visit. Next, vital signs were recorded, blood tests were performed, and an electrocardiogram (ECG) was acquired. Following multi-organ MRI, spirometry, gas transfer and total lung capacity assessment, the questionnaires were filled in (using an electronic data capture platform, CastorEDC) together with a Montreal Cognitive Assessment (MoCA) cognitive assessment, with a CPET marking the end of a study visit.

### Admission details

Details on clinical symptoms, signs, vitals, and laboratory findings during admission were acquired from electronic medical records, following acquisition of consent (after completion of a study visit).

### Vital signs

Following anthropometric measurements (height and weight), temperature was recorded and blood pressure, heart rate, oxygen saturation and respiratory rate were measured.

## Laboratory analysis

The following vacutainer tubes were collected at the beginning of a study visit: one Ethylenediaminetetraacetic acid (EDTA - purple top), two citrate (yellow top), and one heparin (green top) tube. The tubes were sent to the John Radcliffe haematology, biochemistry and microbiology laboratories for complete blood count, liver and renal function assessment, troponin T, N-terminal prohormone of brain natriuretic peptide (NT-proBNP), SARS-CoV-2 antibodies, and C-reactive protein (CRP).

## Electrocardiogram

A 12-lead ECG was performed and interpreted according to the Minnesota Code of Electrocardiographic Findings.[75]

## MRI protocol

MRI imaging was carried out during a single session on a Siemens Prisma 3T with a Siemens 20-channel head coil for neuroimaging and a 32-channel spine array and 30-channel body array used for thoracic and abdominal imaging. In the following descriptions, TR refers to repetition time, TE to echo time, and TI to inversion time.

Control and COVID-19 participant images were analysed together in a blinded fashion.

### Brain MRI

The neuroimaging protocol incorporated structural and functional sequences and lasted approximately 15 minutes. The MRI sequences were as follows:

A) High-resolution T1-weighted Magnetization Prepared RApid Gradient Echo (MPRAGE) – TR/TE/TI=2000/1.95/880 ms, flip angle=8°, matrix=256x256x208, voxel dimension=1 mm isotropic. This sequence is used to assess grey matter (GM) tissue.

B) Diffusion MRI (dMRI) – TR=8500 ms, flip angle=90°, matrix=104x104x72, voxel dimension=2 mm isotropic, b=0,1000 s/mm$^2$, three sequentially applied diffusion gradient directions (x,y,z), blip-reversed b=0. This sequence measures the random motion of water molecules to allow one to 1) infer information about White Matter (WM) microstructural properties and 2) delineate the gross axonal organisation of the brain. With just 3 orthogonal diffusion directions (as commonly done in clinical practice), mean diffusivity can be estimated. The diffusion sequence was kindly provided by the Center for Magnetic Resonance and Research, University of Minnesota, USA.

C) Fluid Attenuated Inversion Recovery (T2-FLAIR) – TR/TE/TI=5000/386/1800 ms, matrix=256x256x192, voxel dimension=1x1x1.05 mm. This sequence is commonly used in clinical practice, for example to characterise white matter (WM) hyperintensities (often referred to as lesions and arising from a range of biological/pathological mechanisms such as vascular injury and inflammation).

D) Susceptibility-weighted MR Imaging (3D-swMRI) – TR/TE1/TE2=27/9.4/20 ms, matrix=256x232x48, voxel dimension=0.9x0.9x3 mm$^3$. This sequence is commonly used in clinical settings to assess traumatic brain injury and stroke, but can also be used to define vascular malformations, cerebral microbleeds, intracranial calcifications, neurodegenerative diseases and brain tumours.

### Lung MRI

Half-Fourier-acquisition single-shot turbo spin-echo (HASTE MRI) - axial; TR/TE=750/49 ms, field of view=380x320 mm, slice thickness/spacing 8/0 mm, 35 slices, matrix=256x123. This was acquired to assess the lungs for parenchymal abnormalities. Images were acquired with parallel imaging, which was applied in the phase-encoding direction.[76] These images show high intensity signals in tissues with high water content,

making lung abnormalities appear bright and surrounded by low intensity air-filled parenchyma.[77]

## Cardiac MRI

The cardiac MRI protocol included routine clinical and advanced parametric mapping sequences. The cardiac MRI sequences were as follows:

A) Cine steady-state free precession (SSFP) imaging - Three long-axis and short-axis stack; typically, TR/TE=3.16/1.38 ms, flip angle=65°, field of view=360×270 mm, matrix=208×139, slice thickness/spacing 7/3 mm. This is used in the clinical setting to assess cardiac (left and right ventricular) mass, volumes and function.

B) Shortened Modified Look Locker Inversion Recovery T1 mapping (ShMOLLI, Siemens prototype sequence WIP1048B) - Base, mid, apex short axis slices; TR/TE=2.7/1.07 ms, flip angle=35°, field of view=360×270 mm, matrix=192×144; slice thickness=8 mm. Inversion times in image acquisitions, waiting periods with conditional on-the-scanner T1 map reconstruction, as previously described.[78] This sequence helps assess the myocardial tissue characteristics which indicates if the myocardium has increased water content or fibrosis.[79]

C) T2 mapping (Siemens Myomaps) - Base, mid, apex short axis; bSSFP readout; TR/TE=3/1.3 ms, flip angle=20°, matrix=192×142, field of view=360×270 mm, slice thickness=8 mm. This sequence is typically used to detect increased water content in myocardial tissue.

D) Late gadolinium imaging was acquired using a T1-weighted phase-sensitive inversion recovery (PSIR) sequence following a bolus injection of 0.15mmol/kg of body weight of gadolinium-based contrast agent (Dotarem) and a 10 ml saline flush. Typical scan parameters: TR/TE/TI=2.9/3.36/subject-specific ms, flip angle=55°, matrix=144×256, field of view 380×285 mm, slice thickness=8 mm. Late gadolinium imaging is used in clinical cardiac MRI to detect regions of focal fibrosis or scar within the myocardium.

E) Post-contrast T1 mapping - Base, mid and apical short-axis T1 maps (ShMOLLI) were acquired 15 minutes after the administration of gadolinium contrast. This sequence is used to estimate the extent of diffuse fibrosis or scar in the myocardium.

All cardiac images from the 2-3, 6 and 18 month visits were analysed using CVI42 software (Circle Cardiovascular Imaging Inc., Calgary, Canada).

### Abdominal MRI

(A) MOLLI-variant T1 map (Siemens Myomaps) was used to assess changes in extracellular water in the liver. Changes in T1 could be due to a number of pathophysiological mechanisms including fibrosis, inflammation and oedema. Axial; TR/TE=2.45/1.05 ms, flip angle=35°, field of view 440×330 mm, matrix=192×144, slice thickness 8mm, ECG-gated shMOLLI sampling pattern and conditional processing.[78]

(B) Multiecho gradient echo iterative decomposition of water and fat with echo asymmetry and least-squares estimation (IDEAL)[80] was used to assess fat and iron in the liver - axial; TR/TE=15/1.1, 2.2, 3.3, 4.4, 5.5, 6.6, 7.7, 8.8, 9.9, 11, 12.1, 13.2 ms; flip angle=6°, field of view 440×400 mm, matrix=128×116, slice thickness 10 mm. These data were reconstructed using the ISMRM fat-water separation toolbox (https://www.ismrm.org/workshops/FatWater12/data.htm) to yield proton density fat fraction (PDFF), $B_0$ and T2* maps.[81]

(C) Kidney MOLLI T1 map with a 5-3s-3 sampling scheme[82] - oblique coronal; TR/TE=2.7/1.15 ms, flip angle=35°, field of view 320×320 mm, matrix=194×192, slice thickness 5.5 mm. As described above, changes in T1 could be due to a number of pathophysiological mechanisms.

### Lung function assessment

DLco, alveolar volume (Va) and measurement of total lung capacity were performed according to the latest published standards.[83,84]

### Cardiopulmonary exercise testing

CPET was performed using a cycle ergometer (Ergoline Ergoselect 100) and a spiroergometry system (Metalyzer 3B). Following two minutes of unloaded cycling, the work rate was increased to 20W, followed by a 10W/min ramp.[85]

### Questionnaires

The Patient Health Questionnaire-15 (PHQ-15) was used to assess for the presence of a number of symptoms common in patients following COVID-19.[86] The Medical research council (MRC) dyspnoea scale[87] was used to assess the effects of breathlessness on daily activities. Fatigue was assessed using the Fatigue Severity Scale (FSS).[88] The Generalised Anxiety Disorder Assessment (GAD-7) and Patient Health Questionnaire depression module (PHQ-9) were used to screen for anxiety and depression among participants, respectively.[89,90] The 36-Item Short Form Survey (SF-36) was used to assess health status and quality of life.[91] Cognitive function was assessed by using the MoCA tool, with scores ranging from 0 to 30 points.[92]

### Statistical methods

For continuous variables with parametric data across all groups, mean and standard deviation were used to describe the data. When non-parametric data was present in one or more groups, median and interquartile range (IQR) were used. Categorical variables were represented as frequency and percentages.

For each continuous variable assessed, the Shapiro-Wilk test was used to determine normality. The statistical tests used to determine group differences in continuous variables between COVID-19 participants and controls consisted of the Student's t-test

(for parametric data), one-way analysis of variance (ANOVA – for parametric data with more than two groups), Mann-Whitney U-test (for non-parametric data) and Kruskal-Wallis test (for non-parametric data with more than two groups). Differences in categorical variables were assessed using Pearson's Chi square test, Fisher's exact test (when 1 or more cells had an expected cell count less than 5) and the Fisher-Freeman-Halton exact test (when a contingency table was larger than 2x2 and 1 or more cells had an expected cell count less than 5).

Paired Student's t-test (parametric) and the Wilcoxon Signed Ranks test (non-parametric) were utilised to assess for intragroup differences in COVID-19 participants (2-3 months vs 6 months, and 6 months vs 18 months). For categorical variables, the McNemar test (2x2 contingency table) and the Stuart-Maxwell test (also known as the Marginal Homogeneity test, used for contingency tables larger than 2x2) were used. Analysis of covariance (ANCOVA) was used to facilitate comparisons between variables in the presence of a covariate.

Pearson's or Spearman's correlation coefficients were used to describe the relationship between two variables, depending on the distribution of the variables.

Ordinal, binominal and linear regression were used to assess the effect of two or more independent variables on an ordinal, binary or continuous outcome, respectively.

## Chapter 3: Long-term impact of COVID-19 on Cardiopulmonary Health and Exercise Capacity


### Abstract

**Background:** The respiratory system is the primary target of COVID-19. Together with early reports of frequent cardiac involvement, COVID-19 may have long-term consequences on cardiorespiratory function and exercise capacity.

**Objectives:** To longitudinally assess the prevalence and investigate potential mechanisms of cardiorespiratory impairment and reduced exercise capacity following moderate to severe COVID-19.

**Methods and results:** Fifty-eight participants with moderate to severe COVID-19, 2-3 months post infection, and 30 matched non-COVID controls underwent blood testing, MRI imaging of their heart and lungs, spirometry, and performed a CPET. COVID-19 participants were invited for repeat assessment 6 months and 18 months post-infection, when gas transfer and total lung capacity assessment were also performed.

CMR imaging, 2-3 months post-infection, revealed elevated myocardial native T1 in participants versus controls (basal T1: 1180ms vs 1150ms, $P<0.001$) which normalised by 6 months. COVID-19 participants and controls had comparable biventricular size and function. COVID-19 participants had a high burden of pulmonary abnormalities on MRI imaging, which improved with time but did not completely resolve.

At 2-3 months post infection, a restrictive pattern was the most common lung abnormality seen in COVID-19 participants (9%), which resolved over time. At 18 months post-infection, gas transfer abnormalities continued to be seen in 1/4$^{th}$ of COVID-19 participants, secondary to both reduced alveolar volume and impaired gas exchange.

During the initial assessment, significantly reduced exercise capacity ($\dot{V}O_2$peak (<80% of predicted) 54% vs 7% in controls, $P<0.001$) was seen in COVID-19 participants. This improved by 6 months ($\dot{V}O_2$peak, (<80% of predicted) 32%) but remained low

compared to controls. Reduced exercise capacity was deemed to be secondary to limiting symptoms and reduced tissue oxygen extraction in the absence of significant cardiopulmonary limitation.

Conclusion: Persistent cardiac abnormalities on CMR imaging were rare. Pulmonary imaging and gas transfer parameters remained abnormal in a substantial proportion of participants 18 months following moderate to severe COVID-19. Neither cardiac nor pulmonary abnormalities explained the observed reductions in exercise capacity; my work suggests that, together with limiting symptoms, reduced tissue oxygen extraction are likely culprits.

## Introduction

The majority of patients hospitalized with COVID-19 demonstrate lung abnormalities on cross-sectional imaging.[93] Ground-glass opacities (increased attenuation in the lungs with preserved bronchial and vascular markings) are the dominant feature of acute lung injury (ALI) during the initial phase of the infection, with linear lung opacities (reticular interstitial pattern) seen later in the course of the disease.[94] ARDS, the most severe form of ALI, was reported in 42% of patients hospitalised with COVID-19 pneumonia early in the pandemic, with 61-81% requiring admission to intensive care.[95] Pulmonary fibrosis is a recognized outcome of both ALI and ARDS, which can have long-term consequences on respiratory function and life expectancy.[96,97]

Myocardial injury (defined as an acute elevation in cardiac troponin above the upper limit of normal) is often identified in hospitalized patients, increasing in incidence with the severity of illness.[5] Within the context of COVID-19, myocardial injury may be ischaemic (type 1 or type 2) or non-ischaemic (such as myocarditis, right ventricular injury) in nature, which can result in cardiac fibrosis and dysfunction.[98] Previous studies of SARS and MERS have also noted a high burden of ongoing pulmonary complications along with impaired exercise tolerance up to 15 years post-infection.[99]

In light of the potential for cardiorespiratory injury in the acute setting of COVID-19 and in the post-acute phase in parallel diseases like SARS and MERS, I set out to assess the prevalence, extent, and longitudinal trajectory of cardiac and respiratory dysfunction, including exercise capacity, in patients following hospitalization with COVID-19.

## Methods

Laboratory analysis was performed at the John Radcliffe biochemistry laboratory. Cardiac injury was assessed using Troponin I. Heart failure was assessed using NT-proBNP.

### MRI Protocol

As previously described, HASTE MRI was used to assess the lungs for parenchymal abnormalities.

Cine SSFP imaging was performed to assess cardiac mass, volumes and function. Three ShMOLLI T1 and Siemens Myomaps T2 maps (basal, mid and apical slices) were performed to assess the tissue characteristics of the myocardium. Late gadolinium imaging was acquired using a T1-weighted PSIR sequence following a bolus injection of 0.15 mmol/kg of body weight of gadolinium-based contrast agent (Dotarem©) and a 10 ml saline flush, to assess for focal myocardial fibrosis. 12-15 minutes after contrast administration, 3 ShMOLLI maps (basal, mid and apical spices) were acquired to assess for the presence and extent of diffuse myocardial fibrosis.

All cardiac images from the 2-3, 6 and 18 month visits were analysed using CVI42 software (Circle Cardiovascular Imaging Inc., Calgary, Canada).

### MRI image analysis

Axial thoracic HASTE images were qualitatively scored by an expert radiologist as 0 (0%), 1 (1–25%), 2 (26–50%), 3 (51–75%), or 4 (76–100%), depending on the extent of parenchymal involvement.

For each cardiac examination, the first phase of the acquisition was selected as the end-diastolic phase. The end-systolic phase was selected by determining the phase in which the left and right ventricular cavities were at their smallest. Left ventricular (LV) and right

ventricular (RV) epicardial and endocardial borders were contoured manually at end-diastole and end-systole. LV papillary muscles were included in LV end-diastolic and end-systolic volumes. Stroke volume (SV) was calculated as [SV = EDV-ESV], and ejection fraction (EF) calculated as [EF = (SV/EDV)X100].[100] Quality control for T1 and T2 maps involved visual assessment of the raw images and $R^2$ maps (T1 maps only). Slices or myocardial segments which failed quality control were excluded from analysis. Epicardial and endocardial contours were drawn on the base, mid and apical slices, and average slice T1 and T2 values derived. Extra-cellular volume (ECV) for the three slices was calculated from pre- and post- contrast T1 maps and haematocrit (Hct) using the formula: ECV = (Δ[1/T1myocardium]/Δ[1/T1blood]) * [1-Hct]).[101]

Late gadolinium enhancement (LGE) analysis consisted of epicardial and endocardial contours drawn on the PSIR images, with a reference region of interest (ROI) drawn over an area of normal myocardial intensity. Artefactual regions were manually excluded. Pixels with over five standard deviations (SDs) above the mean intensity of the reference ROI were defined as 'hyperenhanced'.[102] The percentage of LGE was calculated as [%LGE = (volume of hyperenhanced pixels/volume of myocardium)X100]. Qualitative LGE enhancement was performed by classifying phase-sensitive inversion recovery (PSIR) images into the following categories: 1) No LGE 2) Myocarditis pattern 3) Myocardial infarction 4) LV/RV insertion point 5) Mixed (infarction and myocarditis) and 6) Other (cardiomyopathy).

### Spirometry, Gas Transfer and Total Lung Capacity assessment

As previously described, spirometry assessments were undertaken using a calibrated spirometer (Metalyzer 3B, Cortex Biophysik, Leipzig,Germany) and precalibrated disposable turbines, according to the criteria established by the American Thoracic Society and European Respiratory Society.[103] Measurements were performed with the

participants seated, and the manoeuvre was demonstrated by the operator. Following proper positioning of the mouthpiece and application of a nose clip, participants were asked to inspire rapidly and fully, expire with maximal force and until empty, and finally inspire maximally until completely full. Following a minimum of three manoeuvres, $FEV_1$ and FVC values were reviewed for repeatability (with the aim of achieving two concordant readings within 0.15L of each other). The manoeuvre was repeated until repeatability was achieved. The largest $FEV_1$ and FVC of the concordant readings and respective $FEV_1$/FVC ratio were reported. Bronchodilators were not used. Predicted values for each participant were determined based on age, height, sex and ethnicity, using Global Lung Function Initiative spirometry reference values.[104]

Carbon monoxide transfer coefficient (Kco) and alveolar volume (Va) were assessed using the Vyntus ONE pulmonary function system (Vyaire Medical, Chicago, United States), with methane as the tracer gas and adjusted for haemoglobin and standard pressure (760 mmHg). DLco was then determined via the equation DLco = Kco x Va. Volume and gas calibration took place prior to each assessment. The single breath method was used according to the 2017 American Thoracic Society and European Respiratory Society criteria.[84] Measurements were performed with the participants seated, and the manoeuvre was demonstrated by the operator. Following proper positioning of a disposable mouthpiece and nose clip, participants were asked to breath normally with a regular depth and rate of breathing. Once a stable functional residual capacity (FRC) level was registered, participants were asked to exhale slowly until empty. Participants were then instructed to perform a rapid inhalation until full and hold their breath for 10 seconds, and to avoid Valsalva or Müller manoeuvres during the breath-hold. Following prompting by the operator, participants exhaled in a smooth, unforced manner, without hesitation or interruption. This procedure was repeated at least twice (with at least 3 minutes between trials), until two results that met quality control were

achieved (inspired volume ≥85% of vital capacity, breath hold ≥10 seconds, sample collection completed within 4 seconds of the start of exhalation, and two $DL_{CO}$ measurements within 0.67 $mmol \cdot min^{-1} \cdot kPa^{-1}$ of each other). Predicted values were calculated with respect to the Global Lung Function Initiative reference values.[105]

Total lung capacity was assessed via the nitrogen washout method,[106] using the Vyntus ONE pulmonary function system (Vyaire Medical, Chicago, United States). Measurements were performed with the participants seated, and the manoeuvre was demonstrated by the operator. Following proper positioning of a disposable mouthpiece and nose clip, participants were asked to breath normally with a regular depth and rate of breathing. Once a stable FRC level was registered, participants were asked to exhale slowly until empty, and then resume normal breathing, at which point 100% oxygen was entrained into the circuit. A trial was deemed complete when the nitrogen concentration was <1.5% on at least three successive exhalations. In the event of a leak during the trial (indicated by an increase in nitrogen concentration during the test), the test was repeated (with a delay of at least 10 minutes from the previous trial). Predicted values were calculated with respect to the Global Lung Function Initiative reference values.[105]

### Lung function analysis

$FEV_1$, FVC, DLco, Kco and Va were reported as % of predicted. A value was classified as reduced if it was <LL of normal for that participant (determined using Global Lung Function Initiative reference values).[104,105]

Lung function physiology was classified into four groups: Normal, Obstructive, Restrictive and Mixed, as per ATS/ERS Task Force guidelines.[107] As total lung capacity was not assessed during the first visit, restriction could not be confirmed with certainty, and therefore “probable restriction” was used instead (**Figure 7**).

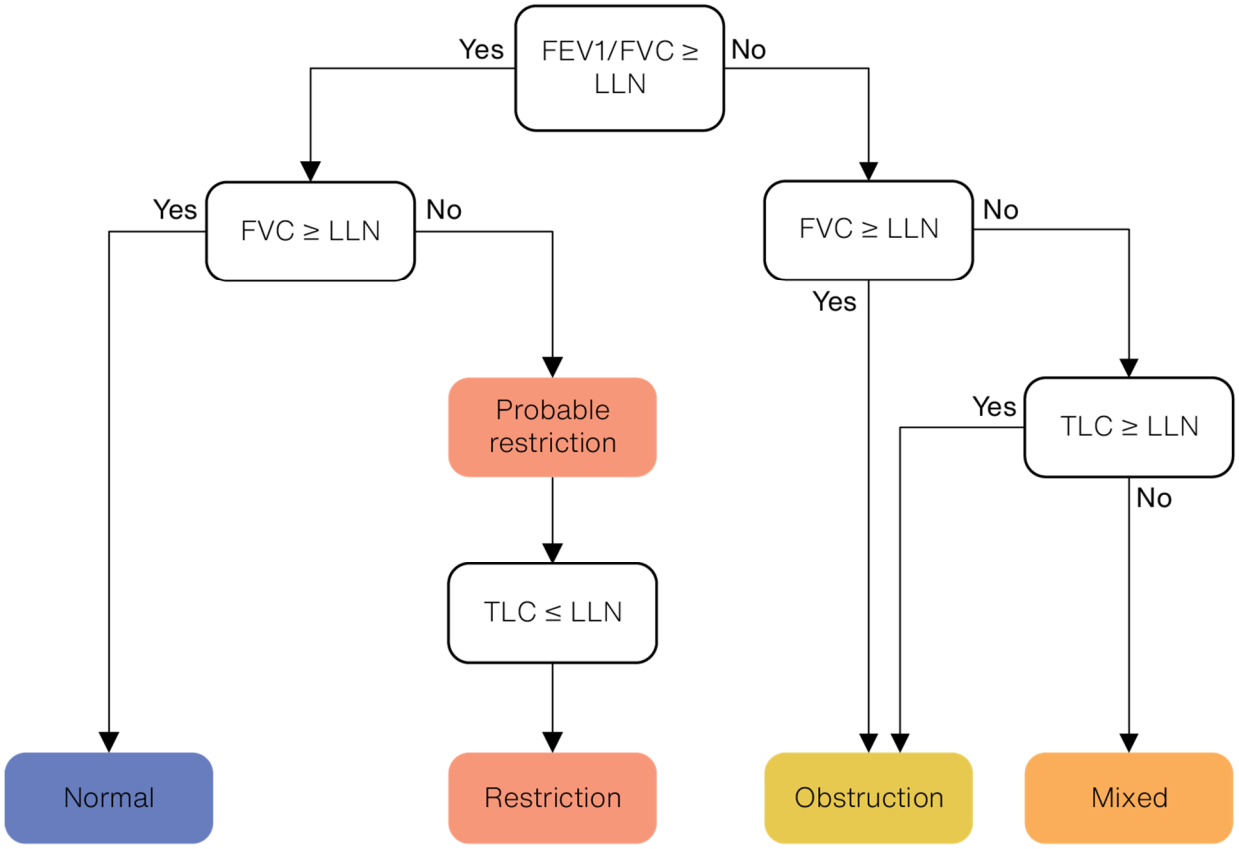


**Figure 7: Flowchart showing the criteria used to classify lung physiology. FEV1 = Forced expired volume in the 1st second. FVC = Forced vital capacity. TLC = Total Lung Capacity. LLN = Lower limit of normal.**

## Cardiopulmonary Exercise Testing

As previously described, CPET was performed using a cycle ergometer according to the latest guidelines.[85,108] The gas analyser was calibrated prior to each test. A facemask made of pliable rubber and incorporating a disposable pre-calibrated gas turbine was fitted to each participant and adjusted to eliminate any leaks. The ergometer saddle height was optimised to provide optimum comfort during the test. As individuals are known to hyperventilate at rest prior to the start of CPET, the test commenced with two minutes of rest followed by two minutes of unloaded cycling.[109] Following this, the work rate was increased to 20 watts (W), followed by a 10W/min ramp. Continuous 12-lead ECG was recorded throughout the test. Oxygen saturation was recorded continuously using a pulse oximeter placed on the right index finger. Blood pressure was measured with a manual sphygmomanometer every 3 to 4 minutes. Criteria for premature test termination included chest pain, blood pressure drop during exercise, severe hypertension (>250/115 mm Hg) and arrhythmia. In the absence of these criteria, participants were encouraged to continue exercise. Following voluntary cessation of exercise, participants performed three minutes of unloaded cycling.

Peak oxygen consumption ($\dot{V}O_2$peak) was predicted using the Wasserman weight algorithm.[110] Reduced oxygen uptake was defined as a value <80% of predicted.[111] Oxygen ($O_2$) pulse (the product of stroke volume and arterial-mixed venous oxygen content difference [$C(a-\tilde{v})O_2$]) was calculated by dividing $\dot{V}O_2$peak by peak heart rate, with <80% of predicted used as the cut-off for reduced values.[111] Maximal test criteria consisted of a respiratory exchange ratio ≥ 1·1 and plateau in oxygen uptake.[112] Maximum heart rate was calculated using the equation 220 – age (in years).[113] Maximal voluntary ventilation (MVV) was calculated by multiplying $FEV_1$ by 40. The anaerobic threshold (AT) was determined using the V-slope method and normalized to peak $\dot{V}O_2$ ($\dot{V}O_2$ at AT/predicted peak $\dot{V}O_2$) x 100). A reduced AT was defined as a value <40% of predicted

$\dot{V}O_2$peak.[114] Input from an expert cardiologist was sought for review of challenging cases. All data points were averaged every 20 seconds.

### Data acquired

Of the 30 controls who attended a study visit, 28 underwent cardiorespiratory imaging (2 had severe claustrophobia precluding imaging) and spirometry testing (2 did not consent to the test). 27 underwent CPET testing (2 did not consent to the test, and 1 was unable to perform CPET due to large body habitus). Controls did not undergo gas transfer and total lung capacity assessment (nor did COVID-19 participants 2-3 months post infection) due to pending approval of an ethics amendment from the research ethics committee.

Of the 58 COVID-19 participants who attended an initial study visit, 53 underwent respiratory imaging (1 had large body habitus precluding imaging, and 4 had limiting claustrophobia). 52 underwent cardiac imaging (a participant requested termination of the MRI following respiratory imaging due to claustrophobia). Spirometry was performed in 56,(2 did not consent to the test), and CPET was performed in 55 (2 did not consent to the test, and 1 had large body habitus precluding CPET).

Of the 46 COVID-19 participants who attended a study visit 6 months following infection, 44 underwent cardiorespiratory imaging (two did not undergo imaging due to claustrophobia). Spirometry, gas transfer and total lung capacity assessment was performed in all. CPET was performed in 42 participants (3 did not consent to the test, 1 had large body habitus precluding CPET).

All 23 participants who attended a visit 18 months post-infection underwent cardiorespiratory imaging, spirometry, gas transfer testing and total lung capacity assessment.

Details for each individual drop-out were provided previously in the methods chapter, Figure 6.

### Statistical Analyses and Definitions

To measure intra-observer variability of left and right ventricular volumes and function, 10 cases were reanalysed after a mean period of 12 months. The coefficient of variability was calculated by the Bland-Altman method (the standard deviation of the difference between the two measurements divided by the mean of the two measures, multiplied by 100).[115]

The upper limits of normal for native T1, native T2 and ECV were defined as control mean + 2 standard deviations. Critical illness was defined as any COVID-19 participant requiring non-invasive ventilation, intubation and ventilation or organ support.

Acute cardiac injury was defined as an acute rise in hypersensitive troponin I above the 99$^{th}$ percentile upper reference limit (>34 ng/L).[116]

Cumulative odds ordinal logistic regression with proportional odds was run to determine the effect of age (continuous), presence of critical illness (binary), and extent of lung involvement on MRI (ordinal), on the change in extent of lung involvement over time (ordinal; 0 = Increased lung involvement, 1 = No change in lung involvement, 2 = Reduced lung involvement). This procedure was repeated twice, with one regression performed to assess the change from 2-3 to 6 months, and another to assess the change from 6 months to 18 months. As only one continuous variable was included in these analyses, the presence of multicollinearity was not assessed. Both models satisfied the assumption of proportional odds, assessed using a full likelihood ratio test comparing the fitted models to models with varying location parameters (2-3 to 6 months: $X^2(6)=3.85$, $P=0.70$; 6 to 18 months: $X^2(5)=8.92$, $P=0.11$).

An analysis of covariance (ANCOVA) was performed to compare mean heart rate recovery following exercise between COVID-19 participants (2-3 months following infection) and controls, after controlling for the increase in heartrate from baseline to maximal exercise. There was a linear relationship between heart rate change and heart rate recovery for each subgroup, as assessed by visual inspection of a scatterplot. There was homogeneity of regression slopes as the interaction term was not statistically significant, $F(1,43)=2.13$, $P=0.15$. Standardized residuals for the subgroups and for the overall model were normally distributed, as assessed by Shapiro-Wilk's test ($P>0.05$). There was homoscedasticity and homogeneity of variances, as assessed by visual inspection of a scatterplot and Levene's test of homogeneity of variance ($P=0.21$), respectively. There were no outliers in the data, as assessed by no cases with standardized residuals greater than ±3 standard deviations.

## Results

### Study Population and demographics

At recruitment, the mean age of COVID-19 participants was 55±13 years and thirty-four (59%) were men (Table 2). Assessments took place at a median interval of 2.3 months (IQR 2.1–2.5), 6.1 months (IQR 6.0 – 6.8), and 18.4 months (IQR 17.2 – 19.1) from disease onset, and 1.5 months (IQR 1.4 – 1.8), 5.5 months (IQR 5.2 – 6.2) and 17.7 months (IQR 16.6 – 18.4) following hospital discharge.

COVID-19 participants and controls were well-matched for gender, co-morbidities and medication use (Table 2). At 18 months, participants were older compared to controls (62 vs 54 years, *P*-value 0.01). There was a higher proportion of COVID-19 participants from black, asian and minority ethnic groups relative to controls. A greater proportion of COVID-19 participants were taking novel oral anticoagulants (NOACs) at 2-3 and 6 months compared to controls.

The median duration of hospitalization was 9 days (IQR 5-17). Twenty (34%) participants required admission to intensive care for management of their acute illness (Table 3). During hospital admission, all participants had a raised CRP (>10 mg/L; median 119.1 mg/L, IQR 75.9 – 185.5 mg/L). Most participants (93%) required some form of supplemental oxygen therapy, with over 1/3$^{rd}$ needing high flow oxygen, non-invasive or invasive ventilation. None required ECMO.

All but one received antibiotic therapy during their admission. Steroids (dexamethasone, prednisolone or hydrocortisone) were administered in 16 (28%) participants.

**Table 2: Demographics and medications of COVID-19 participants and controls.**

| | COVID-19, 2-3m (N=58) | COVID-19, 6m (N=46) | COVID-19, 18m (N=23) | Controls (N=30) | *P*-values | | | |
|---|---|---|---|---|---|---|---|---|
| | | | | | 2-3m vs Controls | 6m vs Controls | 18m vs Controls | 2-3m vs 6m vs 18m |
| Age, years | 55·4 (13·2) | 55·7 (13·3) | 62.3 (10.5) | 53·9 (12·3) | 0·62 | 0·57 | 0.01 | 0.07 |
| Male gender | 34/58 (58·6%) | 29/46 (63·0%) | 15/23 (65.2%) | 18/30 (60·0%) | *0.90* | *0.79* | *0.70* | *0.81* |
| BMI, kg/m$^2$ | 30·8 (26·2 - 36·4) | 30·6 (26·6 - 35·6) | 28.3 (25.5 - 36.3) | 27·3 (23·1 - 35·1) | *0·17* | *0·19* | *0.59* | *0.59* |
| BAME | 13/58 (22·4%) | 10/46 (21·7%) | 3/23 (13.0%) | 1/30 (3·3%) | *0·03* | *0·03* | *0.31* | *0.65* |
| Current/Ex-smoker | 20/58 (34·5%) | 17/46 (37·0%) | 8/23 (34.8%) | 7/30 (23·3%) | *0·28* | *0·21* | *0.36* | *0.96* |
| Diabetes | 9/58 (15.5%) | 8/46 (17.4%) | 3/23 (13.0%) | 3/30 (10·0%) | *0·74* | *0·51* | *1.00* | *0.91* |
| Hypertension | 22/58 (37·9%) | 17/46 (37·0%) | 7/23 (30.4) | 9/30 (30·0%) | *0·46* | *0·53* | *0.97* | *0.81* |
| Coronary artery disease | 2/58 (3·4%) | 1/46 (2·2%) | 1/23 (4.3%) | 0/30 (0·0%) | *0·55* | *1·00* | *0.43* | *1.00* |
| Cerebrovascular Disease | 1/58 (1·7%) | 0/46 (0·0%) | 0/23 (0.0%) | 0/30 (0·0%) | *1·00* | -- | -- | *1.00* |
| Asthma | 20/58 (34·5%) | 17/46 (37·0%) | 8/23 (34.8%) | 6/30 (20·0%) | *0·16* | *0·12* | *0.23* | *0.96* |
| COPD | 3/58 (5·2%) | 2/46 (4·3%) | 0/23 (0.0%) | 0/30 (0·0%) | *0·55* | *0·52* | -- | *0.72* |
| Previous cancer | 2/58 (3.4%) | 2/46 (4.3%) | 1/23 (4.3%) | 3/30 (10/0%) | *0.33* | *0.38* | *0.62* | *1.00* |
| Depression | 3/58 (5.2%) | 3/46 (6.5%) | 0.23 (0.0%) | 1/30 (3.3%) | *1.00* | *1.00* | *1.00* | *0.72* |
| Medications | | | | | | | | |
| ACE inhibitor | 12/58 (20.7%) | 8/46 (17.4%) | 3/23 (13.0%) | 6/30 (20.0%) | *1.00* | *0.77* | *0.72* | *0.79* |
| Beta blocker | 6/58 (10.3%) | 4/46 (8.7%) | 2/23 (4.3%) | 2/30 (6.7%) | *0.71* | *1.00* | *1.00* | *1.00* |
| Calcium channel blocker | 11/58 (19.0%) | 8/46 (17.4%) | 5/23 (21.7%) | 4/30 (13.3%) | *0.57* | *0.75* | *0.48* | *0.91* |
| Diuretic | 4/58 (6.9%) | 3/46 (6.5%) | 1/23 (4.3%) | 2/30 (6.7%) | *1.00* | *1.00* | *1.00* | *1.00* |
| Statin | 12/58 (20.7%) | 9/46 (19.6%) | 4/23 (17.4%) | 5/30 (16.7%) | *0.78* | *0.78* | *1.00* | *1.00* |
| NOAC | 9/58 (15.5%) | 7/46 (15.2%) | 2/23 (13.0%) | 0/30 (0.0%) | *0.025* | *0.038* | *0.08* | *1.00* |
| Warfarin | 1/58 (1.7%) | 1/46 (2.2%) | 0/23 (0.0%) | 0/30 (0.0%) | *1.00* | *1.00* | -- | *1.00* |
| Metformin | 5/58 (8.6%) | 5/46 (10.9%) | 2/23 (8.7%) | 2/30 (6.7%) | *1.00* | *0.70* | *1.00* | *0.92* |
| Gliclazide | 2/58 (3.4%) | 2/46 (4.3%) | 0/23 (0.0%) | 0/30 (0.0%) | *0.55* | *0.52* | -- | *0.83* |
| Antidepressant | 10/58 (17.2%) | 8/46 (17.4%) | 4/23 (17.4%) | 3/30 (10.0%) | *0.53* | *0.51* | *0.45* | *1.00* |
| Salbutamol inhaler | 7/58 (12.1%) | 5/46 (10.9%) | 3/23 (13.0%) | 2/30 (6.7%) | *0.71* | *0.70* | *0.64* | *1.00* |
| Steroid inhaler | 11/58 (19.0%) | 9/46 (19.6%) | 5/23 (21.7%) | 2/30 (6.7%) | *0.20* | *0.18* | *0.22* | *0.96* |

Data are mean (SD) for parametric data, median (IQR) for non-parametric data and n/N (%), where N is the total number of participants with available data. Italicised P-values are from non-parametric tests. COPD – Chronic obstructive pulmonary disease. ACE – Angiotensin converting enzyme. ARB – Angiotensin 2 receptor blocker. NOAC – Novel oral anticoagulant.

| Table 3: Admission details of COVID-19 participants. | | | | |
|---|---|---|---|---|
| | COVID-19, 2-3m | COVID-19, 6m | COVID-19, 18m | *P*-value |
| Median length of stay, days | 8.5 (5.0 - 17.0) | 9.0 (5.0 - 17.5) | 10.0 (5.0 - 19.0) | *0.86* |
| **Treatment** | | | | |
| Antibiotics | 57/58 (98·3%) | 45/46 (97·8%) | 23/23 (100.0%) | *1.00* |
| Antivirals | 4/58 (6·9%) | 2/46 (4·3%) | 1/23 (4.3%) | *0.88* |
| Steroids | 16/58 (27·6%) | 14/46 (30·4%) | 9/23 (39.1%) | *0.63* |
| **WHO Disease Severity Scale** | | | | *0.99* |
| 3 (No oxygen therapy) | 4/58 (6.9%) | 3/46 (6.5%) | 1/23 (4.3%) | |
| 4 (Conventional oxygen) | 27/58 (46.6%) | 20/46 (43.5%) | 8/23 (34.8%) | |
| 5 (NIV or High Flow) | 15/58 (25.9%) | 12/46 (26.1%) | 8/23 (34.8%) | |
| 6 (Invasive Ventilation) | 7/58 (12.1%) | 6/46 (13.0%) | 3/23 (13.0%) | |
| 7 (Organ support) | 5/58 (8.6%) | 5/46 (10.9%) | 3/23 (13.0%) | |
| Required ICU admission | 21/58 (36·2%) | 17/46 (37·0%) | 12/23 (52%) | *0.42* |
| Inotropic support | 4/58 (6·9%) | 4/46 (8·7%) | 2/23 (8.7%) | *0.92* |
| Renal replacement therapy | 2/58 (3·4%) | 2/46 (4·3%) | 2/23 (8.7%) | *0.48* |
| **Acute organ injury** | | | | |
| Acute liver injury | 18/58 (31·0%) | 18/46 (39·1%) | 9/23 (39.1%) | *0.65* |
| Acute kidney injury | 6/58 (10·3%) | 6/46 (13·0%) | 4/23 (17.4%) | *0.64* |
| Acute cardiac injury | 3/38 (7.9%) | 0/29 (0.0%) | 0/13 (0.0%) | *0.30* |
| Pulmonary embolism | 7/58 (12·1%) | 6/46 (13·0%) | 2/23 (8.7%) | *0.94* |

Data are median (IQR) and n/N (%), where N is the total number of participants with available data. Italicised *P*-values are from non-parametric tests. WHO: World Health Organisation. NIV: Non-Invasive Ventilation. ICU: Intensive Care Unit. Acute liver injury defined as blood levels of alanine aminotransferase (ALT) or aspartate aminotransferase (AST) above 3x the upper reference limit (>135 IU/L or >126 IU/L, respectively), alkaline phosphatase or gamma-glutamyltransferase above 2x the upper reference limit (>260 IU/L or >80 IU/L, respectively). Acute kidney injury defined as an increase in serum creatinine of at least 26 umol/L within 48 hours, or 1·5 to 2-fold increase from baseline. Acute cardiac injury defined as an acute rise in hypersensitive troponin I above the 99th percentile upper reference limit (>34 ng/L).

### Blood markers of cardiac health

During admission, troponin I levels were assessed in 38 participants (66%), with three (5%) having acute elevations fulfilling the criteria of acute cardiac injury. One (troponin I 384 ng/L) was secondary to a pulmonary embolism associated with right heart strain on echocardiography. Another (troponin I 315 ng/L) was diagnosed (using in-patient cardiac MRI) with an acute myocardial infarction of the inferior wall and proceeded to undergo percutaneous intervention of his lateral circumflex artery. The third participant's elevated troponin I level (43 ng/L) was deemed to be secondary to sepsis. On serial assessment, none of the participants had elevations in Troponin I.

NT-proBNP was assessed in 4 participants (7%) during admission, with 2 (3%) being above the cut-off of 125 ng/L.[117] One (708.5 ng/L) was attributed to invasive ventilation in the absence of overt fluid overload. The other (1027.7 ng/L) was attributed to COVID-19 pneumonia in the presence of normal biventricular size and function on bedside echocardiography. On serial assessment, one participant had persistently elevated NT-proBNP levels (1848 ng/L at 2-3 months and 1814 ng/L at 6 months), who was known to have a previous diagnosis of heart failure with preserved ejection fraction.

On longitudinal assessment, there were no differences in mean Troponin-I and NT-proBNP levels between COVID-19 participants and controls.

### Electrocardiography

At 2-3 months following infection, ECG analysis revealed atrial fibrillation in one participant, with all other study participants (including controls) demonstrating sinus rhythm. The prevalence of bundle branch block, ST-segment elevation/depression and T wave inversion did not differ between COVID-19 participants (at all time points) and controls ($P$>0·05 for all variables).

## Serial Cardiac Imaging

Coefficients of variability for left and right ventricular volumes and function were comparable to previously published values from other studies:[115]

- Indexed left ventricular end diastolic volume (LVEDVi) – 3.6% (published range 2.1 – 5.6%)
- Indexed left ventricular end systolic volume (LVESVi) – 7.5% (published range 5.8 – 10.1%)
- Left ventricular ejection fraction (LVEF) – 4.6% (published range 0.01 – 5.2%)
- Indexed right ventricular end diastolic volume (RVEDVi) – 6.1% (published range 3.0 – 9.0%)
- Indexed right ventricular end systolic volume (RVESVi) – 8.9% (published range 3.9 – 9.0%)
- Right ventricular ejection fraction (RVEF) – 7.7% (published range 0.08 – 10%)

At 2-3 months, left and right ventricular volumes, mass, and function were not different between COVID-19 participants and controls (Table 4). None of the participants had impaired left or right systolic function (LVEF: Male - <47%, Female: <50%; RVEF: Male: <40%; Female: <45%).[118] Mean slice-averaged basal and mid-ventricular native T1 were statistically significantly elevated in COVID-19 participants (1180 vs 1149ms, $P<0.001$ and 1173 vs 1150ms, $P=0.004$, respectively) compared to controls (Figure 8). Basal myocardial T1 was elevated in 26% (13/50) of COVID-19 participants. Mid myocardial T1 was elevated in 8% (4/51), and average of base and mid myocardial T1 in 24% (12/50) of COVID-19 participants. Overall, 15 (30%) COVID-19 participants had an elevation in basal, mid or apical T1. Native T2, a marker of oedema, was not different between COVID-19 participants and controls. Extracellular volume fraction was comparable between both cohorts. LGE was mildly increased in COVID-19

participants (0.8 vs 0.6%, *P*=0.023). In COVID-19 participants, both basal and mid myocardial T1 correlated moderately with CRP (median 2.0 mg/L, IQR 0.9 – 5.0 mg/L) (Figure 9). Of note, COVID-19 participants had higher CRP levels compared to controls (median 1.2 mg/L, IQR 0.7 – 2.6 mg/L), which approached statistical significance (*P*=0.058).

At 6 and 18-months post COVID-19, left ventricular volumes, mass and function remained comparable to controls (Tables 5 and 6). Small changes in right ventricular volumes and ejection fraction were well within the range of intraobserver variability. None developed systolic left or right cardiac dysfunction. By 6 months, myocardial native T1 decreased and was no longer different from control T1. T2 and ECV values remained comparable to controls throughout follow-up. COVID-19 participants continued to have mildly increased LGE compared to controls.

Participants with severe illness (defined as a requirement for invasive or non-invasive ventilation, and/or organ support during their admission) had lower right ventricular ejection fractions than other COVID-19 participants at all time points (2-3m: 53.5 vs 60.4%, *P*=0.03, 6m: 58 vs 62%, *P*=0.07, 18m: 55 vs 58%, *P*=0.03). No differences in LV function, native T1, native T2 or ECV were observed.

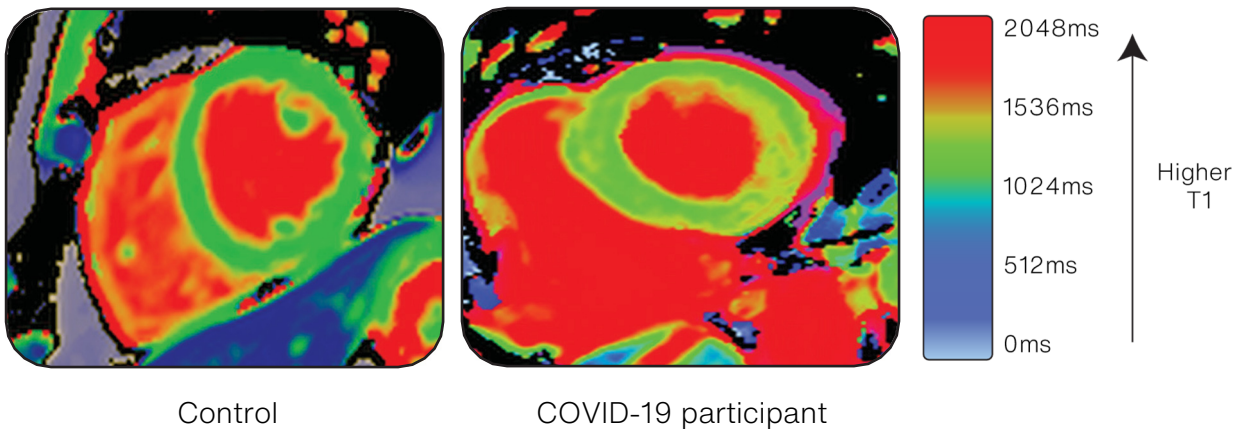


**Figure 8: Basal short axis myocardial native T1 maps from a control (left) and a COVID-19 participant 2-3 months following moderate to severe COVID-19 (right). Note the areas of red within the patient's myocardium, indicative of high native $T_1$ values (reflective of inflammation).**

| Table 4: Cardiac imaging findings in COVID-19 participants 2-3 months post infection and controls. | | | |
|---|---|---|---|
| | COVID-19, 2-3m (N=52) | Controls (N=28) | *P*-value |
| Left ventricular cine analysis | | | |
| End-diastolic volume, mls | 143·8 (127·3 - 165·9) | 153·3 (124·5 - 178·5) | *0·59* |
| End-diastolic volume (indexed), mls/m$^2$ | 73·3 (64·5 - 83·5) | 75·6 (63·4 - 87·5) | *0·51* |
| End-systolic volume, mls | 53·1 (41·5 - 71·7) | 53·1 (47·7 - 70·3) | *0·81* |
| Mass (diastole), g | 116·1 (100·1 - 135·1) | 107·3 (84·3 - 138·3) | *0·39* |
| Mass (indexed), g/m$^2$ | 58·9 (49·8 - 66·2) | 53·8 (48·6 - 63·6) | *0·21* |
| Stroke volume, mls | 89·6 (79·5 - 104·7) | 95·0 (78·4 - 116·5) | 0.54 |
| Ejection fraction, % | 63·0 (7·7) | 63·6 (6·32) | 0·70 |
| Right ventricular cine analysis | | | |
| End-diastolic volume, mls | 164·4 (36·6) | 169·3 (46·5) | 0·61 |
| End-diastolic volume (indexed), mls/m$^2$ | 81·8 (14·0) | 84·3 (18·5) | 0·51 |
| End-systolic volume, mls | 70·4 (23·6) | 72·7 (24·2) | 0·69 |
| Mass, g | 28·8 (25·8 - 35·5) | 33·2 (23·7 - 41·8) | *0·26* |
| Mass (indexed), g/m$^2$ | 14·4 (12·6 - 17·2) | 16·7 (13·9 - 19·3) | *0·19* |
| Stroke volume, mls | 94·0 (19·3) | 96·6 (25·6) | 0·61 |
| Ejection fraction, % | 57·9 (7·8) | 57·6 (6·0) | 0·85 |
| T1 and T2 map analysis | | | |
| Native T1 (basal myocardium), ms | 1179·7 (34·4) | 1149·3 (24) | <0.001 |
| >1197 ms | 13/50 (26·0%) | 1/28 (3·6%) | *0·015* |
| Native T1 (mid myocardium), ms | 1173·1 (33·6) | 1150·2 (32·4) | 0·004 |
| >1215 ms | 4/51 (7·8%) | 0/28 (0%) | *0·29* |
| Native T1 (apical myocardium), ms | 1177·4 (44·7) | 1168·3 (53·2) | 0·42 |
| >1275 ms | 1/50 (2·0%) | 1/28 (3·6%) | *1·00* |
| ECV (basal myocardium), % | 30.1 (2.6) | 28.9 (2.8) | 0·12 |
| >34.52% | 1/35 (2·9%) | 0/21 (0·0%) | *1·00* |
| ECV (mid myocardium), % | 30·1 (27·2 - 31·4) | 29·4 (27·1 - 30·7) | *0·41* |
| >35.87% | 0/37 (0·0%) | 1/23 (4·3%) | *0·38* |
| ECV (apical myocardium), % | 28·7 (27·0 - 31·6) | 29·7 (27·2 - 31·5) | *0·51* |
| >37.87% | 1/40 (2·5%) | 1/23 (4·3%) | *1·00* |
| T2 (basal myocardium), ms | 41·7 (2·2) | 41·6 (2·2) | 0·80 |
| >46 ms | 3/50 (6·0%) | 1/28 (3·6%) | *1·00* |
| T2 (mid myocardium), ms | 41·8 (2·2) | 41·1 (2·3) | 0·21 |
| >46 ms | 1/50 (2·0%) | 1/28 (3·6%) | *1·00* |
| T2 (apical myocardium), ms | 42.9 (41.1 - 45.2) | 42.7 (41.0 - 44.9) | *0·81* |
| >51ms | 1/50 (2·0%) | 1/28 (3·6%) | *1·00* |
| Late gadolinium enhancement analysis | | | |
| % LGE volume enhancement | 0·8 (0·5 - 1·9) | 0·6 (0·3 - 1) | *0·023* |
| Myocarditis pattern | 6/52 (11·5%) | 2/28 (7·1%) | |
| Myocardial infarction | 1/52 (1·9%) | 0/28 (0·0%) | |
| LV/RV insertion point | 7/52 (13·5%) | 1/28 (3·6%) | |
| Mixed | 0/52 (0·0%) | 0/28 (0·0%) | |
| Other | 0/52 (0·0%) | 0/28 (0·0%) | |
| Pericardial effusion >10mm | 1/52 (1·9%) | 0/28 (0·0%) | |

Data are mean (SD), median (IQR) and n/N (%), where N is the total number of participants with available data. Italicised *P*-values are from non-parametric tests. ECV = Extracellular volume. LGE = Late Gadolinium enhancement.

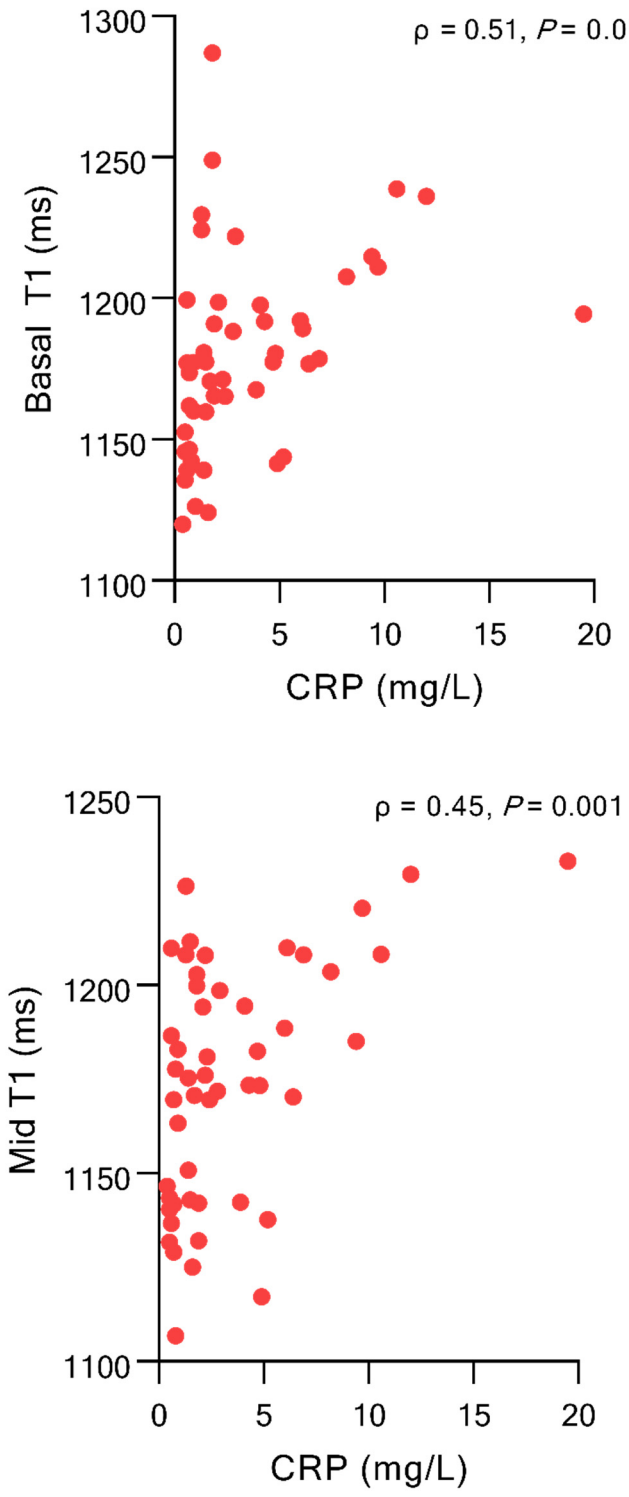


**Figure 9: Scatter plots showing the relationship between basal and mid T1 with CRP in COVID-19 participants.** ρ = Spearman's rho.

Table 5: Paired cardiac imaging findings in COVID-19 participants 2-3 and 6 months post-infection and controls.

| | COVID-19, 2-3m (N=44) | COVID-19, 6m (N=44) | Controls | *P*-values | |
|---|---|---|---|---|---|
| | | | | 2-3m vs 6m | 6m vs Controls |
| Left ventricular cine analysis | | | | | |
| End-diastolic volume, mls | 146.3 (127.5 - 173.6) | 151·1 (125·0 - 183·4) | 153·3 (124·5 - 178·5) | *0·21* | 0·78 |
| End-diastolic volume (indexed), mls/m$^2$ | 73.6 (66.6 - 86) | 76·7 (66·4 - 86·6) | 75·6 (63·4 - 87·5) | *0·59* | 0·90 |
| End-systolic volume, mls | 55.2 (43.5 - 72.8) | 54·6 (44·3 - 71·0) | 53·1 (47·7 - 70·3) | *0·31* | *0·90* |
| Mass (diastole), g | 117.6 (101.2 - 136.4) | 119·5 (98·8 - 134·0) | 107·3 (84·3 - 138·3) | *0·25* | 0·25 |
| Mass (indexed), g/m$^2$ | 59.6 (49.7 - 66.9) | 57·0 (50·2 - 65·2) | 53·8 (48·6 - 63·6) | *0·15* | *0·37* |
| Stroke volume, mls | 91.0 (76.4 - 80.7) | 96.7 (21.9) | 96.7 (24.9) | 0·06 | 1·00 |
| Ejection fraction, % | 61.9 (7.6) | 62·7 (6·8) | 63·6 (6·32) | 0·27 | 0·58 |
| Right ventricular cine analysis | | | | | |
| End-diastolic volume, mls | 167.3 (38.7) | 160.0 (40.4) | 169·3 (46·5) | 0·023 | 0·38 |
| End-diastolic volume (indexed), mls/m$^2$ | 83.1 (14.8) | 78·8 (15·8) | 84·3 (18·5) | 0·005 | 0·18 |
| End-systolic volume, mls | 73.1 (23.8) | 65.0 (23.1) | 72·7 (24·2) | <0.001 | 0·19 |
| Mass, g | 31.2 (26.2 - 37.9) | 32·6 (28·8 - 39·8) | 33·2 (23·7 - 41·8) | *0·13* | *0·88* |
| Mass (indexed), g/m$^2$ | 14.6 (13.6 - 18.9) | 16·4 (14·4 - 19·1) | 16·7 (13·9 - 19·3) | *0·31* | *0·90* |
| Stroke volume, mls | 94.2 (20.3) | 95.0 (20.9) | 96·6 (25·6) | 0·68 | 0·78 |
| Ejection fraction, % | 57.0 (7.1) | 60.2 (6.3) | 57·6 (6·0) | <0.001 | 0·085 |
| T1 and T2 map analysis | | | | | |
| Native T1 (basal myocardium), ms | 1178.4 (31.1) | 1151.6 (38.3) | 1149·3 (24) | <0.001 | 0·65 |
| >1197 ms | 11/40 (27.5%) | 3/40 (7.5%) | 1/28 (3·6%) | *0·065* | *0·64* |
| Native T1 (mid myocardium), ms | 1172.6 (34.1) | 1144.9 (42) | 1150·2 (32·4) | <0.001 | 0·62 |
| >1215 ms | 4/41 (9.8%) | 1/41 (2.4%) | 0/28 (0%) | *0·38* | *1·00* |
| Native T1 (apical myocardium), ms | 1175.2 (41.2) | 1152.8 (46.8) | 1168·3 (53·2) | 0·001 | 0·22 |
| >1275 ms | 0/41 (0.0%) | 1/41 (2·3%) | 1/28 (3·6%) | *1·00* | *1·00* |
| ECV (basal myocardium), % | 30.5 (28.4 - 31.2) | 27·9 (25·5 - 30·2) | 28·3 (26·8 - 31·5) | *0·001* | *0·19* |
| >34.52% | 0/23 (0.0%) | 1/23 (4.3%) | 0/21 (0·0%) | *1·00* | *0·53* |
| ECV (mid myocardium), % | 30.1 (26.9 - 31.3) | 27.7 (26.3 - 29.9) | 29·4 (27·1 - 30·7) | *0·03* | 0·35 |
| >35.87% | 0/31 (0.0%) | 0/31 (0·0%) | 1/23 (4·3%) | -- | *0·35* |
| ECV (apical myocardium), % | 29.3 (3.4) | 28.6 (2.8) | 29·7 (27·2 - 31·5) | 0·32 | *0·24* |
| >37.87% | 0/27 (0.0%) | 0/27 (0·0%) | 1/23 (4·3%) | *1·00* | *0·39* |
| T2 (basal myocardium), ms | 41.7 (1.9) | 41.5 (2.1) | 41·6 (2·2) | 0·71 | 0·80 |
| >46 ms | 0/40 (0.0%) | 1/40 (2·5%) | 1/28 (3·6%) | *1·00* | *1·00* |
| T2 (mid myocardium), ms | 41.7 (2) | 41.5 (1.8) | 41·1 (2·3) | 0·50 | 0·53 |
| >46 ms | 1/40 (2.5%) | 1/40 (2·5%) | 1/28 (3·6%) | *1·00* | *1·00* |
| T2 (apical myocardium), ms | 42.3 (41.0 - 45.0) | 42.9 (41.1 - 45.0) | 43.3 (40.8 - 46.6) | *0·51* | 0·33 |
| >51ms | 1/40 (2.5%) | 0/40 (0·0%) | 1/28 (3·6%) | *1·00* | *0·39* |
| Late gadolinium enhancement analysis | | | | | |
| % LGE volume enhancement | 0.8 (0.5 - 2.1) | 0·7 (0·1 - 2·2) | 0·6 (0·3 - 1) | *0·91* | 0·62 |
| Myocarditis pattern | 4/40 (10.0%) | 4/40 (10.0%) | 2/28 (7·1%) | | |
| Myocardial infarction | 0/40 (0·0%) | 0/40 (0·0%) | 0/28 (0·0%) | | |
| LV/RV insertion point | 5/40 (12.5%) | 5/40 (12.5%) | 1/28 (3·6%) | | |
| Mixed | 0/40 (0·0%) | 0/40 (0·0%) | 0/28 (0·0%) | | |
| Other | 0/40 (0·0%) | 0/40 (0·0%) | 0/28 (0·0%) | | |
| Pericardial effusion >10mm | 0/40 (0·0%) | 0/40 (0·0%) | 0/28 (0·0%) | | |

Data are mean (SD), median (IQR) and n/N (%), where N is the total number of participants with available data. Italicised *P*-values are from non-parametric tests. ECV = Extracellular volume. LGE = Late Gadolinium enhancement.

Table 6: Paired cardiac imaging findings in COVID-19 participants 6 and 18 months post-infection and controls.

| | COVID-19, 6m (N=23) | COVID-19, 18m (N=23) | Controls (N=28) | *P*-values | |
|---|---|---|---|---|---|
| | | | | 6m vs 18m | 18m vs Controls |
| Left ventricular cine analysis | | | | | |
| End-diastolic volume, mls | 150.6 (136.7 - 176.8) | 156.4 (138.1 - 184.3) | 153·3 (124·5 - 178·5) | 0.005 | 0.65 |
| End-diastolic volume (indexed), mls/m$^2$ | 77.4 (67.8 - 85.6) | 76.2 (68.5 - 91.1) | 75·6 (63·4 - 87·5) | 0.01 | 0.53 |
| End-systolic volume, mls | 59.1 (47.1 - 70.5) | 56.8 (51.2 - 72.5) | 53·1 (47·7 - 70·3) | 0.09 | 0.25 |
| Mass (diastole), g | 123.4 (106 - 135.2) | 123.6 (111.8 - 136) | 107·3 (84·3 - 138·3) | 0.98 | 0.26 |
| Mass (indexed), g/m$^2$ | 60.8 (54.3 - 65.9) | 60.1 (52.3 - 65.4) | 53·8 (48·6 - 63·6) | 0.70 | 0.10 |
| Stroke volume, mls | 93.3 (21) | 95.3 (20.9) | 96.7 (24.9) | 0.10 | 0.83 |
| Ejection fraction, % | 61 (5.4) | 60.7 (4.7) | 63·6 (6·32) | 0.62 | 0.07 |
| Right ventricular cine analysis | | | | | |
| End-diastolic volume, mls | 156.1 (36.8) | 154.9 (35.3) | 169·3 (46·5) | 0.29 | 0.23 |
| End-diastolic volume (indexed), mls/m$^2$ | 77.6 (14.2) | 77.3 (14.1) | 84·3 (18·5) | 0.66 | 0.14 |
| End-systolic volume, mls | 64.2 (19.1) | 67.7 (16.9) | 72·7 (24·2) | *0.03* | 0.41 |
| Mass, g | 32.2 (27.1 - 36.5) | 32.2 (27.6 - 36.3) | 33·2 (23·7 - 41·8) | 0.87 | *0.41* |
| Mass (indexed), g/m$^2$ | 15.7 (14.0 - 17.3) | 15.8 (13.9 - 17.8) | 16·7 (13·9 - 19·3) | 0.94 | *0.43* |
| Stroke volume, mls | 91.9 (20.2) | 87.1 (20.2) | 96·6 (25·6) | 0.001 | 0.16 |
| Ejection fraction, % | 59.4 (4.9) | 56.4 (3.8) | 57·6 (6·0) | 0.001 | 0.42 |
| T1 and T2 map analysis | | | | | |
| Native T1 (basal myocardium), ms | 1149.4 (29.3) | 1147.1 (31.2) | 1149·3 (24) | 0.67 | 0.78 |
| >1197 ms | 1/23 (4.3%) | 1/23 (4.3%) | 1/28 (3·6%) | *1.00* | *1.00* |
| Native T1 (mid myocardium), ms | 1145.8 (35.7) | 1147.4 (36.3) | 1150·2 (32·4) | 0.80 | 0.78 |
| >1215 ms | 0/23 (0.0%) | 1/23 (4.3%) | 0/28 (0%) | *1.00* | *0.45* |
| Native T1 (apical myocardium), ms | 1151.4 (49.3) | 1158.4 (54) | 1168·3 (53·2) | 0.44 | 0.51 |
| >1275 ms | 1/23 (4.3%) | 0/23 (0.0%) | 1/28 (3·6%) | *1.00* | *1.00* |
| ECV (basal myocardium), % | 27.0 (25.3 - 30.3) | 28.2 (24.1 - 29.8) | 28·3 (26·8 - 31·5) | *0.80* | 0.11 |
| >34.52% | 1/19 (5.3%) | 0/19 (0.0%) | 0/21 (0·0%) | *1.00* | -- |
| ECV (mid myocardium), % | 27.8 (25.6 - 32.0) | 27.7 (24.3 - 29.6) | 29·4 (27·1 - 30·7) | 0.07 | 0.08 |
| >35.87% | 0/23 (0.0%) | 0/23 (0.0%) | 1/23 (4·3%) | -- | *1.00* |
| ECV (apical myocardium), % | 28.8 (26.6 - 30.6) | 29.6 (25.4 - 31.8) | 29·7 (27·2 - 31·5) | 0.84 | *0.49* |
| >37.87% | 0/19 (0.0%) | 0/19 (0.0%) | 1/23 (4·3%) | -- | *1.00* |
| T2 (basal myocardium), ms | 41.3 (2) | 40.9 (2.2) | 41·6 (2·2) | 0.35 | 0.26 |
| >46 ms | 1/23 (4.3%) | 0/23 (0.0%) | 1/28 (3·6%) | *1.00* | *1.00* |
| T2 (mid myocardium), ms | 41.4 (1.6) | 41.6 (1.9) | 41·1 (2·3) | 0.71 | 0.41 |
| >46 ms | 0/22 (0.0%) | 0/22 (0.0%) | 1/28 (3·6%) | *1.00* | *1.00* |
| T2 (apical myocardium), ms | 43.3 (41.6 - 44.9) | 41.8 (40.5 - 44.6) | 43.3 (40.8 - 46.6) | 0.34 | 0.16 |
| >51ms | 0/23 (0.0%) | 0/23 (0.0%) | 1/28 (3·6%) | -- | *1.00* |
| Late gadolinium enhancement analysis | | | | | |
| % LGE volume enhancement | 1.9 (0.3 - 2.3) | 1.3 (0.7 - 2.4) | 0·6 (0·3 - 1) | *0.44* | *0.007* |
| Myocarditis pattern | 4/23 (17.4%) | 4/23 (17.4%) | 2/28 (7·1%) | | |
| Myocardial infarction | 0/23 (0.0%) | 0/23 (0.0%) | 0/28 (0·0%) | | |
| LV/RV insertion point | 2/23 (8.7%) | 2/23 (8.7%) | 1/28 (3·6%) | | |
| Mixed | 0/23 (0.0%) | 0/23 (0.0%) | 0/28 (0·0%) | | |
| Other | 0/23 (0.0%) | 0/23 (0.0%) | 0/28 (0·0%) | | |
| Pericardial effusion >10mm | 0/23 (0.0%) | 0/23 (0.0%) | 0/28 (0·0%) | | |

Data are mean (SD), median (IQR) and n/N (%), where N is the total number of participants with available data. Italicised *P*-values are from non-parametric tests. ECV = Extracellular volume. LGE = Late Gadolinium enhancement.

## Respiratory Imaging

2-3 months following infection, 60% of COVID-19 participants had pulmonary parenchymal hyperintensities on MRI, compared to 3/28 (11%) in controls ($P$<0.001, Figure 10). 23% had >75% involvement of their lung parenchyma. Parenchymal hyperintensities were more frequent in COVID-19 participants with critical illness compared to those without (90% vs 44%, $P$=0.001).

By 6 months, although the proportion of COVID-19 participants with lung parenchymal abnormalities remained high (69%), there was a significant improvement in the extent of lung involvement ($P$=0.005), with none having hyperintensities involving more than 75% of their lung parenchyma. 20/43 (46.5%) had a reduced volume of lung involvement compared to the initial assessment. Only 9 COVID-19 participants (20.9%) demonstrated an increased burden in pulmonary hyperintensities.

At 18 months, there was a significant change in the extent of lung parenchymal abnormalities ($P$=0.027). While 16/23 (70%) COVID-19 participants continued to exhibit pulmonary hyperintensities on MRI imaging, 7/23 (30.4%) had a reduced burden of lung involvement compared to the second assessment, 13 (56.5%) had comparable findings, and 3 (13%) had an increased burden of hyperintensities. COVID-19 participants continued to have a higher burden of pulmonary abnormalities compared to controls ($P$<0.0001), even when considering only those without critical illness during their admission ($P$<0.001 for all time points vs controls).

A higher burden of parenchymal abnormalities was associated with an increase in the odds (i.e. likelihood) of improvement in lung hyperintensities from 2-3 to 6 months post-infection (odds ratio 6.5, $P$<0.0001). No relationship was seen with age (Odds ratio 0.96, $P$=0.09) and the presence of critical illness (Odds ratio 0.70, $P$=0.69). Similar findings were seen from 6 to 18 months, although the association between the

burden of parenchymal abnormalities and improvement over time did not reach statistical significance (Odds ratio 3.86, *P*=0.058).

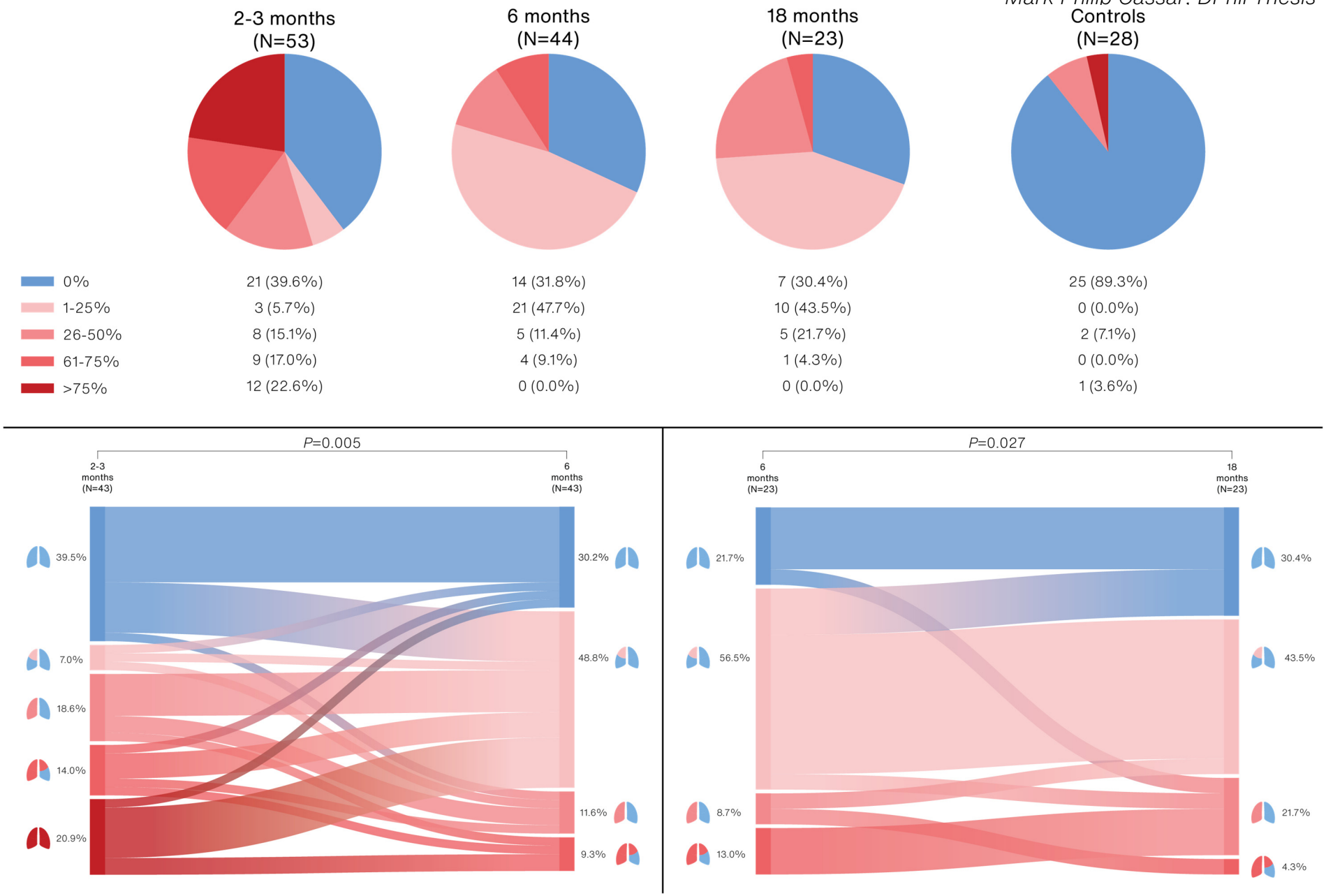


**Figure 10: Pie charts showing the extent of MRI parenchymal abnormalities in COVID-19 participants and controls, together with Alluvial diagrams showing longitudinal changes in COVID-19 participant parenchymal abnormalities from 2-3 to 6 months and 6 months to 18 months.**

### Respiratory Function Assessment

At 2-3 months post-infection, COVID-19 participants had lower $FEV_1$ and FVC and a slightly higher $FEV_1$/FVC compared to controls (Table 7). Most COVID-19 participants (84%) had normal lung function on spirometry (Figure 12). 3 (5%) had an obstructive pattern, 5 (9%) had a probable restrictive pattern and 1 (2%) had a mixed obstructive/restrictive pattern of lung function impairment.

At 6 months, $FEV_1$ was no longer different from controls ($P$=0·10), whereas FVC remained slightly lower ($P$=0·024, Figure 11). The $FEV_1$/FVC ratio became comparable to controls ($P$=0.24). By 18 months, $FEV_1$, FVC and $FEV_1$/FVC continued to approach control values, and all became comparable to controls.

Over time, a trend of improvement in COVID-19 participants with a restrictive lung physiology was observed (with 4 COVID-19 participants with a restrictive pattern at 2-3 months having normal lung function by 6 months, Figure 12). Obstructive lung physiology appeared to persist over time and developed in 2/46 (4.3%) at 6 months and 1/23 (4.3%) at 18 months, although 4/6 (66.7%) with obstructive physiology across all time points had a past medical history of asthma or COPD.

Reduced gas transfer (DLco <LL of normal) was seen in 17/46 COVID-19 participants (37%) at 6 months and 6/23 (26%) at 18 months ($P$=1.0, Table 8). Between 6 and 18 months, some COVID-19 participants with impaired gas transfer improved, while others with normal gas transfer developed mild impairment (Figure 12). At 6 and 18-months post-infection, COVID-19 participants with parenchymal hyperintensities on MR imaging had lower DLco compared to those without (6 months: DLco (% predicted) 77% vs 91%, $P$-value 0.009; 18 months: DLco (% predicted) 77% vs 93%, $P$=0.02). Of note, a history of lung disease preceding COVID-19 did not influence DLco amongst COVID-19 participants (at 6 months: DLco (preceding lung

disease) 83% vs 80% in those without, *P*=0.48; at 18 months: DLco (preceding lung disease) 84% vs 81% in those without, *P*=0.61).

Reduced Va with normal Kco was the most common pattern of gas transfer impairment seen at 6 and 18 months (Figure 13). Of the 17 COVID-19 participants with impaired gas transfer at 6 months, 13 had reduced Va, 1 had reductions in both Va and Kco, and 1 had a reduced Kco with normal Va. Of the 6 COVID-19 participants with reduced gas transfer at 18 months, 3 had reduced Va, 2 had reduced Va and Kco, and 1 had reduced Kco with a normal Va.

| Table 7: Spirometry findings in COVID-19 participants at 2-3 months and controls. | | | |
|---|---|---|---|
| | COVID-19, 2-3m | Controls | *P*-value |
| Spirometry | | | |
| $FEV_1$, % predicted | 101·4 (19·7) | 118·7 (22·1) | <0.001 |
| <LLN | 4/56 (7.1%) | 1/28 (3·6%) | *0.46* |
| FVC, % predicted | 108·3 (22·8) | 131·4 (21·8) | <0.001 |
| <LLN | 6/56 (10.7%) | 0/28 (0·0%) | *0.08* |
| $FEV_1$/FVC | 0·77 (0·73 - 0·80) | 0·75 (0·70 - 0·78) | *0·027* |
| <LLN | 4/56 (7.1%) | 2/28 (7.1%) | *0.66* |
| Data are mean (SD), median (IQR) and n/N (%), where N is the total number of participants with available data. Italicised *P*-values are from non-parametric tests. LLN = Lower limit of normal. | | | |

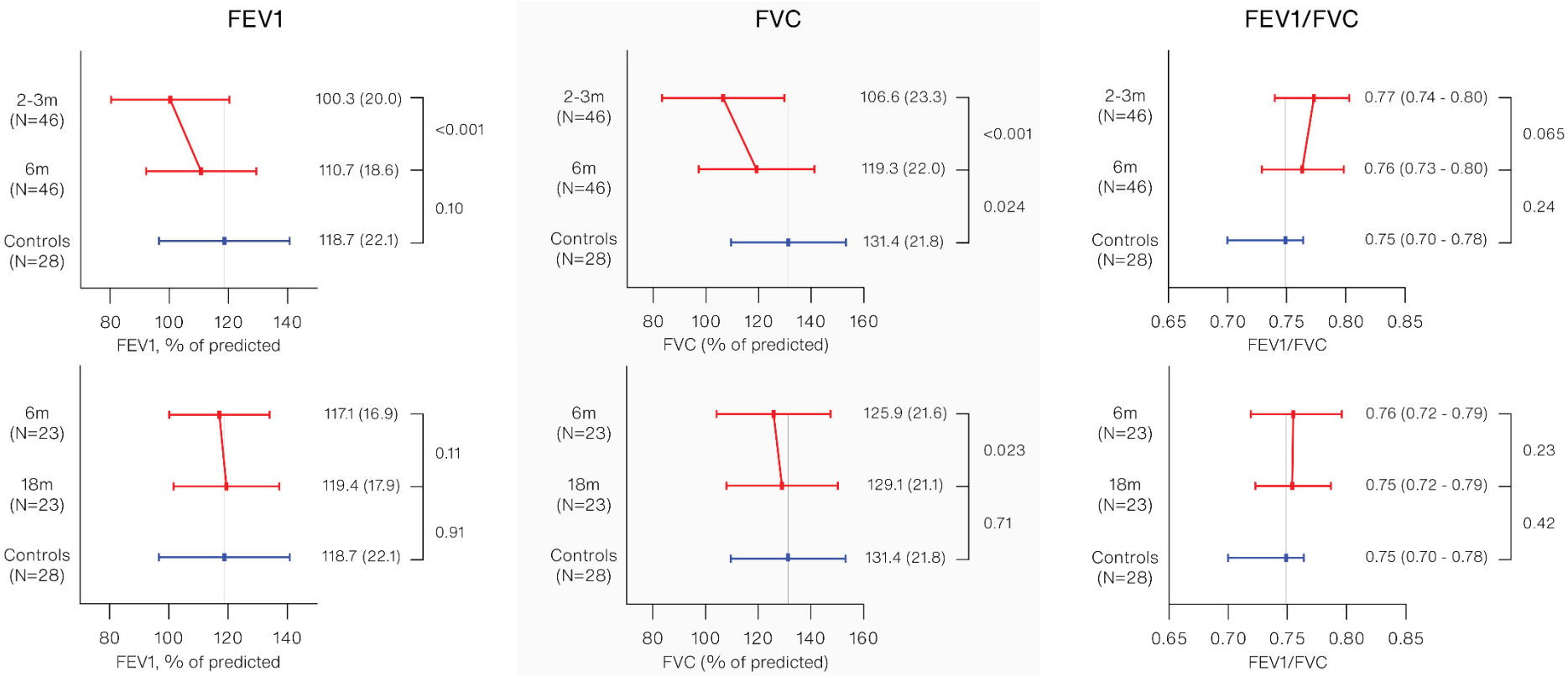


**Figure 11: Serial pulmonary function tests in patients from 2-3 to 6 months (first row), and 6 to 18 months (second row), compared with control data. Only paired data is visualised. Red bars depict COVID-19 participant data, while blue bars depict control data. Bars depict either mean +/- SD or median and IQR. Descriptor values (mean[SD] or median[IQR]) are provided next to each bar. Significance brackets are provided together with their corresponding *P* values, with the first signifying comparison between COVID-19 participants at different time points, and the 2nd representing comparison between COVID-19 participants and controls.**

| Table 8: Gas transfer findings in COVID-19 participants at 6- and 18-months post-infection. The second column depicts 6-month participant data who attended a visit at 18 months (i.e. paired data). | | | | |
|---|---|---|---|---|
| | COVID-19, 6m (N=46) | COVID-19, 6m (N=23) | COVID-19, 18m (N=23) | *P*-value |
| Gas Transfer | | | | |
| DLCO, % of predicted | 79.1 (68.3 - 88.5) | 79.2 (76.0 - 84.3) | 80.3 (72.7 - 84.5) | *0.99* |
| <LLN | 17/46 (37.0%) | 5/23 (21.7%) | 6/23 (26.1%) | *1.00* |
| $K_{CO}$, % of predicted | 100.9 (91.1 - 111) | 101.8 (89.8 - 108.9) | 102.6 (88.2 - 106.2) | *0.13* |
| <LLN | 6/46 (13·0%) | 4/23 (17.4%) | 3/23 (13.0%) | *1.00* |
| $V_a$, % of predicted | 76.8 (70.9 - 89.8) | 82.7 (73.9 - 92.9) | 78.5 (74 - 90.8) | *0.66* |
| <LLN | 24/46 (52·2%) | 9/23 (39.1%) | 12/23 (52.2%) | *0.25* |
| Data are mean (SD), median (IQR) and n/N (%), where N is the total number of participants with available data. Italicised *P*-values are from paired non-parametric tests. LLN = Lower limit of normal. | | | | |

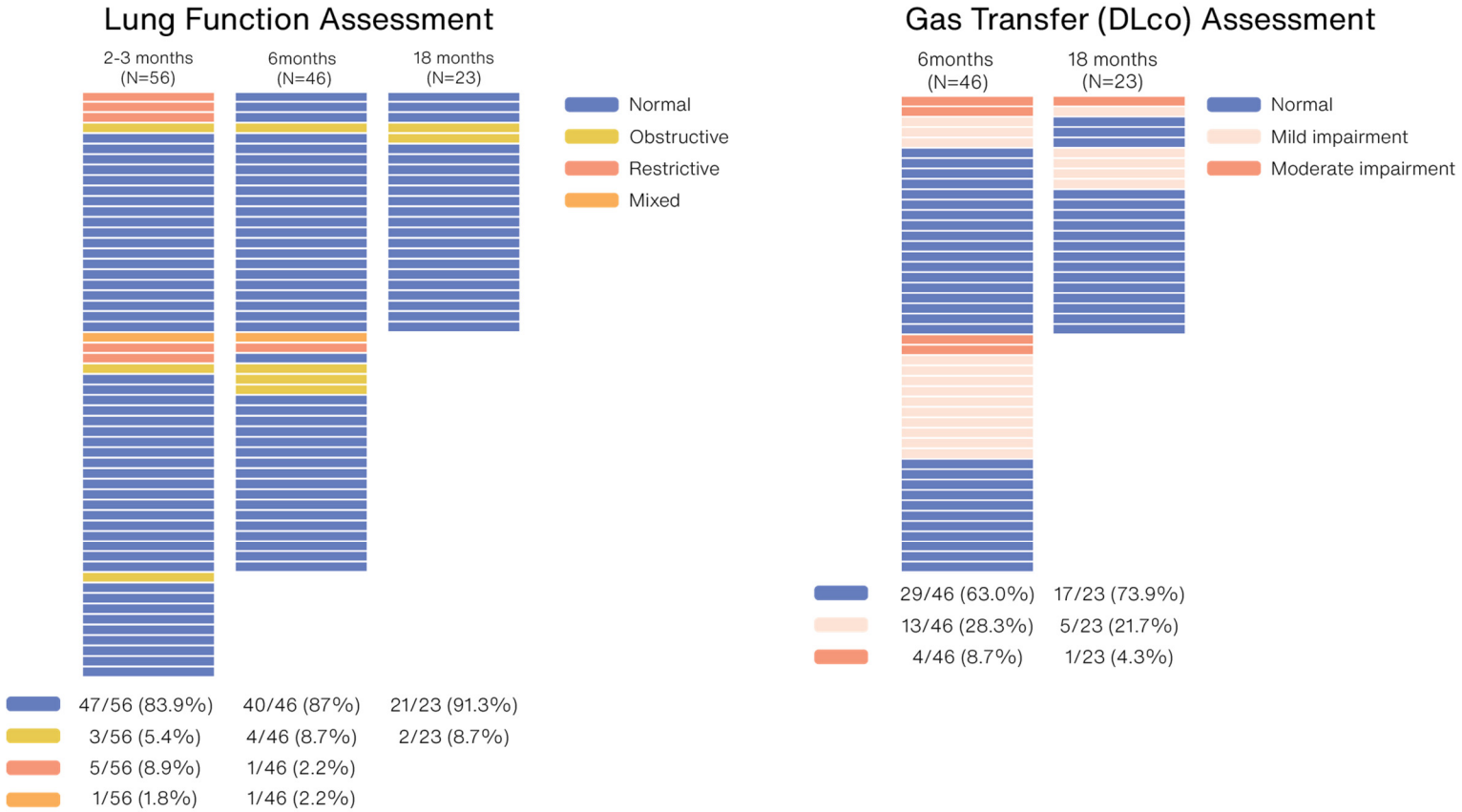


**Figure 12: Heat maps showing lung function and gas transfer status in COVID-19 participants over time. Each row represents one participant.**

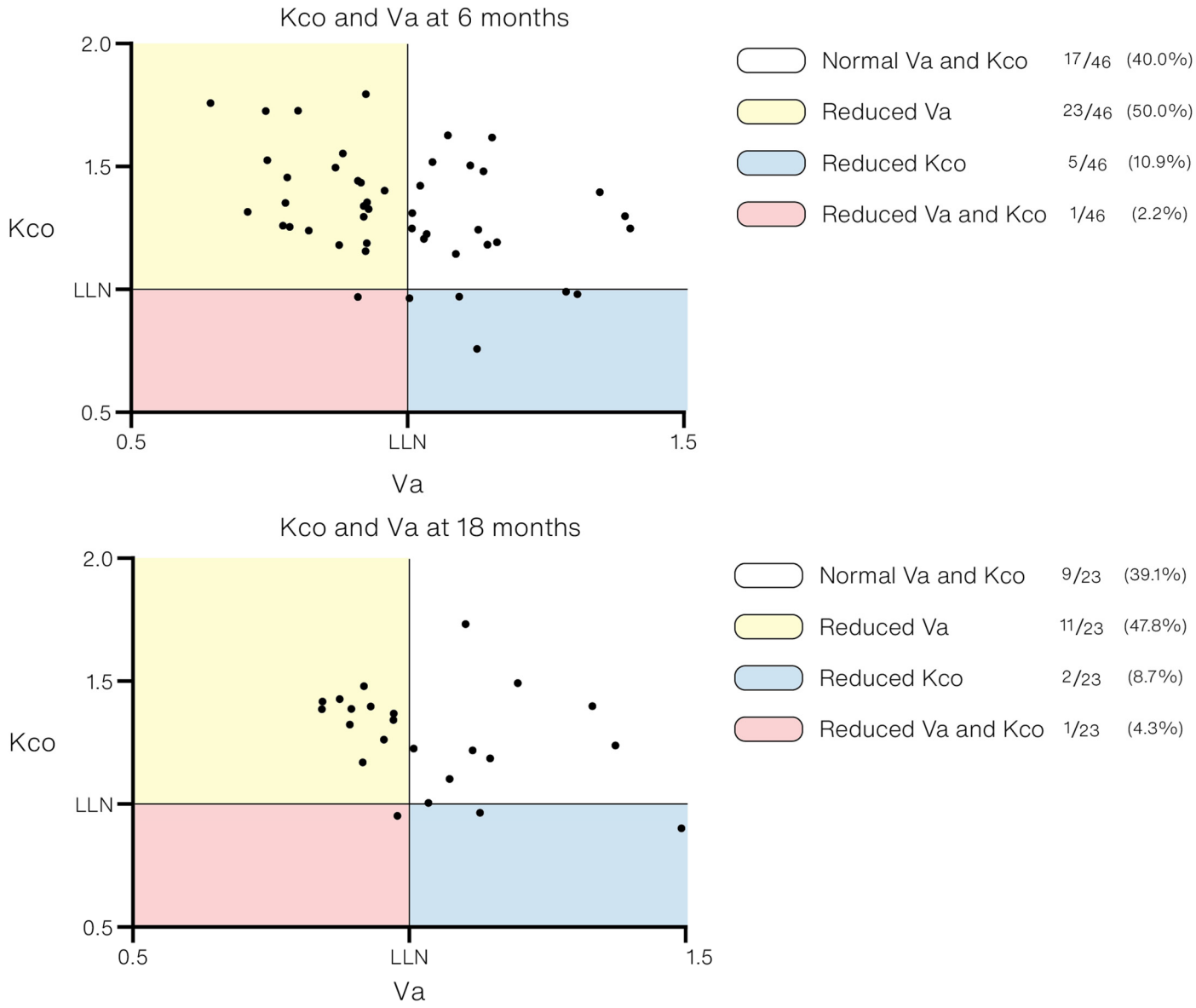


**Figure 13: Scatter plots showing Kco and Va values normalised to the predicted lower limit of normal (LLN) for each COVID-19 participant, at 6 and 18 months. Participants within yellow portions = Reduced Va. Participants within blue portion = Reduced Kco. Participants within red portion = Reduced Va and reduced Kco. Kco = Carbon monoxide transfer coefficient. Va = Alveolar volume. LLN = Lower limit of normal.**

## Cardiopulmonary Exercise Testing

At 2-3 months post-infection, COVID-19 participants had lower mean oxygen uptake at peak exercise compared to controls ($\dot{V}O_2$peak, 80.5% vs 112.7% of predicted, *P*<0.001), with 28/51 COVID-19 participants (55%) having an abnormally low $\dot{V}O_2$peak (<80% predicted, **Table 9**). The first ventilatory threshold, a ventilatory surrogate for anaerobic threshold (AT), occurred earlier in COVID-19 participants. Reductions in haemoglobin (seen in 7/51 (13.7%)) were mild in severity (median 115 g/L, range 102 – 129 g/L), as were NT-proBNP measures above the upper limit of normal (observed in 9/51 (17.6%), median 145 ng/L, range 126 – 195 ng/L). No signs of myocardial ischaemia (ST segment deviations) were seen during exercise, and none of the participants developed chest pain.

Peak $O_2$ pulse, a surrogate marker of stroke volume, arterial oxygen content and tissue oxygen extraction, was lower in COVID-19 participants (91.4% vs 103.3% of max predicted, *P*=0.006).

The ventilatory equivalent for carbon dioxide ($\dot{V}E/\dot{V}CO_2$) slope, a marker of ventilatory efficiency and ventilation/perfusion matching,[119] was steeper (lower lung efficiency) in COVID-19 participants (33.4, vs 28.2 in controls (*P*<0.001)). COVID-19 participants with MRI lung abnormalities had steeper slopes compared to those without (37.7 vs 32.0, *P*=0.011). DLco (% predicted) was inversely correlated with $\dot{V}E/\dot{V}CO_2$ slope (r=-0.373, *P*=0.046). Despite reduced ventilatory efficiency, respiratory limitation in COVID-19 participants was rare, with only 3/51 (5.9%) having a breathing reserve of <20% at peak exercise.

24/46 COVID-19 participants (49%) performed a submaximal test (cessation of exercise without cardiorespiratory limitation), compared to 4 (15%) controls (*P*=0.003); 10 terminated exercise due to fatigue, 5 due to breathlessness and 9 due

to muscle ache. One test was stopped at the operator's discretion (hypertensive response). Of the four controls with a submaximal test, three terminated exercise due to fatigue, while one stopped due to muscle ache.

When assessing oxygen uptake in maximal tests only ($\dot{V}O_2$max), this remained reduced compared to controls (95.5% vs 112.3% of predicted, *P*=0.016). Of the 5/26 (19.2%) COVID-19 participants with a reduced $\dot{V}O_2$max, 1 had a reduced breathing reserve suggestive of respiratory limitation, and 3 had a reduction in AT and $O_2$ pulse. Only 1 had a reduced haemoglobin (male; 118g/L). None had elevations in NT-proBNP.

End-tidal partial pressure of $CO_2$ ($ETCO_2$), reflective of $CO_2$ concentration in ventilated alveoli, was reduced at all stages of exercise (baseline, at AT, peak exercise and during recovery) between COVID-19 participants and controls. The temporal change of $ETCO_2$ during exercise was similar in COVID-19 participants and controls (Figure 14A), and not suggestive of acute or chronic hyperventilation.[120]

Heart rate recovery in the first minute following cessation of exercise was slower in COVID-19 participants (16.6 vs 21.9 beats, *P*=0.018). However, when adjusted for the heart rate increase during exercise (difference between heart rate at peak exercise and heart rate at baseline), no statistically significant difference was found (adjusted means of heart rate recovery: COVID-19: 18.5bpm. Controls: 19.6bpm. *P*=0.60).

At 6 months post-infection, $\dot{V}O_2$peak improved but was still reduced relative to controls (Table 9). As previously observed, reductions in Hb (median 11 g/L, range 114 – 122 g/L) and elevations in NT-proBNP (median 175 ng/L, range 153 – 301 ng/L) were mild. Despite improvement in the AT, occurring later during exercise, it remained different from controls (42% of predicted $\dot{V}O_2$max vs 47% of predicted $\dot{V}O_2$max, *P*=0·041). $O_2$ pulse improved and became comparable to controls (95% of predicted vs 103% of predicted, *P*=0·13). The $\dot{V}E/\dot{V}CO_2$ slope improved by 6 months (*P*=0·033)

but remained high compared to controls (*P*=0·002). Respiratory limitation was rare, seen in only 2/41 COVID-19 participants (4.8%).

The prevalence of submaximal tests reduced to 26% (*P*=0·37 for comparison with controls). In those with a maximal test, $\dot{V}O_2$max was no longer different from controls (*P*=0·12).

Of the 13/41 COVID-19 participants (31.7%) with reduced $\dot{V}O_2$peak, 6 months post-infection, 7/13 (53.8%) terminated exercise in the absence of any cardiorespiratory limitation (submaximal tests) due to fatigue, breathlessness and lower back/lower limb pain. Of the 6/13 COVID-19 participants (46.2%) with impaired exercise tolerance and a maximal test, despite reduced $O_2$ pulse seen in five COVID-19 participants and four having an early AT, none had significant anaemia, elevated NT-proBNP or reduced breathing reserve at peak exercise (Figure 14B).

The severity of illness during admission was not associated with peak or maximal oxygen consumption at 2-3 months and 6 months (*P*>0·20 for all comparisons).

Table 9: Relevant haematological and CPET findings in COVID-19 participants and controls.

| | COVID-19, 2-3m (N=51) | COVID-19 2-3m (N=41) | COVID-19 6m (N=41) | Controls (N=27) | *P*-values | | |
|---|---|---|---|---|---|---|---|
| | | | | | 2-3m vs Controls | 6m vs Controls | 2-3m vs 6m |
| **Relevant haematological parameters** | | | | | | | |
| Haemoglobin, g/L | 135.4 (13.7) | 137.1 (13.7) | 141.2 (14.7) | 141.5 (12.7) | 0.06 | 0.98 | 0.003 |
| <120 (females)/<130 (males) | 7/51 (13.7%) | 5/41 (12.2%) | 5/41 (12.2%) | 1/27 (3.7%) | *0.25* | *0.39* | *1.00* |
| NT-proBNP, ng/L | 55.7 (31.9 - 108.9) | 56.5 (32.3 - 113.6) | 45.0 (30.0 - 96.8) | 45.3 (22.5 - 77.5) | *0.36* | *0.53* | *0.30* |
| ≥125 | 9/51 (17.6%) | 8/41 (19.5%) | 7/41 (17.1%) | 1/27 (3.7%) | *0.15* | *0.13* | *1.00* |
| **CPET (all tests)** | | | | | | | |
| Maximal tests performed | 26/51 (51·0%) | 22/41 (53.7%) | 30/41 (73·2%) | 23/27 (85·2%) | *0·003* | *0·37* | *0·067** |
| $\dot{V}O_2$peak, % of predicted | 80·5 (23·1) | 80.9 (24.5) | 93·3 (29·7) | 112·7 (27·0) | <0·001 | 0·007 | <0·001 |
| < 80% | 28/51 (54·9%) | 22/41 (53.7%) | 13/41 (31·7%) | 2/27(7·4%) | *<0·001* | *0·034* | *0·012* |
| Anaerobic threshold (% of predicted $\dot{V}O_2$max) | 40·7 (36·2 - 47·5) | 40.3 (35.4 - 46.5) | 42·0 (39·0 - 51·7) | 46·8 (43·3 - 51·3) | *<0·001* | *0·041* | *0·030** |
| <40% | 20/48 (41·7%) | 17/38 (44.7%) | 14/39 (35·9%) | 0/27 (0·0%) | *<0·001* | *<0.001* | *0·43** |
| Oxygen pulse, % of predicted | 81·1 (66.7 - 90.0) | 80.2 (66.7 - 89.2) | 88.8 (75.0 - 102.9) | 101.0 (88.8 - 114.6) | <0·001 | *0·020* | *0·003* |
| Breathing reserve, % of predicted $\dot{V}E$max | 44·8 (15·3) | 43.2 (15.5) | 42·4 (15·7) | 40·7 (11·0) | 0·22 | 0·62 | 0·71 |
| <20% | 3/51 (5·9%) | 3/41 (7.3%) | 2/41 (4·8%) | 1/27 (3·7%) | *1·00* | *1·00* | *1·00* |
| $\dot{V}E/\dot{V}CO_2$ Slope | 33·4 (29·2 - 40·3) | 33.4 (28.9 - 39.4) | 31·3 (28·6 - 34·5) | 28·2 (26·7 - 30·0) | *<0·001* | *0·002* | *0·033* |
| Baseline End tidal $CO_2$ tension, mm Hg | 30.4 (4.1) | 30.1 (4.12) | 30.3 (4.5) | 32.2 (2.7) | 0.043 | 0.03 | 0.88 |
| End tidal $CO_2$ tension at AT, mm Hg | 35.0 (3.7) | 34.9 (3.7) | 36.7 (3.7) | 38.4 (3.8) | <0.001 | 0.04 | <0.001 |
| **CPET (maximal tests only)** | | | | | | | |
| $\dot{V}O_2$max, % of predicted | 95·5 (19·9) | 95.8 (21.2) | 100·6 (27·6) | 112·3 (27·0) | 0·016 | 0·12 | 0·49* |
| <80% | 5/26 (19·2%) | 4/22 (18.2%) | 6/30 (20.0%) | 1/23 (4·3%) | *0·13*[a] | *0·22*[a] | *1.00** |
| Breathing reserve, % of predicted $\dot{V}E$max | 34·9 (12·1) | 32.5 (11.1) | 38.0 (12.8) | 38·9 (9·9) | 0·21 | 0·80 | 0·79* |
| Oxygen pulse, % of predicted | 89.1 (82.2 - 102.8) | 87.4 (78,4 - 102.8) | 89.6 (77.71 - 107.5) | 103·3 (20·9) | 0·039 | 0·13[c] | 0·45* |
| <80% | 6/26 (23.1%) | 6/22 (27.3%) | 8/30 (26.7%) | 2/23 (8.7%) | *0.17* | *0.16* | *1.00** |
| HR recovery slope, bpm | 16·6 (7·1) | 16.4 (7.1) | 21.4 (13.2) | 21·9 (7·5) | 0·018 | 0·67[c] | 0.10* |
| End tidal $CO_2$ tension at peak exercise, mm Hg | 31.2 (4.0) | 31.1 (3.9) | 31.9 (3.9) | 33.8 (3.6) | 0.007[+] | 0.11 | 0.46* |
| End tidal $CO_2$ tension during recovery, mm Hg | 30.0 (4.2) | 29.8 (4.1) | 30.7 (3.6) | 32.5 (4.0) | 0.043 | 0.15 | 0.40* |

Data are mean (SD), median (IQR) and n/N (%), where N is the total number of participants with available data. Italicised P-values are from non-parametric tests. * are unpaired tests when comparing longitudinal COVID-19 participant data. $\dot{V}O_2$ = oxygen consumption. $\dot{V}E/\dot{V}CO_2$ = Ventilatory equivalent for carbon dioxide. AT = Anaerobic threshold.

A

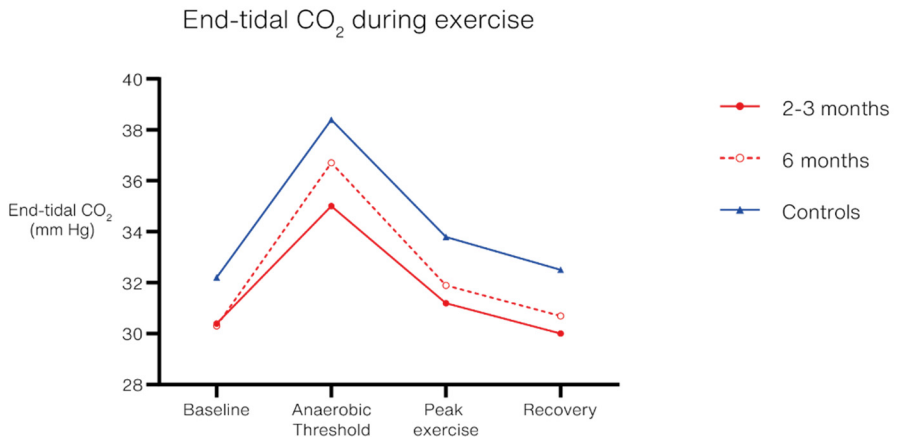


B

| 13 (31%) patients at 6 months had reduced $\dot{V}O_2$peak | |
|---|---|
| Seven submaximal tests | Six maximal tests |
| Early AT: 4 | Early AT, Reduced $O_2$ pulse: 4<br>Normal AT, Reduced $O_2$ pulse: 1 |
| Normal Hb levels, NT-proBNP, LV/RV function. Preserved breathing reserve | |

**Figure 14. A: The temporal change of $ETCO_2$ (mmHg) during exercise in COVID-19 participants and controls. B: Characteristics of COVID-19 participants with a reduced $\dot{V}O_2$peak 6 months following COVID-19.**

## Discussion

The main findings of the present study are as follows:

1) 2-3 months post-infection, a significant proportion of COVID-19 participants had elevations in myocardial native T1 which normalized by 6 months.
2) While spirometric measures normalized on serial assessment, a significant proportion of COVID-19 participants continued to exhibit gas transfer impairment.
3) Although exercise capacity improved by 6 months post-infection, a substantial proportion had reductions in exercise capacity secondary to symptomatic limitation and/or early occurrence of anaerobic respiration.

Throughout the pandemic, several studies have embraced the power of CMR imaging to assess the impact of COVID-19 on the heart. In one of the first published reports, Puntmann and colleagues described a surprisingly high prevalence (60%) of active myocardial inflammation (defined as elevations in native T1 and T2) in patients predominantly treated at home, at a median of 71 days following COVID-19 diagnosis.[121] In contrast, Starekova and colleagues reported a far lower prevalence of active myocarditis (1.4%) among 145 student athletes 15 days following diagnosis.[122] In a report focusing on patients with severe COVID-19 associated with elevations in troponin I (a significantly ill cohort at the highest risk of cardiac injury), CMR performed at a median of 6 weeks following diagnosis revealed active myocarditis in 8%.[123] Separate to the large variation in prevalence estimates (which may be due to differences in cohort characteristics, variations in methodologies used and differences in the timing of CMR imaging relative to COVID-19 diagnosis), one must also question the paradoxically higher rates of myocarditis reported on MR imaging compared to histological-confirmed cases on autopsy, which are below 2%.[48] It is important to recognize that myocarditis is rarely diagnosed with MR imaging alone. Typically,

patients present with symptoms such as chest pain, fever, and shortness of breath, often accompanied by elevated troponin I levels and ECG abnormalities.[124] Although MR imaging offers a valuable perspective on cardiac involvement in diseases, its findings must be interpreted carefully, especially outside established clinical contexts where its diagnostic validity has been confirmed. The reported abnormalities in native myocardial T1, T2, and late gadolinium enhancement observed on MRI imaging, in light of the low incidence of myocarditis in deceased COVID-19 patients, likely represent non-myocarditis oedema or alterations in the extracellular matrix rather than myocarditis with myocyte necrosis. In the present study, COVID-19 participants had higher native T1 values compared to controls, with 30% having values above the UL of normal, with these findings resolving by 6 months. Of note, none had evidence of active myocarditis according to the Modified Lake Louise Criteria,[125] in keeping with the rare incidence of myocarditis documented at post-mortem.[48] The observed isolated elevations in native myocardial T1 suggest that these early tissue abnormalities are likely due to dynamic alterations in the extracellular environment (hyperaemia[126] or changes in extracellular proteins/matrix) influenced by circulating cytokines that have also demonstrated temporal changes (improvement) in inflammatory cytokines (IL-1, IL-2, IL-6, IL-18, TNF, IFNL1) in COVID-19 patients on serial assessments.[127,128]

Separate to reports of myocarditis, impaired left and right systolic function has also been described (using CMR as well as other imaging modalities, such as echocardiography), albeit at a lower prevalence (ranging from 3 to 18%).[123,129,130] Of note, such studies recruited patients with significant comorbidities (such as heart failure and ischaemic heart disease) predating COVID-19 diagnosis, making the inference of causal associations tenuous. In the present study, only COVID-19 participants with mild or no co-morbidities were recruited, together with a matched

control group. The absence of significant left or right systolic impairment is in keeping with the low prevalence (7%) of cardiac dysfunction (defined by levels of NT-BNP) reported by a large UK-wide prospective follow-up study of post-hospitalised COVID-19 patients by Evans and colleagues.[131]

Multi-faceted lung function assessment together with pulmonary imaging provided important mechanistic insights into persistent lung injury following infection with COVID-19. The initial restrictive patterns observed on spirometry, 2-3 months following infection, resolved with time. Abnormalities in DLco at 6 months were common, and little change was seen 18 months post-infection. These findings have been echoed by Wu and colleagues; in a longitudinal assessment of respiratory outcomes in patients previously hospitalised with COVID-19, the most common abnormality observed was a reduction in gas transfer (DLco), with the authors postulating that this may be secondary to interstitial abnormalities or pulmonary vascular abnormalities.[132] In the present study, impaired diffusion capacity (assessed using DLco, the product of Kco, the carbon monoxide transfer coefficient, and Va, the alveolar volume) was most often secondary to reductions in alveolar volume with preservation of Kco, a phenomenon described by others shortly after discharge (1 month) and in patients 6 – 12 months following infection.[133,134] While this pattern of gas transfer derangement could be explained by discrete loss of alveolar subunits with the remaining alveoli being unaffected,[135] the interpretation is not always straight-forward; as alveolar volume decreases, lung capillaries become less distended resulting in an increase in capillary filling, and hence, an increase in Kco (in the absence of alveolar membrane defects).[136] Prediction formulae do not adjust Kco for alveolar volume (while equations to carry out this adjustment exist, they have not undergone rigorous clinical validation), inevitably resulting in overestimation of Kco in such cases.[137] In fact, some authors argue that a normal Kco in the presence of a reduced alveolar volume should

raise suspicions of concomitant impairment of gas exchange secondary to alveolar membrane abnormalities (as Kco should be supranormal in the absence of alveolar membrane pathology).[137] Hyperpolarized $^{129}Xe$ MRI, a relatively new technique to assess lung function, overcomes these limitations by obtaining measurements directly form the alveoli, alveolar-capillary membrane and red blood cells.[138] Using this technique, Grist and colleagues found that patients (both hospitalised and those managed in the community), 5 – 9 months following infection, had impaired gas transport across the alveolar membrane (reduced Xe red blood cell:Xe plasma ratio) in the presence of normal ventilation, compared to healthy volunteers.[139] These findings suggest that, separate to loss of alveolar sub-units, damage to the alveolar epithelium (without frank fibrosis) and/or a reduction in pulmonary capillary blood volume (secondary to the previously described alveolar capillary thrombosis seen in post-mortem studies) may also play a role in the underlying pathophysiology of impaired lung function post-COVID-19.

Comprehensive cardiopulmonary exercise testing revealed steeper $\dot{V}E/\dot{V}CO_2$ slopes and lower $ETCO_2$ throughout exercise in COVID-19 participants when compared with controls. While hyperventilation could explain these findings, one would expect static $ETCO_2$ throughout exercise (in chronic hyperventilation) or sudden drops in $ETCO_2$ during periods of acute hyperventilation (resulting in an erratic pattern of $ETCO_2$ over time).[120,140,141] In contrast, COVID-19 participants had normal $ETCO_2$ kinetics, with $ETCO_2$ peaking at the anaerobic threshold and decrementing thereafter. A more plausible explanation is ventilation perfusion (V/Q) mismatch, with increased physiological dead space (resulting in dilution of alveolar gas with ambient air) accounting for the mildly reduced $ETCO_2$ partial pressures observed in COVID-19 participants.[142] This is further supported by the fact that $VE/VCO_2$ slope (a marker of

V/Q mismatch) correlated with MRI lung abnormalities and inversely correlated with DLco.

Reduced exercise capacity was observed in over half of COVID-19 participants 2-3 months following COVID-19. By 6 months, this improved significantly but remained low in 1/3rd. The observed reduction in peak $\dot{V}O_2$ is partially accounted for by the high occurrence of submaximal tests due to intrusive symptoms. While exercise capacity in those who performed a maximal test ($\dot{V}O_2$max) became comparable to controls by 6 months, the early attainment of the anaerobic threshold (the exercise $\dot{V}O_2$ above which aerobic respiration is supplemented with anaerobically produced ATP, and coincides with the development of lactic acidosis[119]) persisted, being observed in 42% of COVID-19 participants. Of note, the anaerobic threshold is not affected by participant effort or motivation. Any mechanism that limits the delivery or utilization of oxygen within skeletal muscle can result in premature attainment of the anaerobic threshold. In broad terms, one can classify these mechanisms into abnormalities in oxygen delivery or oxygen carriage, cardiac dysfunction, pulmonary vascular disease, peripheral artery disease or tissue oxygen extraction.[119] Despite evidence suggestive of V/Q mismatch, breathing reserve was only exhausted in two COVID-19 participants, implying that respiratory limitation had very little impact on exercise capacity. None of the COVID-19 participants had significant reductions in haemoglobin, nor did any have evidence of left or right systolic impairment on MRI. Although pulmonary pressures were not assessed, right ventricular volumes were comparable to controls, and any elevations in NT-proBNP (a sensitive marker to cardiac stress that has been shown to be raised in the presence of elevated pulmonary pressures[143,144]) were mild. The pattern of change of $ETCO_2$ with exercise adds valuable information in discerning the cause of early anaerobic threshold; COVID-19 participants and controls had similar findings, with $ETCO_2$ peaking at the anaerobic threshold. This is in contrast to the

pattern observed in patients with pulmonary hypertension ($ETCO_2$ decreases immediately following the initiation of exercise) or left ventricular failure ($ETCO_2$ would follow a similar pattern, but the change from one stage of exercise to another would be much smaller in magnitude).[145] While peripheral vascular disease was not assessed, the participants recruited were generally well prior to COVID-19, with no history of arterial disease or intermittent claudication. In addition, comparisons were made with comorbidity-matched controls, and not only with predicted reference values.

Considering the above, reduced tissue oxygen extraction is a potential mechanism that could explain the early attainment of anaerobic threshold (as well as the higher frequency of reduced $O_2$ pulse, due to a reduction in the alveolar-venous oxygen difference) and has been described in a number of reports. Baratto and colleagues utilised level 3 CPET (incorporating exercise echocardiography and arterial blood sampling through a radial catheter) in 25 patients immediately prior to hospital discharge. Patients had reduced tissue oxygen extraction at peak exercise compared to controls in the presence of normal cardiac function.[146] Given that assessment was done at such close proximity to the time of infection together with the presence of mild anaemia and lower arterial oxygen content at peak exercise within the patient group, cautious interpretation of the results is required. Further evidence was provided by Singh and colleagues, who assessed 10 patients 1 year following infection. Patients had lower tissue oxygen extraction compared to matched controls, in the absence or anaemia or reduced arterial oxygen content at peak exercise.[147] The authors postulate that dysregulated vasodilatation and vasoconstriction during exercise (previously documented in patients with chronic fatigue syndrome) secondary to a small fibre neuropathy could be the cause of such findings. Given the association of endothelial dysfunction and dysregulation of fibrinolysis during COVID-19, together with the documentation of microthrombi within different vascular beds, capillary obstruction

restricting the delivery of oxygen to skeletal muscle may also pay a role. Mitochondrial dysfunction is another mechanism that could account for such findings; SARS-CoV-2 may alter mitochondrial function directly (through localisation of viral RNA within mitochondria),[148] and reduced autophagy and mitophagy have also been reported, potentially resulting in an accumulation of damaged mitochondria.[149,150]

## Clinical Implications

My findings suggest that, in patients without a history of significant cardiorespiratory disease, acute or chronic cardiac dysfunction secondary to COVID-19 is rare. Lung imaging abnormalities and reductions in gas transfer persist long after resolution of the acute illness, which suggests a reduction in physiological reserve and may have future implications on health and longevity. Reduced exercise capacity 6 months post-infection was not due to respiratory limitation; the use of exercise testing post-COVID-19 has a low yield for identifying treatable causes of limited exercise tolerance.

## Study limitations

The study is limited by the small sample size which limits the external validity of the results. In the absence of stress cardiac imaging, it was not possible to exclude significant inducible ischaemia with certainty. However, none of the participants stopped their CPET because of angina or developed ischaemic changes on their exercise ECGs. Gas transfer testing and total lung capacity assessment was not available 2-3 months post-infection. However, these results would have been difficult to interpret given that resolution of the acute infection may have still been ongoing. The absence of arterial blood gas sampling or echocardiography during CPET did not permit assessment of tissue oxygen extraction, cardiac output during exercise and

pulmonary dead space. Not all COVID-19 participants came back for follow-up assessments which could in turn bias prevalence estimates in this study. However, participants who returned for follow-up were representative of the original population at all time points.

## Conclusions

In this study, cardiac dysfunction in participants with moderate to severe COVID-19 was rare. Elevated native myocardial T1 was observed shortly after infection which resolved with time. This is likely secondary to the inflammatory climate of acute infection with resultant changes in the extracellular environment, and unlikely to represent direct cellular injury by SARS-CoV-2. A significant proportion of COVID-19 participants had gas transfer abnormalities 18 months post-infection, which are likely due to a combination of loss of discrete alveolar subunits and damage to the alveolar epithelium. Limitations in exercise capacity improve, but do not normalize, with time. 6 months post-infection, reduced tissue oxygen extraction (in the absence of cardiorespiratory limitation) together with submaximal effort due to intrusive symptoms were thought to be the main contributors of persistent reductions in exercise capacity.

## Chapter 4 – Long-term impact of COVID-19 on hepatic and renal health post COVID-19 hospitalization


### Abstract

Introduction: Acute kidney injury and hepatic dysfunction are frequently associated with moderate to severe COVID-19, which may persist following resolution of the acute phase.

Objectives: To assess the longitudinal impact of moderate to severe COVID-19 on hepatic and renal health.

Methods and results: Fifty-eight participants with moderate to severe COVID-19, 2-3 months post infection, and 30 matched COVID-19 naïve controls underwent blood testing and MRI imaging of their liver and kidneys. COVID-19 participants were invited for repeat assessment 6 months and 18 months post-infection, during which albuminuria was also assessed.

During admission, 33% had evidence of acute hepatic injury. On longitudinal assessment, serum markers of hepatic impairment normalised. MRI imaging showed elevated hepatic iron-corrected T1 in COVID-19 participants 2-3 months post-infection versus controls (838ms vs 792ms, *P*=0.009), which became comparable to controls by 6 months (804ms, *P*=0.41 vs controls). Regarding renal health, 10 % of COVID-19 participants had acute kidney injury. However, 52% of COVID-19 participants at 18 months post-infection had reduced renal function (eGFR) when compared to their initial assessment. A validated mechanism used to predict the risk of CKD failed to identify COVID-19 participants who underwent a significant reduction in renal function. Renal MR imaging revealed elevated renal cortical T1 2-3 months post infection and reductions in corticomedullary differentiation (a marker of renal structural health). Although renal cortical T1 normalised with time, this was not accompanied by an

improvement in renal function. Renal cortical T1, 2-3 months post-infection, was strongly negatively correlated with eGFR 18 months post-infection.

Conclusion: Hepatic impairment during acute COVID-19 is common and resolves with time. A downward trajectory of renal function was observed on longitudinal assessment, and was not predicted by a widely used CKD risk instrument. Renal tissue abnormalities as measured by MR at 2-3 months after COVID-19 were strongly associated with impaired renal function 18 months post-infection.

## Introduction

While SARS-CoV-2 primarily targets the lungs, extra-pulmonary organ involvement was recognized early in the pandemic, with acute kidney injury and acute derangement of liver function being described in nearly a third of patients requiring management in intensive care.[6] Insights gained from post-mortem studies have provided important clarifications regarding the mechanisms underlying acute kidney and hepatic injury. Renal injury appears to be characterized by derangement of glomerular and proximal tubule integrity and function, secondary to direct invasion (via ACE2 receptor-mediated cell entry) of podocytes and brush border cells, together with indirect insult secondary to hypoxia, hypotension and the hyperinflammatory environment characteristic of COVID-19.[49,50] In contrast, despite high ACE2 receptor expression by cholangiocytes, SARS-CoV-2 mediated hepatic injury is primarily due to hypoxia in the absence of direct cell invasion.[51,53]

The liver and kidneys carry out a wide range of metabolic and homeostatic functions that are critical to health. It is therefore unsurprising that chronic liver and renal disease are associated with significant increases in morbidity and mortality.[151,152]

Given the potential for long-term hepatic and renal dysfunction following hospitalization with COVID-19, I set out to assess the prevalence, extent, and longitudinal trajectory of renal and hepatic injury in patients following hospitalization with COVID-19.

## Methods

Laboratory analysis was performed at the John Radcliffe biochemistry laboratory. Renal function assessment consisted of the following markers: creatinine, estimated glomerular filtration rate (eGFR) and spot urine albumin:creatinine ratio (ACR). Markers of liver function consisted of alaline transaminase (ALT), aspartate transaminase (AST), alkaline phosphatase, gamma-glutamyl transaminase (GGT) and bilirubin.

### MRI Protocol

As previously described, MOLLI-variant T1 maps (Siemens Myomaps) were used to assess fibrosis, inflammation and oedema in the liver.[78] Multiecho gradient echo IDEAL[80] was used to assess fat and iron in the liver, with the data reconstructed using the ISMRM to yield proton density fat fraction (PDFF), $B_0$ and T2* maps.[81] Kidney MOLLI T1 maps were used to assess oedema, inflammation and fibrosis.

### MRI image analysis

Liver MRI images were analysed by placing three 15 mm diameter circular regions of interest within the liver parenchyma, avoiding vessels and bile ducts as much as possible, and any fat/water swaps visible in the PDFF maps. Iron-corrected T1, a biomarker of hepatic inflammation and fibrosis which corrects for the T1-shortening properties of iron,[153] was calculated using a method developed in-house.[81] Average values of PDFF, T2*, and iron-corrected T1 for the liver were recorded.

Renal T1 mapping was assessed using manually defined ROIs in the cortex and medulla. Corticomedullary T1 difference (CMD), a marker of renal structural integrity and health,[154] was calculated using the following equation:

$CMD = T1_{medulla} - T1_{cortex}$.[155]

### Data acquired

Of the 30 controls who attended a study visit, all underwent biochemical blood testing. 28 underwent abdominal imaging (2 had severe claustrophobia precluding imaging).

Of the 58 COVID-19 participants who attended an initial study visit, 52/58 (89.7%) underwent abdominal imaging (1 had large body habitus precluding imaging, 4 had limiting claustrophobia, and 1 participant requested termination of the MRI following respiratory imaging due to claustrophobia). Urine ACR was only collected following approval of a protocol amendment, and available for 6 month and 18 month visits only.

Of the 46 COVID-19 participants who attended a study visit 6 months following infection, biochemical testing (including ACR) was performed in all. 44/46 (95.7%) underwent abdominal imaging (2 did not undergo imaging due to claustrophobia).

Of the 23 participants who attended a visit 18 months post-infection, all underwent biochemical testing. 22/23 (95.7%) had ACR assessed. All underwent abdominal imaging.

## Statistical Analyses and Definitions

Statistical analysis was performed as previously described in the methods chapter. Critical illness, as previously described, was defined as any COVID-19 participant requiring non-invasive ventilation, intubation and ventilation or organ support.

Multivariate binary logistic regression was used to assess the relationship between patient/disease characteristics and a significant drop in eGFR of >5ml/min/1.73m$^2$ between the first and final visit. To maintain the absence of multicollinearity, age, diagnosis of hypertension, presence of type 1 or 2 diabetes, acute kidney injury (AKI) during admission, steroid administration during admission and risk of chronic kidney disease (CKD) progression (based on eGFR and urine ACR at 6 months post-infection) were included as independent variables in the multivariate analysis. COVID-19 severity

was not included in the model as this moderately correlated with the presence or absence of AKI during admission ($\rho$=0.53, $P$<0.001), and would have therefore resulted in multicollinearity. The Box-Tidwell test demonstrated linearity of the continuous variable age with respect to the logit of the dependent variable.

Multivariate linear regression was used to assess the relationship between patient/disease characteristics and eGFR at the final visit. To maintain the absence of multicollinearity, age, diagnosis of hypertension, presence of type 1 or 2 diabetes, AKI during admission, steroid administration during admission, risk of CKD progression and average renal cortical T1 at 2-3 months post-infection were included as independent variables in the analysis. There was independence of residuals, as assessed by a Durbin-Watson statistic of 2.35. There was homoscedasticity, as assessed by visual inspection of a plot of studentized residuals versus unstandardized predicted values.

Liver test abnormalities were defined as ALT >45 IU/L, AST >42 IU/L, GGT >49 IU/L, ALP >130 IU/L, and total bilirubin >21 µmol/L, based on the upper limits determined by the local laboratory. Liver injury was classified into the following groups:[156]

- Hepatocyte type: ALT and/or AST > 3× the ULN
- Cholangiocyte type: ALP or GGT >2x the ULN
- Mixed type: Any combination of the above.

AKI was defined as an increase in serum creatinine of at least 26 umol/L within 48 hours, or at least a 1·5 fold increase from baseline.[152] Elevated creatinine was defined as a value >90 umol/L, based on local laboratory reference ranges.

eGFR was used to classify renal function as follows:[157]

Normal: ≥90 ml/min/1.73m$^2$

Mildly decreased: 60-89 ml/min/1.73m$^2$

Mildly to moderately decreased: 45-59 ml/min/1.73m$^2$

Moderately to severely decreased: 30-44 ml/min/1.73m$^2$

Severely decreased: 15-29 ml/min/1.73m$^2$

Kidney failure: <15 ml/min/1.73m$^2$

Urine ACR was interpreted as follows:

Normal: <3mg/mmol

Moderately increased: 3-30mg/mmol

Severely increased: >30mg/mmol

## Results

### Renal and hepatic dysfunction during admission

As previously described, none of the participants recruited to the study had a previous history of CKD. During admission with COVID-19, a total of 6 participants (10%, median age 55 years, range 52 – 77 years) fulfilled the criteria of acute kidney injury (median creatinine 244 µmol/L, range 73 – 1002 µmol/L). Given that not all participants had a creatinine recorded prior to admission, together with the impact of intravenous fluid administration on creatinine levels, this may be an underestimation of the true figure. All participants with AKI but one were male. All required intubation and mechanical ventilation, with 2/58 (3.4%) requiring renal replacement therapy. Peak creatinine during admission moderately correlated with peak CRP ($\rho$=0.45, $P$<0.001), D-dimer ($\rho$=0.47, $P$=0.001) and disease severity classified according to the WHO disease severity scale ($\rho$=0.44, $P$<0.001).

During admission with COVID-19, elevated ALT was the most common marker of hepatic derangement, seen in 51% of participants (median 111 IU/L, range 47 – 499 IU/L). Elevations in alkaline phosphatase were observed in 32% of participants (median 174 IU/L, range 135 – 473 IU/L). Liver injury was observed in a third of participants, with the hepatocyte type of injury being by far the most common (Table 10). Participants with COVID-19 associated hepatic injury had a longer admission time compared to those without (17 [9-19] days vs 7[4-10] days, $P$<0.001). There was a weak correlation between ALT levels and peak CRP ($\rho$=0.37, $P$=0.006) and disease severity ($\rho$=0.38, $P$=0.003).

| Table 10: Admission hepatic, renal and relevant haematological blood results during admission. | |
|---|---|
| | COVID-19 (admission) (N=58) |
| **Haematology and Coagulation** | |
| Haemoglobin, g/L | 141·0 (125·5 - 150·5) |
| <120 (females)/<130 (males) | 12/58 (20·6%) |
| D-dimer, µg/L | 780·0 (636·0 - 1490·0) |
| >500 | 27/31 (87.1%) |
| **Hepatic panel** | |
| Total bilirubin, mmol/L | 10·0 (7·0 - 13·8) |
| Alanine transaminase, IU/L | 34·0 (22·3 - 62·8) |
| >45 | 38/57 (50.7%) |
| Alkaline phosphatase, IU/L | 91.0 (70.0 - 150.0) |
| >130 | 18/57 (31.6%) |
| Hepatic injury | 19/57 (33.3%) |
| Hepatocyte type | 15/57 (26.3%) |
| Cholangiocyte type | 1/57 (1.8%) |
| Mixed type | 3/57 (5.2%) |
| **Renal function and electrolytes** | |
| Potassium, mmol/L | 3·8 (3·7 - 4·1) |
| Sodium, mmol/L | 136·0 (2·9) |
| Peak creatinine, umol/L | |
| >90 | 17/58 (29.3%) |
| eGFR, ml/min/1·73m$^2$ | |
| ≥90 | 31/58 (53·4%) |
| 60-89 | 21/58 (36·2%) |
| 45-59 | 3/58 (5·2%) |
| 30-44 | 2/58 (3·4%) |
| 15-29 | 1/58 (1·7%) |
| <15 | 0/58 (0·0%) |
| **Inflammatory markers** | |
| C-reactive protein, mg/L | 119·1 (75·9 - 185·5) |
| >10 | 58/58 (100%) |

Data are mean (SD), median (IQR) and n/N (%), where N is the total number of participants with available data. eGFR = Estimated glomerular filtration rate.

### Hepatic health

In participants 2-3 months following infection with COVID-19, median ALT, AST, alkaline phosphatase (ALP) and GGT were comparable to controls (Table 11). In total, 21/58 COVID-19 participants (36%) had at least one hepatic marker above the upper limit of normal. GGT was the most frequently elevated marker (seen in 28%), followed closely by ALT (19%). Elevations in hepatic markers were overall small in magnitude, with only 4 participants (7%) fulfilling criteria of hepatic injury (3 were of the mixed type, while 1 was of the hepatocyte type). In contrast to what was seen during admission, none of the markers correlated with CRP or disease severity.

By 6 months post-infection, ALT, AST, ALP and GGT continued to improve (Table 12). There was a reduced prevalence of hepatic injury, with only 1 participant (2%) having evidence of hepatic injury (mixed type, Figure 15). At 18 months post-infection, serum markers of hepatic health remained stable (Table 13), and none developed hepatic injury.

| Table 11: Markers of hepatic health in COVID-19 participants 2-3 months post infection and controls. | | | |
|---|---|---|---|
| | COVID-19, 2-3m (N=58) | Controls (N=30) | *P*-value |
| **Hepatic panel** | | | |
| Total bilirubin, mmol/L | 10·0 (6·8 - 14·0) | 8·0 (7·0 - 11·5) | *0·51* |
| ALT, IU/L | 23·5 (18·8 - 39·0) | 23·5 (16·0 - 28·0) | *0·19* |
| >45 IU/L | 11/58 (19.0%) | 1/30 (3.3%) | *0.04* |
| AST, IU/L | 23·0 (18·0 - 28·0) | 21·0 (18·0 - 27·0) | *0·36* |
| >42 IU/L | 4/55 (7.3%) | 0/25 (0.0%) | *0.22* |
| Alkaline Phosphatase, IU/L | 72·0 (60·0 - 85·5) | 65·5 (55·8 - 80·3) | *0·21* |
| >130 IU/L | 2/58 (3.4%) | 0/30 (0.0%) | *0.43* |
| GGT, IU/L | 33·0 (21·8 - 52·3) | 29·0 (18·5 - 47·5) | *0·25* |
| >49 IU/L | 15/54 (27.8%) | 6/25 (24.0%) | *0.72* |
| Hepatic injury | | | *0.70* |
| Hepatocyte type | 1/58 (1.7%) | 0/30 (0.0%) | |
| Cholangiocyte type | 0/58 (0.0%) | 0/30 (0.0%) | |
| Mixed type | 3/58 (5.2%) | 0/30 (0.0%) | |

Paired data are mean (SD), median (IQR) and n/N (%), where N is the total number of participants with available data. Italicised P-values are from non-parametric tests. ALT = Alanine transaminase. AST = Aspartate aminotransferase. GGT = Gamma-glutamyl transferase.

| Table 12: Paired markers of hepatic health in COVID-19 participants 2-3 and 6 months post infection. | | | |
|---|---|---|---|
| | COVID-19, 2-3m (N=46) | COVID-19, 6m (N=46) | *P*-value |
| **Hepatic panel** | | | |
| Total bilirubin, mmol/L | 10·0 (6·0 - 14·0) | 10.5 (7·0 - 14.3) | *0.17* |
| ALT, IU/L | 23.5 (19.0 - 38.3) | 24.0 (18.8 - 37.0) | *0.63* |
| >45 IU/L | 8/46 (17.4%) | 5/46 (10.9%) | *0.51* |
| AST, IU/L | 23·0 (18·0 - 28·0) | 21·0 (18·0 - 26·0) | *0.07* |
| >42 IU/L | 3/43 (7.0%) | 0/46 (0.0%) | *0.25* |
| Alkaline Phosphatase, IU/L | 72·0 (60·0 - 87.0) | 69.0 (54.8 - 83.0) | *0.20* |
| >130 IU/L | 0/46 (0.0%) | 0/46 (0.0%) | -- |
| GGT, IU/L | 33·0 (21·8 - 53.8) | 29·0 (22.0 - 40.5) | *0.002* |
| >49 IU/L | 13/42 (31.0%) | 10/46 (21.7%) | *0.13* |
| Hepatic injury | | | *0.50* |
| Hepatocyte type | 1/46 (2.2%) | 0/46 (0.0%) | |
| Cholangiocyte type | 0/46 (0.0%) | 0/46 (0.0%) | |
| Mixed type | 2/46 (4.3%) | 1/46 (2.2%) | |

Paired data are mean (SD), median (IQR) and n/N (%), where N is the total number of participants with available data. Italicised P-values are from non-parametric tests. ALT = Alanine transaminase. AST = Aspartate aminotransferase. GGT = Gamma-glutamyl transferase.

| Table 13: Paired markers of hepatic health in COVID-19 participants 6 and 18 months post infection. | | | |
|---|---|---|---|
| | COVID-19, 6m (N=23) | COVID-19, 18m (N=23) | P-value |
| **Hepatic panel** | | | |
| Total bilirubin, mmol/L | 11.0 (7.0 - 15.0) | 12.0 (7.0 - 17.0) | *0.17* |
| ALT, IU/L | 23.0 (16.0 - 29.0) | 21.0 (19.0 - 29.0) | 0.82 |
| >45 IU/L | 0/23 (0.0%) | 1/23 (4.3%) | *1.00* |
| AST, IU/L | 20.0 (18.0 - 24.0) | 23.0 (19.0 - 26.0) | *0.11* |
| >42 IU/L | 0/23 (0.0%) | 1/23 (4.3%) | *1.00* |
| Alkaline Phosphatase, IU/L | 69.0 (50.0 - 83.0) | 73.0 (55.0 - 88.0) | 0.11 |
| >130 IU/L | 0/23 (0.0%) | 1/23 (4.3%) | *1.00* |
| GGT, IU/L | 26.0 (18.0 - 34.0) | 25.0 (17.0 - 32.0) | *0.37* |
| >49 IU/L | 3/23 (13.0%) | 1/23 (4.3%) | *0.50* |
| Hepatic injury | 0/23 (0.0%) | 0/23 (0.0%) | -- |

Data are mean (SD), median (IQR) and n/N (%), where N is the total number of participants with available data. Italicised P-values are from non-parametric tests. ALT = Alanine transaminase. AST = Aspartate aminotransferase. GGT = Gamma-glutamyl transferase.

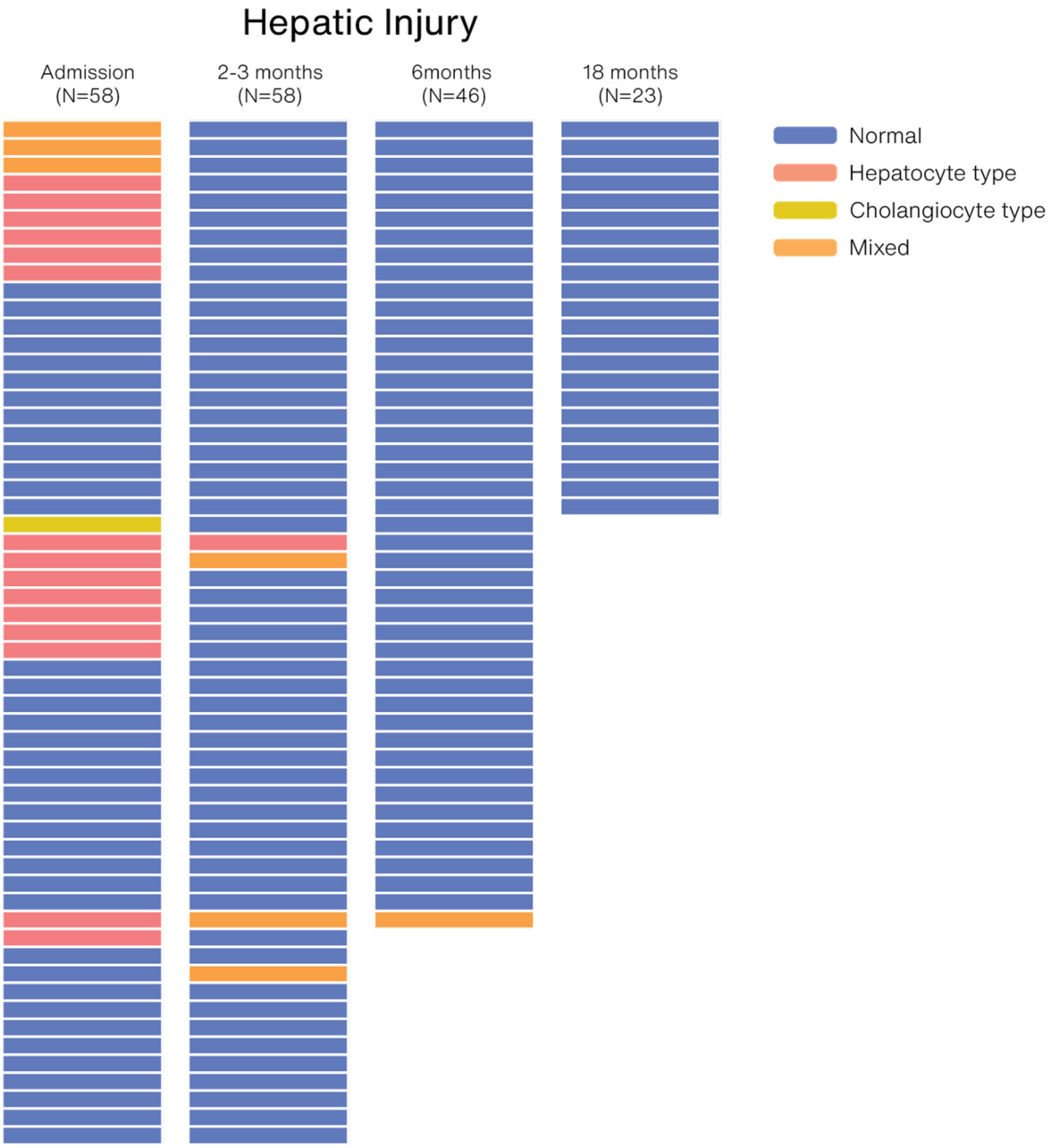


**Figure 15. A heat map showing the prevalence of hepatic injury during admission and on follow-up.**

MRI imaging of the liver 2-3 months post-infection revealed elevated hepatic iron-corrected T1 (a marker of fibrosis, inflammation or oedema) in COVID-19 participants compared to controls (838 vs 792ms, *P*=0.009, Table 14, Figures 16 and 17). COVID-19 participant iron-corrected T1 moderately correlated with CRP (ρ=0.59, *P*<0.001). Iron-corrected T1 did not differ in COVID-19 participants with or without hepatic injury during admission. T2*, a marker inversely correlated with hepatic iron content, was comparable in COVID-19 participants and controls. None of the participants had evidence of hepatic iron overload (T2* <4ms).[158] Proton density fat fraction (PDFF, a marker of hepatic fat) was higher in COVID-19 participants compared to controls, although this was not statistically significant.

On follow-up assessment, iron-corrected T1 improved in COVID-19 participants and was comparable to controls 6 months following COVID-19. T2* increased and PDFF decreased, both remaining comparable to controls.

By 18 months, iron-corrected T1 did not undergo any significant change. COVID-19 participants had slightly higher T2* and higher PDFF values compared with controls (Figure 17).

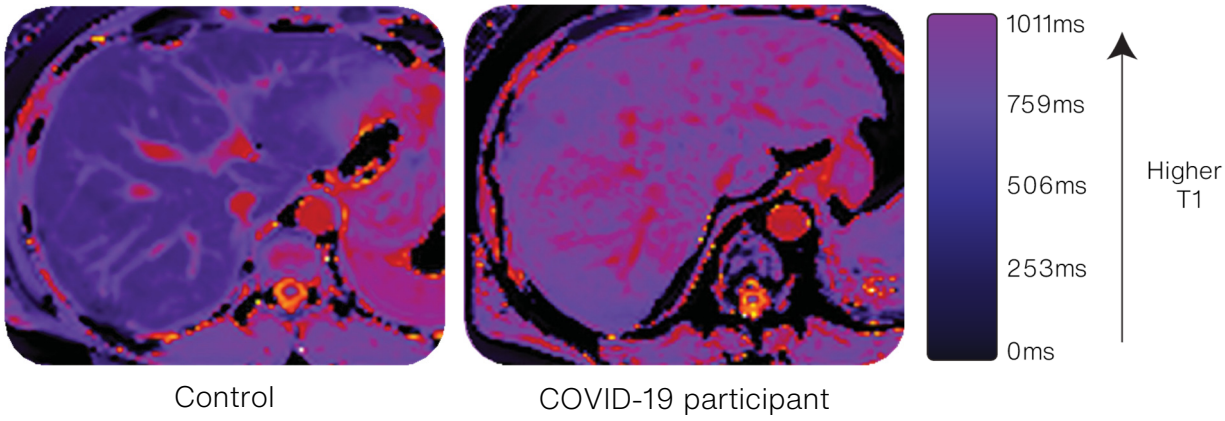


**Figure 16: Hepatic native T1 images from a control participant (left) and a COVID-19 participant 2-3 months following moderate to severe COVID-19 (right). Heterogenous hyperintense areas can be seen within the participant's liver parenchyma, indicative of increased T1.**

| Table 14: Hepatic T1, T2* and PDFF in COVID-19 participants 2-3 months post-infection and controls. | | | |
|---|---|---|---|
| | COVID-19, 2-3m (N=52) | Controls (N=28) | *P*-value |
| **Hepatic MRI imaging** | | | |
| Iron-corrected T1, ms | 838 (804.3 - 899.8) | 792 (732.2 - 856.1) | *0.009* |
| T2*, ms | 17.7 (4.4) | 17.2 (3.5) | 0.60 |
| PDFF, % | 4.9 (3.1 - 9.5) | 3.7 (2.1 - 6.5) | *0.18* |
| Data are mean (SD) and median (IQR) PDFF = Proton density fat fraction. | | | |

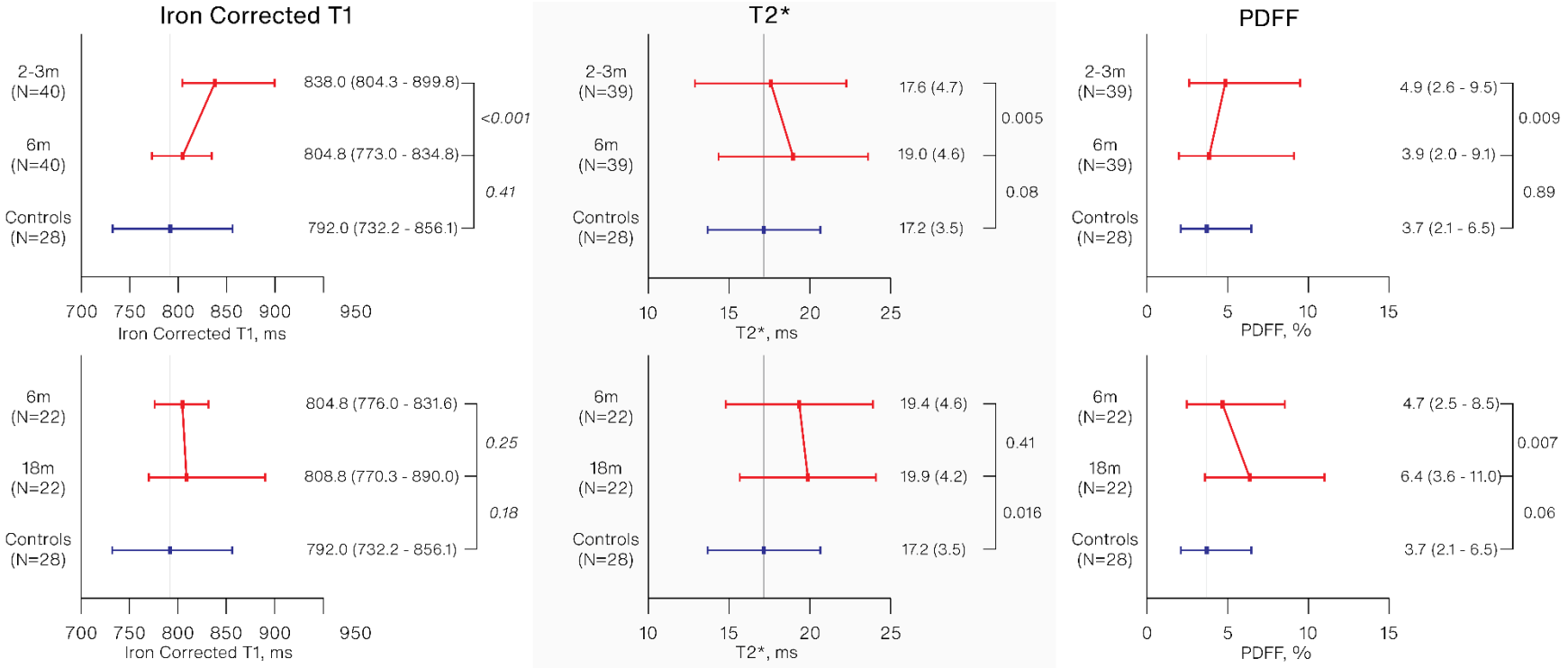


**Figure 17. Serial hepatic iron-corrected T1, T2* and PDFF (Proton density fat fraction) in COVID-19 participants from 2-3 to 6 months (first row), and 6 to 18 months (second row), compared with control data. Red bars depict COVID-19 participant data, while blue bars depict control data. Bars depict either mean +/- SD or median and IQR. Descriptor values (mean[SD] or median[IQR]) are provided next to each bar. Significance brackets are provided together with their corresponding *P* values, with the first signifying comparison between COVID-19 participants at different time points, and the 2nd representing comparison between COVID-19 participants and controls.**

## Renal Health

2-3 months following infection, COVID-19 participants had comparable creatinine concentrations with controls (Table 15). Although the proportions of COVID-19 participants and controls classified as having reduced renal function (based on eGFR) were comparable, COVID-19 participants with reduced kidney function had lower eGFR values (COVID-19: 75.5ml/min/1·73m$^2$ (65.5 – 84.8); Controls: 84.0ml/min/1·73m$^2$ (78.5 – 85.0); *P*=0.09). One COVID-19 participant had mildly to moderately decreased renal function (eGFR 56 ml/min/1·73m$^2$), and 2 had moderately to severely decreased renal function (eGFRs 43 and 41ml/min/1·73m$^2$).

At 6 months post-infection, COVID-19 participants had a significant reduction in eGFR (4 had a higher eGFR, 26 had unchanged values and 16 had a lower eGFR; *P*=0.01 (Figure 20)). Despite having an eGFR of >90ml/min/1.73m$^2$, 4 participants (9%) had a mild risk of progression, and 1 (2%) had a moderate risk of progression, due to the presence of albuminuria. The two participants (4%) with the lowest eGFRs had a high risk of progression to CKD. In spite of this, overall the majority had a low risk of progression to end stage kidney disease (74%, Figure 18).

By 18 months, COVID-19 participants continued to have a lower eGFR when compared to the initial assessment (2 had an improvement in eGFR, 9 had stable eGFR, and 12 had a deterioration in eGFR; *P*=0.006, Figure 20). The risk of CKD progression remained stable in 19 (83%) participants, improved in 3 (13%), and became worse in 1 participant (4%) (Figure 19). Despite this, 6 (26%) had a decline in eGFR of >5ml/min/1.73m$^2$ (median decline 8ml/min/1.73m$^2$, range 7 – 13), suggestive of rapid progression of renal disease.[157] Interestingly, these COVID-19 participants had a low (5 participants) or mildly increased risk (1 participant) of CKD progression at 6 months. There was no correlation between the risk of CKD progression (at 6 and 18 months)

and change in eGFR from 6 to 18 months. The disparity between CKD risk and deterioration in renal function was again seen with multivariate logistic regression, resulting in a statistically significant model ($P$=0.030) which explained 76% (Nagelkerke $R^2$) of the variance in a significant drop in eGFR between the first and final visit (specificity 100%, sensitivity 90.0%). Of the 6 predictor variables (age, diagnosis of hypertension, presence of type 1 or 2 diabetes, COVID-19 severity, AKI during admission, steroid administration during admission and risk of CKD progression), only age was statistically significant ($P$=0.03, $P$-value range for other variables 0.61-1.00), with each year increasing the odds of a significant drop in eGFR by 1.5 (95% confidence interval 1.03 – 2.07).

Across all time points, COVID-19 participants who had an AKI during admission had lower eGFR values compared to those without significant renal dysfunction during admission ($P$<0.03 for all time points, Figure 21).

| Table 15: Measures of renal function in COVID-19 participants 2-3 months post infection and controls. | | | |
|---|---|---|---|
| | COVID-19, 2-3m (N=58) | Controls (N=30) | *P*-value |
| **Renal function** | | | |
| Creatinine, µmol/L | 69·5 (60·0 - 79·3) | 79·0 (63·0 - 89·0) | *0·16* |
| >90 µmol/L | 8/58 (13.8%) | 5/30 (16.7%) | *0.76* |
| eGFR, ml/min/1·73m$^2$ | | | |
| ≥90 | 38/58 (65·5%) | 17/30 (56·7%) | *0·53* |
| 60-89 | 17/58 (29·3%) | 13/30 (43·3%) | |
| 45-59 | 1/58 (1·7%) | 0/30 (0·0%) | |
| 30-44 | 2/58 (3·4%) | 0/30 (0·0%) | |
| 15-29 | 0/58 (0·0%) | 0/30 (0·0%) | |
| <15 | 0/58 (0·0%) | 0/30 (0·0%) | |
| Data are median (IQR) and n/N (%), where N is the total number of participants with available data. Italicised P-values are from non-parametric tests. eGFR = Estimated glomerular filtration rate. | | | |

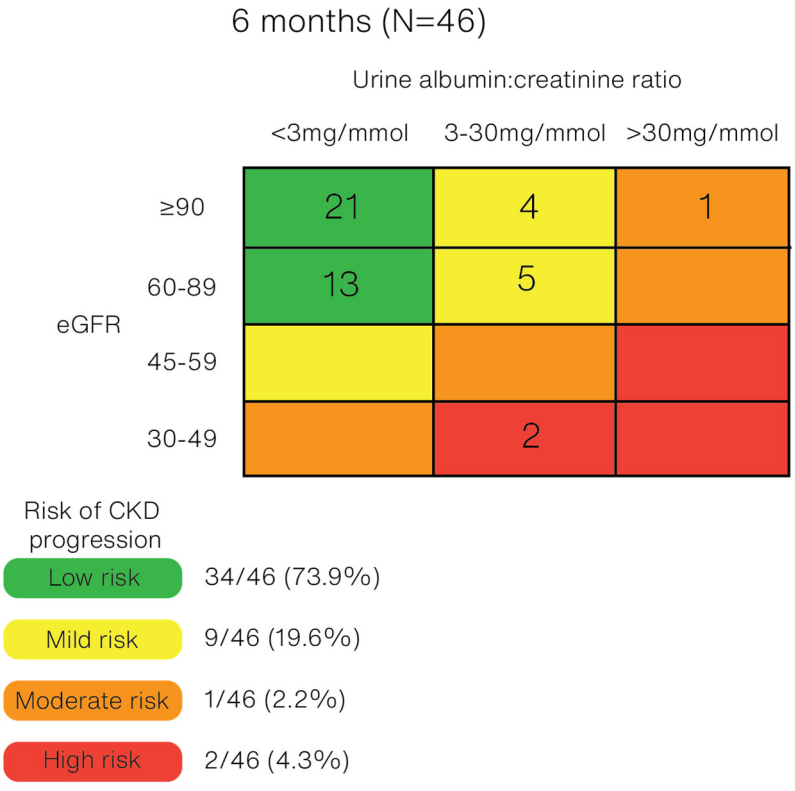


**Figure 18. CKD heat map showing the risk of CKD progression in COVID-19 participants, 6 months following infection. eGFR units ml/min/1·73m$^2$.**

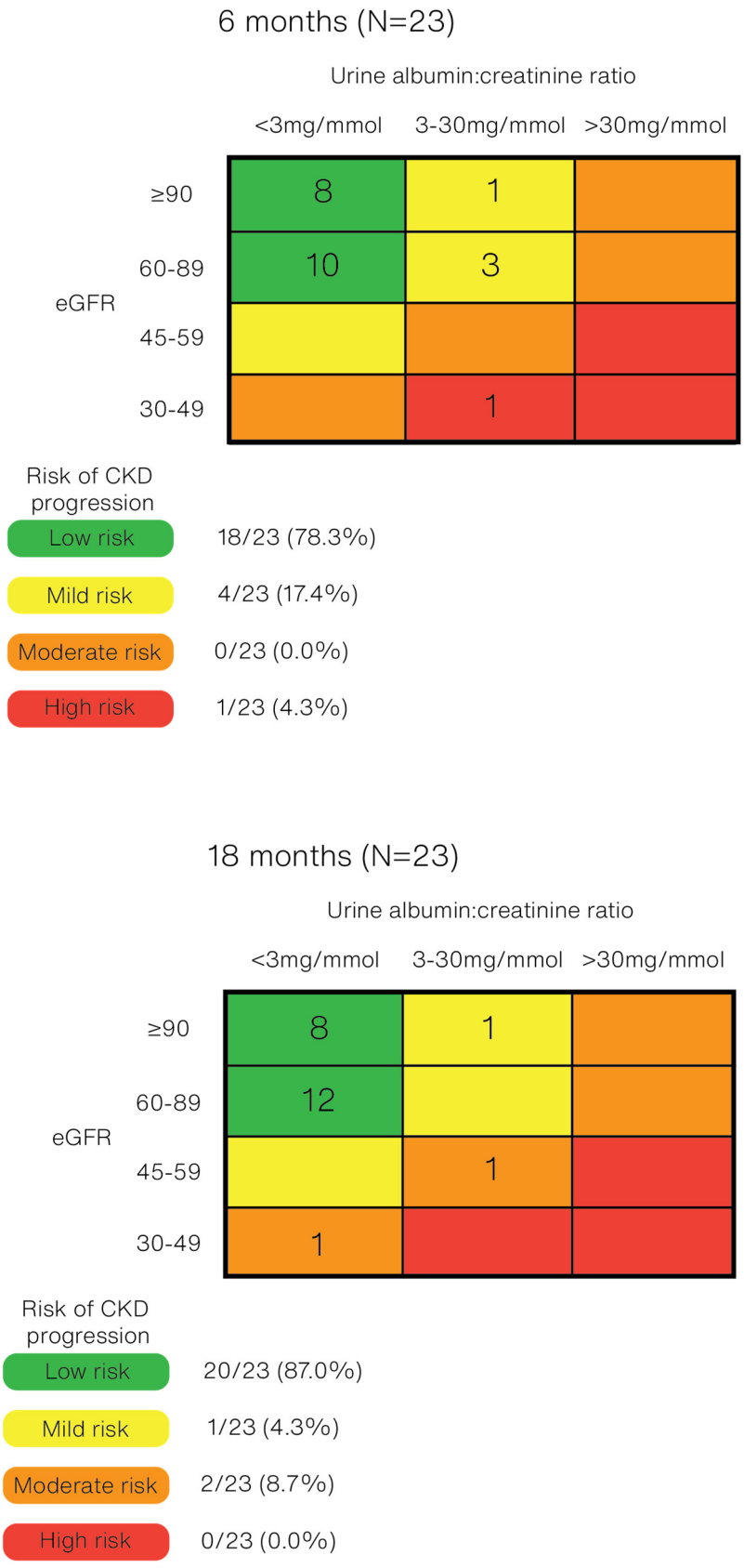


**Figure 19. CKD risk maps showing the risk of CKD progression in COVID-19 participants who attended a visit 6- and 18-months following infection. Only paired data is shown. eGFR units ml/min/1·73m².**

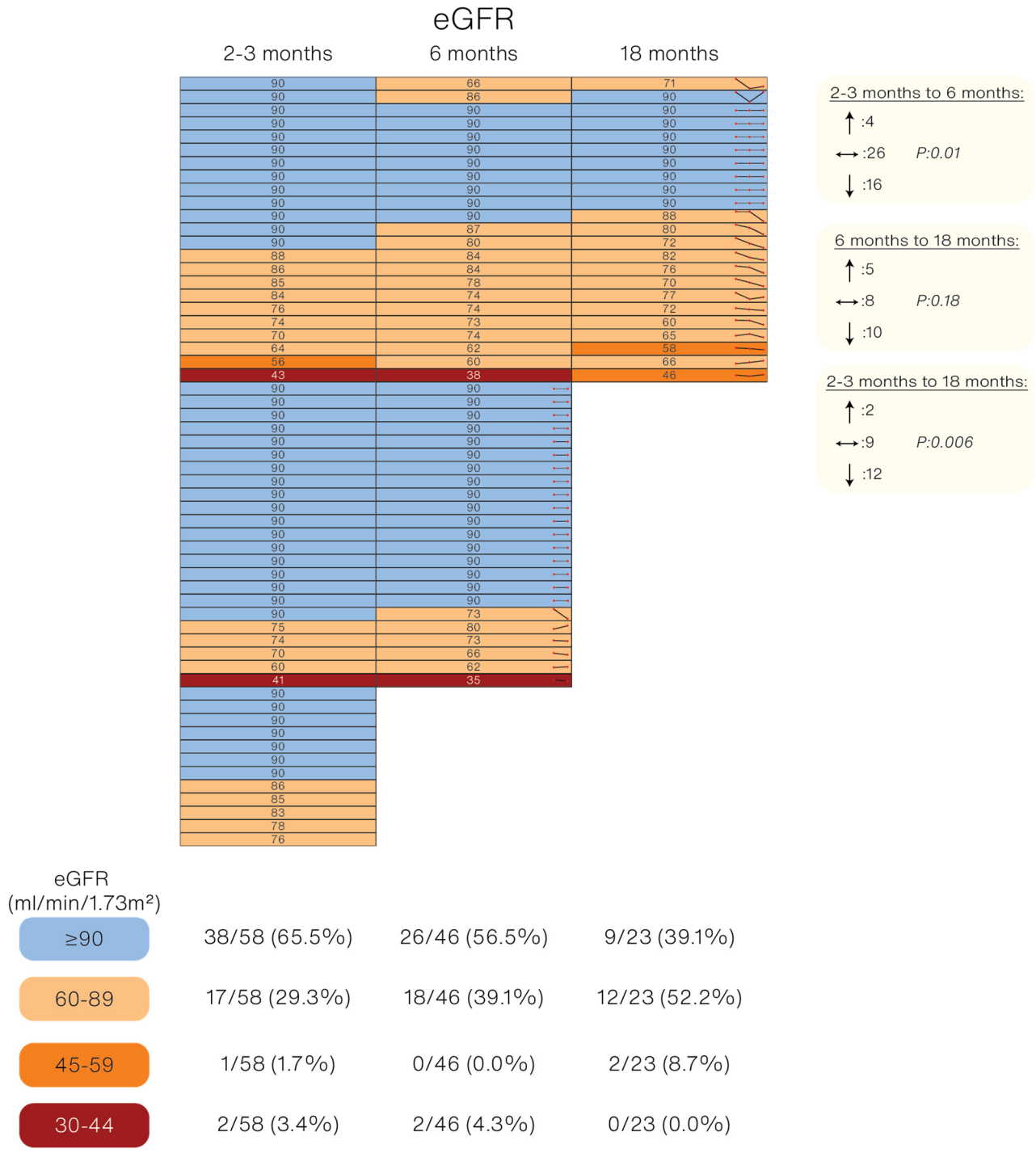


**Figure 20. Heat map showing eGFR values for all COVID-19 participants recruited into the study, together with trend-lines for participants who attended 2 or more visits. ↑: Increase in eGFR. ↔: No change in eGFR. ↓: Reduction in eGFR.**

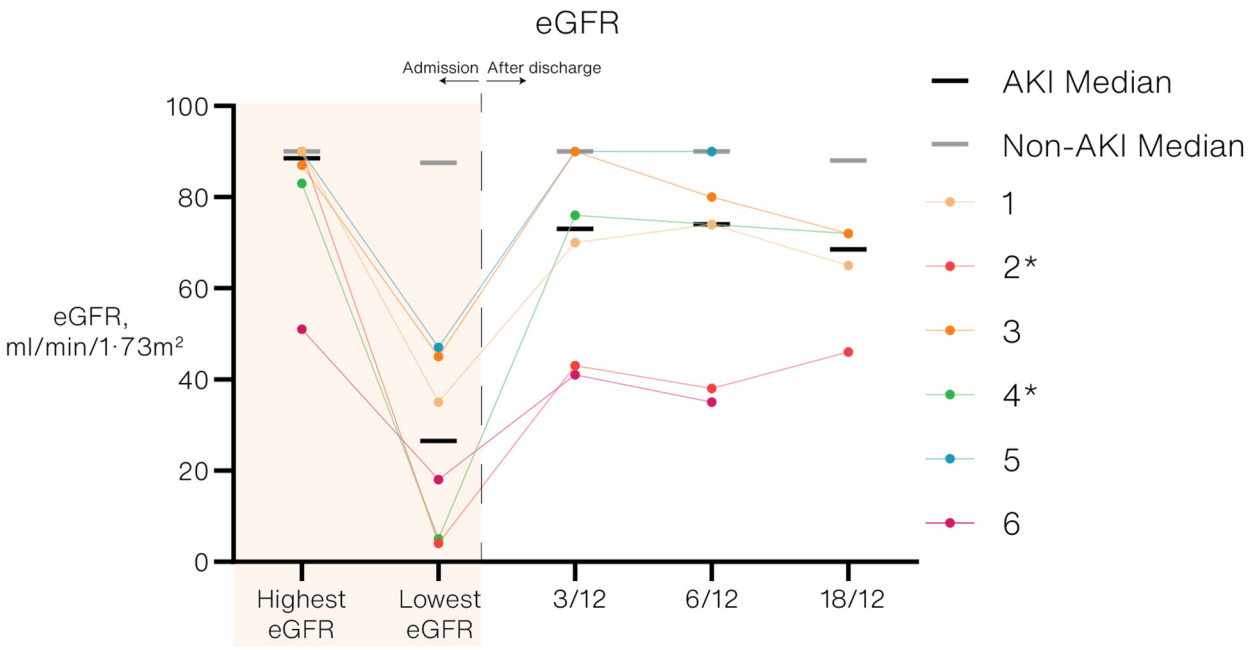


**Figure 21. Plot showing individual eGFR values during admission and on follow-up in COVID-19 participants with AKI, and median eGFR values for participants with an AKI (black lines) and those without renal dysfunction during admission (grey lines). * indicates participants who underwent renal replacement therapy**

On MRI imaging, 2-3 months following infection, participants had higher average renal cortical T1 and lower corticomedullary differentiation (CMD) compared to controls (**Table 16, Figure 22**). Average cortical T1 moderately correlated with CRP (ρ=0.43, *P*<0.001) and severity of illness (ρ=0.45, *P*<0.001), and was moderately inversely correlated with the lowest eGFR during admission (ρ=-0.46, *P*<0.001).

By 6 months, average cortical T1 significantly improved (1549 vs 1592ms, *P*<0.001) and became comparable to controls (1523ms, *P*=0.14). COVID-19 participants continued to have lower CMD compared to controls (**Figure 23**).

MRI measures of renal health remained stable 18 months following infection, and the reduced CMD relative to controls persisted.

COVID-19 participants with an AKI had persistently higher cortical T1 and lower CMD compared to those without AKI during admission (**Table 17**). Renal cortical T1 2-3 months post-infection negatively correlated with eGFR assessed at all time points, with the relationship becoming stronger over time. A similar positive correlation was observed between CMD and eGFR (**Table 18**). In a statistically significant multivariate linear regression model to predict eGFR 18 months post-infection ($F(6,15) = 4.70$, *P*=0.007, adjusted $R^2 = 0.51$), of the variables age, history of hypertension, history of diabetes, AKI during admission, steroid administration during admission and average renal cortical T1 2-3 months post infection, only renal cortical T1 contributed significantly to the model (β=-0.1, *P*=0.012).

There was a dissociation in the trajectories of eGFR and renal cortical T1 over time; from 2-3 to 6 months, change in eGFR moderately correlated with change in T1 (ρ=0.44, *P*=0.005), meaning that renal cortical T1 improved (i.e. decreased) in COVID-19 participants while renal function declined (of the 15 participants with a decline in eGFR from 2-3 to 6 months and underwent imaging, 12 had an improvement in renal

cortical T1). From 6 months to 18 months post infection, no relationship between change in eGFR and change in renal cortical T1 was seen (r=0.17, *P*=0.44).

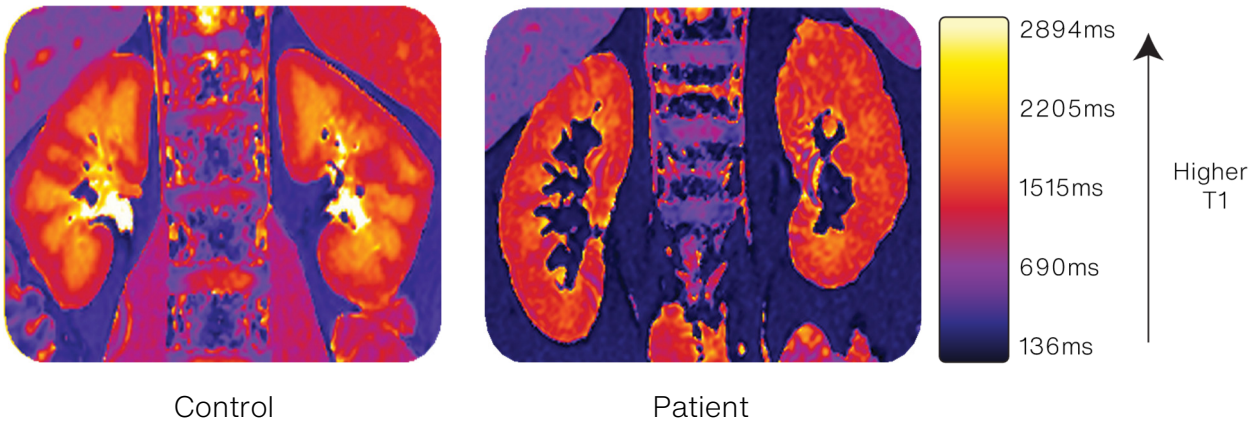


**Figure 22: Renal native T1 images from a control (left) and a COVID-19 participant 2-3 months following moderate to severe COVID-19 (right). The clear distinction between the outer cortex and inner medulla is absent in the COVID-19 participant's kidneys.**

| Table 16: Renal T1 parameters in COVID-19 participants 2-3 months post-infection and controls. | | | |
|---|---|---|---|
| | COVID-19, 2-3m (N=51) | Controls (N=28) | *P*-value |
| **Renal MRI imaging** | | | |
| Average Cortical T1, ms | 1597.5 (91.2) | 1523.1 (65.5) | <0.001 |
| Average Medullary T1, ms | 1992.6 (71.6) | 1988.8 (73.7) | 0.82 |
| CMD, ms | 395.1 (85.4) | 465.7 (63.5) | <0.001 |
| Data are mean (SD). P-values are from parametric tests. CMD = Corticomedullary differentiation. | | | |

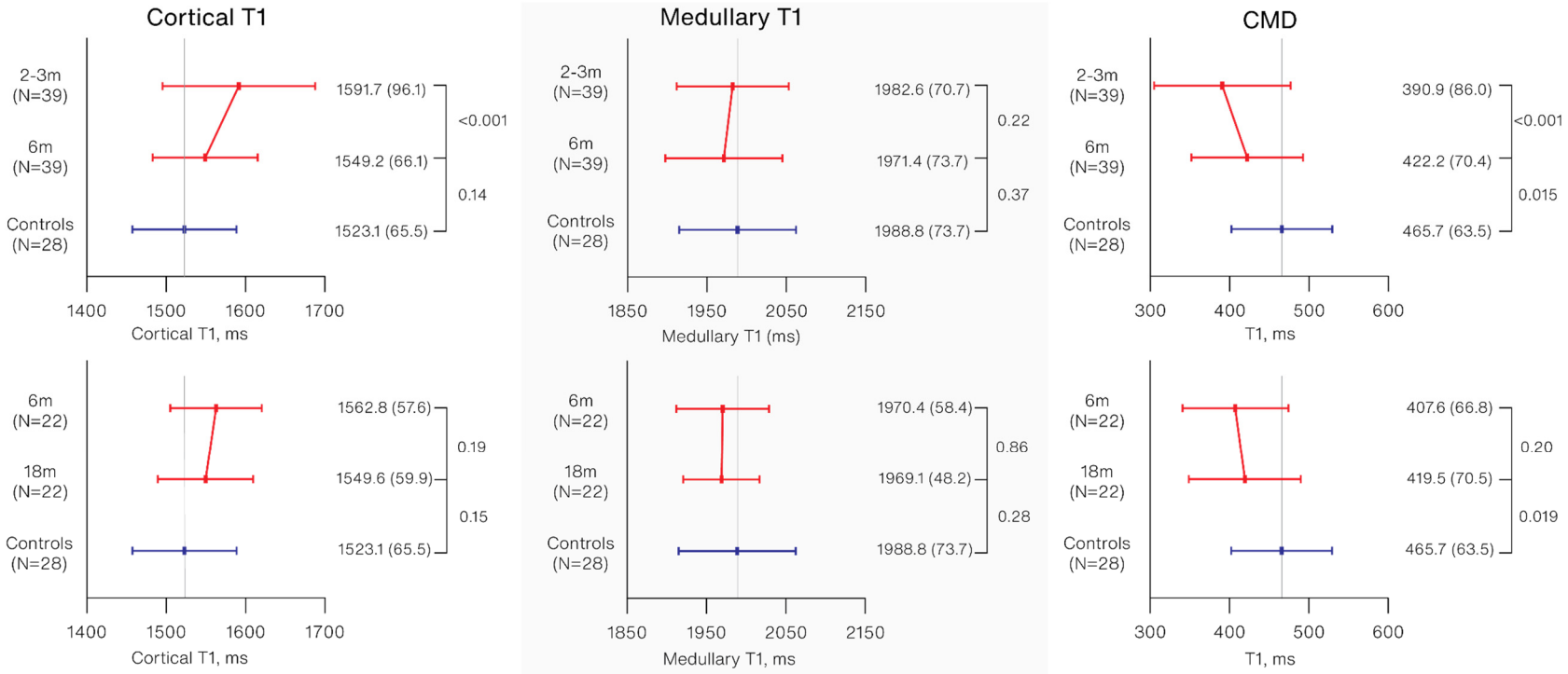


**Figure 23. Paired serial cortical T1, medullary T1 and CMD (corticomedullary differentiation) in COVID-19 participants from 2-3 to 6 months (first row), and 6 to 18 months (second row), compared with control data. Data are mean (SD). Red bars depict COVID-19 participant data, while blue bars depict control data. Bars depict either mean +/- SD or median and IQR. Descriptor values (mean[SD] or median[IQR]) are provided next to each bar. Significance brackets are provided together with their corresponding *P* values, with the first signifying comparison between COVID-19 participants at different time points, and the 2nd representing comparison between COVID-19 participants and controls.**

| Table 17: Cortical T1 and CMD in COVID-19 participants with and without AKI during admission. | | | | | | |
|---|---|---|---|---|---|---|
| | AKI during admission | | No AKI during admission | | *P*-values | |
| | Cortical T1 | CMD | Cortical T1 | CMD | Cortical T1 | CMD |
| 2-3 months | 1711.3 (89.7) | 317.7 (59.5) | 1582.3 (80.8) | 405.5 (83.4) | <0.001 | 0.016 |
| 6 months | 1619 (35.8) | 372.6 (47.5) | 1536.6 (69.6) | 433 (70.7) | 0.008 | 0.026 |
| 18 months | 1608.6 (81.6) | 366.8 (90.5) | 1536.5 (47.5) | 431.2 (62.5) | 0.025 | 0.10 |
| Data are mean (SD). P-values are from parametric tests. AKI = Acute kidney injury. CMD = Corticomedullary differentiation. | | | | | | |

| Table 18: Relationship between renal MRI parameters 2-3 months post-infection and eGFR at 2-3, 6 and 18 months post infection. | | |
|---|---|---|
| | Renal Cortical T1, 2-3m | CMD, 2-3m |
| eGFR, 2-3 months post infection | ρ=-0.44, *P*<0.001 | ρ=0.46, *P*<0.001 |
| eGFR, 6 months post infection | ρ=-0.63, *P*<0.001 | ρ=0.54, *P*<0.001 |
| eGFR, 18 months post infection | ρ=-0.68, *P*<0.001 | ρ=0.71, *P*<0.001 |
| ρ=Spearman's correlation coefficient, *P*=P-value. | | |

## Discussion

The main findings of the present study are as follows:

1) Acute hepatic injury during admission with COVID-19 was seen in a third of participants. Hepatic function improved on longitudinal assessment, with no evidence of hepatic dysfunction observed 18 months post infection.
2) Despite a low prevalence of hepatic dysfunction at 2-3 months post-COVID-19, participants had higher iron-corrected liver T1 which normalised over time.
3) Acute kidney injury was uncommon during admission with COVID-19 (observed in 10%). Despite this, there was a downward trajectory of renal function (assessed using eGFR) following infection, in contrast with their calculated predicted risk of chronic kidney disease.
4) 2-3 months post infection, participants had renal tissue abnormalities (elevated renal cortical T1 and reduced corticomedullary differentiation) on MR imaging. Despite resolution of elevated renal cortical T1 over time, evidence of impaired renal health (reduced corticomedullary differentiation on MRI) persisted.

Hepatic injury is a recognized acute complication of COVID-19, ranging in incidence from 1 to 53%.[159] In the present study, 1/3$^{rd}$ of COVID-19 participants had elevated hepatic markers fulfilling criteria of hepatic injury during their hospital admission, with the hepatocellular pattern being the most common type observed. Numerous studies have described similar findings, with predominant derangements of ALT/AST and a low incidence of elevations in alkaline phosphatase or GGT (markers indicative of a cholangiocyte pattern of hepatic injury). [160,161]

Longitudinal assessment revealed normalization of liver enzymes over time, with none of the participants having evidence of hepatic injury 18 months post-infection. Others have reported similar findings; in a longitudinal study of 594 patients discharged from hospital following admission with COVID-19, only 7.6% of patients had abnormal liver

function (defined as an ALT or AST above the upper limit of normal, and therefore not necessarily fulfilling acute liver injury criteria) compared to 43% during admission.[162] In a similar study providing more granular results, elevated hepatic markers above 2 times the upper limit of normal were rare 12 months post-discharge (ALT: 0.4%; AST: 0.4%; GGT: 0.9%). [53,163]

The pattern of hepatic injury and its trajectory over time provide important insights into the mechanisms contributing to hepatic injury during acute infection. Early in the pandemic, direct infection was postulated to contribute to liver injury, given the detection of SARS-CoV-2 RNA in faeces together with the known high ACE2 receptor density on the surface of cholangiocytes.[164] While Puelles and colleagues were successful in isolating SARS-CoV-2 RNA from liver tissue obtained at autopsy, tissue samples were ground prior to nucleic acid extraction, making it impossible to determine whether SARS-CoV-2 was localised within the intracellular environment.[165] Studies using immunohistochemistry and in-situ hybridisation (in liver samples obtained from both living and deceased patients) have thus far failed to demonstrate direct SARS-CoV-2 invasion of liver cells.[51,52] The fact that the incidence and magnitude of liver function test derangements are comparable between COVID-19 and influenza patients (with derangements appearing later in the course of COVID-19)[166] suggests that the liver is but a bystander of COVID-19 and not a direct target of SARS-CoV-2.[167] The predominant hepatocyte pattern of liver injury observed and reported by others, together with evidence of non-specific liver injury on post-mortem studies suggests that COVID-19 associated hepatic dysfunction is likely multifactorial and secondary to ischaemia, hepatotoxicity from drugs, and/or a deranged hypercoagulable state that frequently accompanies COVID-19.[51,52,168]

On MRI imaging of the liver, the most notable finding was an elevated iron-corrected T1 in participants 2-3 months post-infection compared with controls, which normalised

by 6 months. As previously described, iron-corrected T1 is a marker sensitive to the presence of inflammation, oedema and/or fibrosis.[153] Given that iron corrected T1 correlated with CRP 3 months post-infection and became comparable to controls by 6 months suggests a state of transitory inflammation/oedema shortly following infection which resolves with time. COVID-19 participants had a higher PDFF, a non-invasive measure of hepatic fat content, at all time points compared with controls (which approached statistical significance 18 months post-infection). Studies using ultrasound and CT have shown a high prevalence of hepatic steatosis/fatty liver disease during and following infection with COVID-19, raising the possibility that COVID-19 may lead to or promote the development of fatty liver disease.[169-171] While other infections like viral hepatitis, HIV, and Helicobacter pylori are known to be associated with hepatic steatosis,[172] the assertion that COVID-19 leads to fatty liver disease may run the risk of reverse causation bias. Fatty liver disease has been well established as a significant risk factor for severe COVID-19, with the risk of severe illness reported to be >6 times higher in the presence of obesity and concomitant fatty liver disease, and >3 times higher in the presence of fatty liver disease alone following adjustment for obesity, diabetes and metabolic syndrome.[173,174] The increased risk of severe COVID-19 in the presence of fatty liver disease has been postulated to be secondary to excessive release of inflammatory markers (such as IL-6, which is known to play a central role in the cytokine storm that typifies severe COVID-19 and has been found in higher concentrations in patients with fatty liver disease).[175]

While COVID-19 illness varies significantly in severity ranging from asymptomatic infection to critical illness with multiorgan dysfunction, AKI is a relatively common complication occurring in up to 46% in some studies, with a substantial number of patients requiring acute dialysis.[176] In the present study, longitudinal assessment revealed that COVID-19 participants who developed AKI during admission had lower

eGFR values compared to those without, and a significant number (both with and without AKI during their admission) had a downward trajectory in renal function over time (with 52% having a lower eGFR 18 months following infection compared to their initial assessment). Similarly, Gu and colleagues, in a cohort study comprising of 1734 patients previously hospitalized with COVID-19, observed reductions in eGFR (in both those with and without AKI during admission) 1 year following discharge, with patients who had COVID-19 associated AKI displaying a more dramatic reduction in renal function.[177] While AKI can occur in a number of diseases and is not a unique feature of COVID-19, recent evidence has revealed two important points:[178] First, COVID-19 associated AKI is accompanied by a greater decrease in eGFR compared to non-COVID-19 AKI. Second, patients with COVID-19 associated AKI were less likely to achieve renal recovery compared to patients with non-COVID-19 AKI.

Similarly, higher rates of AKI were seen in patients hospitalized with COVID-19 (23%) compared to controls hospitalized with Influenza A or B (13%).[179] These findings suggest that, separate to the numerous mechanisms that result in AKI within the context of a critical illness (such as hypotension and hypoxia), the unique tropism of SARS-CoV-2 for ACE2 receptor enriched proximal tubular cells and podocytes within the kidney (with SARS-CoV-2 RNA being detected within such cells in autoptic specimens)[180] may contribute to not only acute but also long-term derangements in renal health. The presence of fibrin thrombus within glomerular capillary loops on autoptic specimens, reminiscent of thrombotic microangiopathies,[181] a group of haematological diseases associated with hypercoagulability and endothelial dysfunction (features which are known to occur in COVID-19), could also play a role.

Another important finding of the present study was the dissociation between a validated mechanism to predict risk of chronic kidney disease and the actual outcomes of the COVID-19 participants recruited; no relationship was seen between CKD risk

and a significant reduction in eGFR over time. In fact, the 6 participants who showed the most significant drop in eGFR from 6-to-18 months had a low (5 participants) or mild (1 participant) risk of progression. This is in keeping with findings by Bowe and colleagues,[182] who describe a higher risk of AKI, greater longitudinal eGFR loss and higher prevalence of end-stage kidney disease in patients 1 year after COVID-19 diagnosis (in both hospitalized and non-hospitalised patients with or without COVID-19 associated AKI) compared with non-infected controls, with the authors concluding that renal follow-up should be integral to post-acute COVID-19 care pathways.

Separate to serological markers, the use of MRI imaging to assess renal health yielded important findings. 2-3 months following infection, participants had elevated renal cortical T1 values which correlated with CRP, becoming comparable to controls 6 months post infection. This is likely due to ongoing resolution of the acute inflammatory environment following discharge from hospital, similar to the myocardial T1 findings described previously. Additionally, renal cortical T1 2-3 months post-infection moderately-strongly inversely correlated with eGFR measured at all time points of the study, suggesting that participants with elevated renal cortical T1 shortly following discharge have higher magnitudes of renal impairment in the short and long term. Most surprising is the fact that a reduction in cortical T1 was not accompanied by an improvement in renal function. On the contrary, participants whose cortical T1 improved from 2-3 to 6 months post-infection suffered a drop in renal function. This suggests that while inflammation and/or oedema may be important contributors to acute renal dysfunction within the context of COVID-19, their resolution does not herald an improvement in renal health. Deranged inflammation, a hallmark of COVID-19, is known to result in tubulointerstitial fibrosis,[183] recognized as the final pathway common to all diseases that result in progressive renal dysfunction.[184] Jansen and colleagues observed increased interstitial fibrosis in the renal tissue of COVID-19

kidneys (all but 1 being post-mortem) compared to sex, age and comorbidity-matched controls (which included patients admitted to ITU with ARDS and influenza).[185] The potential presence of tubulointerstitial fibrosis following resolution of acute inflammation may also account for the persistent reduced corticomedullary differentiation observed in COVID-19 participants, a marker of renal health and influenced by the architecture of the renal extracellular matrix.[186]

## Clinical Implications

My data suggests that hepatic injury during acute COVID-19 resolves with time. A significant number of COVID-19 participants suffered a progressive deterioration in renal function post-infection. The use of a validated mechanism to predict the risk of renal dysfunction did not correctly identify participants whose renal function deteriorated over time. This suggests that renal function post moderate to severe COVID-19 should be monitored closely, especially in those who suffered an AKI during admission or developed severe illness.

## Study limitations

This was a single-centre study limited by a relatively small sample size. While not all COVID-19 participants returned for repeat assessment, the paired results provided show that dropout did not result in attrition bias. COVID-19 participants with significant co-morbidities were excluded from recruitment, which may limit the external validity of my study findings. Albuminuria was not assessed during the initial study visit, and therefore the risk of renal progression 2-3 months post-infection could not be assessed. However, as elevated cortical T1 was evident during this time point (which

improved significantly by 6 months), transient hyperalbuminuria could have been present, which would not have provided a true estimation of renal progression risk.

## Conclusion

In this chapter, moderate to severe COVID-19 was associated with significant rates of hepatic dysfunction and AKI during the acute phase. While blood and imaging markers of hepatic dysfunction resolved with time and are likely due to non-specific injury, a deterioration in renal function was observed in a significant number of COVID-19 participants. The tropism of SARS-CoV-2 for proximal tubular cells and podocytes is likely a unique mechanism of renal injury in COVID-19. Renal cortical T1 shortly after infection predicted renal function 18 months post-infection. Improvement in renal cortical T1 did not herald an improvement of renal function, suggesting that COVID-19 associated renal injury is progressive; this warrants further research and has significant clinical implications on the future care of such patients.

## Chapter 5 –Impact of COVID-19 on cerebral function, cognition, mental health and quality of life


### Abstract

Introduction: Acute neurological injury is a known feature of COVID-19, which may have long-term consequences on neurological function, cognition, mental health and quality of life.

Objectives: To assess for manifestations of neurological injury following moderate to severe COVID-19, as well as assess the longitudinal trajectory of cognition, mental health and quality of life following recovery from acute illness.

Methods and results: Fifty-eight patients with moderate to severe COVID-19 2-3 months post infection and 30 matched COVID-19 naïve controls underwent MRI brain imaging and completed questionnaires to assess cognition (MoCA), depression (PHQ-9), anxiety (GAD-7), quality of life (SF-36), symptom burden (PHQ-11), breathlessness (MRC dyspnoea scale) and fatigue (FSS). COVID-19 participants were invited for repeat imaging and qualitative questionnaire assessments 6 months and 18 months post-infection.

During admission, one participant suffered an acute ischaemic stroke. Longitudinal qualitative assessment of MR brain imaging did not reveal significant differences between COVID-19 participants and controls. At 2-3 months post infection, participants had lower total MoCA scores compared to controls (median 27 (25 – 29) vs median 28 (27-29)), and cognitive performance in the executive/visuospatial domain was impaired. COVID-19 participants had higher PHQ-9 and GAD-7 scores. By 6 months, participants displayed better cognitive performance and markers of depression and anxiety improved, becoming comparable to controls.

At 2-3 months post infection, participants had significant impairment in all quality of life domains. Longitudinal assessment revealed significant improvement in all

domains, although COVID-19 participants continued to suffer from reduced general health compared with controls 18 months post-infection. Similarly, while symptom burden was reduced by 18 months, COVID-19 participants continued to experience limiting breathlessness (40% experiencing dyspnoea when walking up a hill) which did not associate with ECG, CMR, lung function or CPET measures.

Conclusion: Cognition, mental health and quality of life improved following infection with moderate to severe COVID-19, although limitations due to reduced general health and breathlessness persisted. No relationship was seen between breathlessness and objective measures of cardiopulmonary health.

## Introduction

Early in the pandemic, alarmingly high rates of neurological symptoms associated with acute COVID-19 were reported, ranging in severity from dizziness to hemiplegia and loss of consciousness. Concomitantly, brain imaging during acute illness revealed unexpectedly high rates of acute cerebrovascular disease (predominantly ischaemic stroke).[187] As the pandemic progressed and global lockdowns were enforced, increased rates of anxiety and depression in the general population were noted.[188] Although the impact of psychological trauma (following the death of a loved one to disease) and reduced social interaction cannot be overlooked, evidence was published suggesting that COVID-19 itself may be a separate contributing biological factor for the high prevalence of mood symptoms.[189]

Previously published studies investigating the long-term outcomes of patients following infection during previous coronavirus outbreaks (SARS and MERS) describe high rates of mental morbidity (anxiety and depression), fatigue and reductions in quality of life up to four years post infection.[68,69]

Given the high rates of neurological sequalae reported early in the pandemic, together with the concerning outcomes of SARS and MERS survivors, I set out to investigate the longitudinal impact of moderate to severe COVID-19 on cerebral and mental health, cognition, quality of life and symptoms.

## Methods

### Brain MRI protocol

The neuroimaging protocol incorporated structural and functional sequences and lasted approximately 15 minutes. This included High-resolution T1-weighted Magnetization Prepared RApid Gradient Echo (MPRAGE), Fluid Attenuated Inversion Recovery (T2-FLAIR), Diffusion MRI (dMRI) and Susceptibility-weighted MR Imaging (3D-swMRI), as previously described in the methods.

### Brain MRI image analysis

All data were manually quality-control checked. Images were qualitatively assessed by an expert neuroradiologist. Images that passed quality control were assessed using a standard DICOM viewer for the following:

- Small vessel disease: This is a major component of white matter hyperintensities and appears as relatively well-defined, punctate lesions which typically spare the U-fibers and do not involve the cerebellum or corpus callosum. These lesions are associated with degeneration and ageing.[190] The FLAIR sequence was primarily used for initial evaluation and screening of small vessel disease. DWI and SWI sequences were used to provide additional information about the extent and severity of small vessel disease and were always used in combination during evaluation. Small vessel disease was reported as present or absent.
- Other white matter hyperintensities: These appear as less discrete and more diffusely distributed compared to small vessel disease, and usually represent other causes of inflammation and demyelination.[191] T2-FLAIR was the primary sequence used, supplemented by MPRAGE, DWI and SWI, which provided additional information about the extent and severity of white matter

hyperintensities. The severity of white matter hyperintensities was graded as mild, moderate or severe. The pattern of white matter hyperintensities was classified as subcortical, periventricular, deep, diffuse or mixed.

- Cortical signal/diffusion abnormalities: Restricted diffusion is a reliable marker of ischaemia/stroke.[192] The DWI sequence was used to determine cortical signal/diffusion abnormalities (which appear hyperintense), due to its sensitivity for detecting changes in the diffusion of water molecules in the cortex. T1 and T2-weighted sequences were used to provide additional information about the structure and composition of the tissues. Cortical diffusion abnormalities were reported as present or absent, and details provided in those with an abnormality present (such as extent and location).
- Brain volume: MPRAGE (T1-weighted) was used for the determination of brain volume/volume loss. T2-FLAIR also provided additional information about brain volume by identifying areas of tissue damage or atrophy. Brain volume was reported as normal, and in those with atrophy, this was graded as mild, moderate or severe.
- Haemorrhage: SWI was the primary sequence used. Given the diamagnetic properties of haemoglobin, haemorrhage results in a distortion of the magnetic field and appears bright on SWI images. MPRAGE and T2-FLAIR supplemented analysis by providing information about the age and location of haemorrhage, as well as any associated oedema or mass effect. Haemorrhage was reported as present or absent, with descriptive details provided in those with an abnormality.

### Questionnaires

The Patient Health Questionnaire-15 (PHQ-15), an instrument for assessing the burden of somatic symptoms, was used to assess for the presence of a number of symptoms common in patients following COVID-19.[86]

The MRC dyspnoea scale[87] was used to assess the effects of breathlessness on daily activities. This scale was used to measure perceived respiratory disability on a scale of 1 (no breathlessness) to 5 (unable to leave the house and breathless whilst dressing or undressing). Participants with a grade of 2 (unable to keep up with normal men/women their own age on the level, but able to walk about a mile or more at his/her own speed due to breathlessness) or above were defined as having limiting breathlessness.

The Fatigue Severity Scale (FSS) is a symptom-specific outcome scale aimed at providing a standardised quantification of fatigue burden.[88] The FSS comprises of nine statements, describing the severity and impact of fatigue, with a scale of possible responses ranging from 1 (“strongly disagree”) to 7 (“strongly agree”). FSS was reported as the mean score over the nine items; a higher mean score (≥4) was used to indicate significant fatigue.

The Generalised Anxiety Disorder Assessment (GAD-7), a seven-item instrument, was used to screen for and measure the severity of generalised anxiety disorder among participants.[89] Scores of 5, 10 and 15 were used as cut-offs for mild, moderate and severe anxiety, respectively.

The Patient Health Questionnaire depression module (PHQ-9),[90] a multipurpose instrument for screening, diagnosing and monitoring depression, was used to assess for evidence of depression. Scores of 5, 10, 15 and 20 were used as cut-offs mild, moderate, moderately severe and severe depression, respectively.

The 36-Item Short Form Survey (SF-36) assesses health status and quality of life. Scores for each domain (a total of 8) were calculated using the survey scoring instructions; all scores range from 0 (worst) to 100 (best), with higher scores indicating better quality of life.[91]

Cognitive function was assessed by using the Montreal Cognitive Assessment (MoCA) Tool, with scores ranging from 0 to 30 points .[92] A score of 18-25 is indicative of mild cognitive impairment, 10-17 is moderate, and <10 is severe.

### Data acquired

Of the 30 controls who attended a study visit, 28 underwent brain imaging (2 had severe claustrophobia precluding imaging). All 30 controls completed the full complement of questionnaires except for one participant, who was unable to complete the FSS due to having to leave the study appointment early.

Of the 58 COVID-19 participants who attended an initial study visit, 54 underwent brain imaging (4 had limiting claustrophobia). 55 completed the full complement of questionnaires; one participant only filled in the MOCA, while a further two did not fill in the FSS.

Of the 46 COVID-19 participants who attended a study visit 6 months following infection, 41 underwent diagnostic brain imaging (2 did not undergo imaging due to claustrophobia, 2 refused brain imaging due to claustrophobia with the head coil, and 1 had significant motion artefact). 45 participants answered all the questionnaires; one participant had to terminate the visit early due to a family emergency, and therefore was unable to provided questionnaire responses.

Of the 23 participants who attended a visit 18 months post-infection, all underwent brain imaging and filled in their questionnaires. In addition, some participants who were

unable to attend a third visit agreed to provide questionnaire responses over the phone. The following number of total responses were registered:

- SF36: 45
- MRC Dyspnoea Scale: 38
- FSS: 38
- PHQ15: 37
- GAD7 and PHQ9: 36

## Statistical Analyses and Definitions

Statistical analysis was performed as previously described.

Binomial logistic regression was performed to ascertain the effects of age, weight, sex, history of admission with COVID-19, history of hypertension, history of diabetes and smoking history on 1) the likelihood that participants have small vessel disease and 2) the likelihood that participants have other white matter hyperintensities on brain imaging. The logistic regression models were statistically significant ($\chi^2$ (8) = 42.72, $P< 0.01$ and $\chi^2$ (8) = 49.8, $P< 0.01$, respectively).

Binomial logistic regression was used to assess the effects of MRI brain parameters on the likelihood of cognitive impairment (defined as a MoCA score of ≤25) at 2-3- and 6-months post-infection. Brain volume (normal or reduced), small vessel disease (present or absent), other white matter hyperintensities (present or absent), and cortical diffusion abnormalities (present or absent) were included as independent variables. The logistic regression models were not statistically significant (2-3 months: $\chi^2$ (8) = 12.09, $P$=0.15; 6 months: $\chi^2$ (8) = 49.8, $P$=0.28, respectively).

Univariate and multivariate binary logistic regression were used to assess the association between limiting breathlessness (defined as an MRC dyspnoea scale score of ≥2) and objective measures of cardiopulmonary health at 2-3 months, 6

months and 18 months post-infection. To maintain the absence of collinearity, NT-proBNP (<125 ng/L or ≥125 ng/L), ECG (normal or abnormal), indexed left and right ventricular end diastolic volumes, left and right ventricular ejection fraction, mid myocardial T1, mid myocardial T2, volume of late gadolinium enhancement, FEV1, FVC, DLco, peak oxygen consumption and $\dot{V}E/\dot{V}CO_2$ slope were included as independent variables in the multivariate analysis. The Box-Tidwell test was used to demonstrate maintenance of linearity in the logit between the continuous independent variables and the dependent variable (limiting breathlessness).

## Results

### Cerebral injury during admission

As previously described, none of the participants had a past medical history of cerebral infarction or TIA. Three reported a history of mild depression.

During a prolonged admission (54 days) with acute COVID-19, one participant underwent a CT brain whilst intubated due to persistent high fevers. This revealed a large area of hypoattenuation within the left occipital lobe, consistent with a subacute left posterior cerebral artery infarct. Following extubation, the participant was noted to have a new right hemianopia consistent with the imaging findings. The participant was fit and well prior to infection, with no significant past medical history (including non-smoker).

### Findings from brain imaging

2-3 months post infection, brain volume was normal in most participants (96%), with only two having evidence of mild atrophy (aged 56 and 71 years). White matter hyperintensities compatible with small vessel disease were observed in 19/54 COVID-19 participants (35%), all mild in severity (Table 19). This was comparable with controls, with 6/28 (21%) having evidence of mild small vessel disease ($P$=0.14). Binomial logistic regression revealed that of all the variables used to predict the likelihood of small vessel disease, only age ($P$<0.001, Exp(B) 1.22) and history of diabetes ($P$<0.045, Exp(B) 14.042) were statistically significant predictors. Other white matter hyperintensities (mostly mild) were seen in 21/54 COVID-19 participants (39%), with the mixed pattern of distribution being most common. This was comparable to controls, with 6/28 (21%) having other white matter hyperintensities on brain imaging ($P=0.14$). In contrast to small vessel disease, only age was a statistically significant predictor ($P$<0.001, Exp(B) 1.27). One participant had diffusion

abnormalities on MRI, who was known to have suffered a right posterior cerebral artery infarct during admission. None had evidence of haemorrhage.

Repeated brain imaging at 6 months and 18 months post-infection was unremarkable, with no significant changes seen. There was no new onset (or resolution) of small vessel disease or white matter hyperintensities. None of the participants developed a new cerebral infarct or haemorrhage in the 18 month follow-up period.

Table 19: Brain MRI findings in COVID-19 participants and controls.

| | COVID-19, 2-3m (N=54) | Controls (N=28) | *P*-value |
|---|---|---|---|
| **Brain MRI imaging** | | | |
| Brain Volume | | | *0.60* |
| Normal | 52/54 (96.3%) | 26/28 (92.9%) | |
| Mild Atrophy | 2/54 (3.7%) | 2/28 (7.1%) | |
| Small Vessel Disease | 19/54 (35.2%) | 5/28 (17.9%) | *0.13* |
| Other WMH | 21/54 (38.9%) | 6/28 (21.4%) | *0.14* |
| Subcortical | 1/21 (4.8%) | 0/6 (0.0%) | |
| Periventricular | 4/21 (19.0%) | 1/6 (16.7%) | |
| Deep | 6/21 (28.6%) | 3/6 (50.0%) | |
| Diffuse | 0/21 (0.0%) | 1/6 (16.7%) | |
| Mixed | 10/21 (47.6%) | 1/6 (16.7%) | |
| Severity of other WMH | | | |
| Mild | 16/21 (76.2%) | 4/6 (66.7%) | |
| Moderate | 4/21 (19.0%) | 2/6 (33.3%) | |
| Severe | 1/21 (4.8%) | 0/6 (0.0%) | |
| Diffusion Abnormalities | 1/54 (1.9%) | 0/28 (0.0%) | *1.00* |
| Haemorrhage | 0/54 (0.0%) | 0/28 (0.0%) | .. |

Data are n/N (%), where N is the total number of participants with available data. Italicised P-values are from non-parametric tests. WMH = White matter hyperintensities.

## Cognitive assessment

At 2-3 months post infection, participants had lower total MoCA scores compared to controls (median 27 (25 – 29) vs median 28 (27-29)), although this failed to reach statistical significance (*P*=0.15). 16/58 (28%) had scores compatible with cognitive impairment, with the majority being mild in severity (Table 20). Cognitive performance in the executive/visuospatial domain was impaired in COVID-19 participants compared to controls (MoCA visuospatial score ≤4 in 40% of COVID-19 participants vs 16% in controls, *P*=0.01). Weak borderline significant inverse relationships were observed between total MoCA score and disease severity (ρ=-0.23, *P*=0.08) and between total MoCA score and admission time (ρ=-0.25, *P*=0.06).

By 6 months post infection, total MoCA scores improved (6m: median 29.0 (27.5 – 30.0); 2-3m: median 27.0 (26.0 – 29.0), *P*<0.001, Table 21). Total MoCA score increased in 30 participants (67%), remained the same in 9 (20%), and was lower in 5 (11%). Of interest, the participant who suffered a cerebral infarct during admission demonstrated the greatest improvement in cognition, with their MoCA score increasing from 6 to 20. The reduction in MoCA scores observed were small in magnitude (-1 in 4 participants (9%) and -2 in 2 (4%)); these occurred in participants who achieved high scores 2-3 months post-infection and did not fulfil criteria of cognitive impairment at 6 months. Only 4 participants (9%) had evidence of mild cognitive impairment. COVID-19 participants demonstrated a significant improvement in visuospatial, language and delayed recall scores. When compared with controls, no differences were seen.

A binomial logistic regression model was used to assess the effects of COVID-19 severity and MRI brain abnormalities on the likelihood of cognitive impairment (a MoCA score of ≤25). Neither disease severity nor presence of small vessel disease, other

white matter hyperintensities, diffusion abnormalities or reduced brain volume predicted cognitive impairment (range of *P*-values for individual predictor variables: 2-3 months: 0.53 – 1.00; 6 months: 0.99 – 1.00).

| Table 20: MoCA scores in COVID-19 participants 2-3 months post-infection and controls. | | | |
|---|---|---|---|
| | COVID-19, 2-3m (N=58) | Controls (N=30) | *P*-value |
| **Visuospatial (Max score 5)** | **5.0 (4.0 - 5.0)** | **5.0 (5.0 - 5.0)** | ***0.017*** |
| 5 | 34/58 (58.6%) | 25/30 (83.3%) | *0.10* |
| 4 | 15/58 (25.9%) | 4/30 (13.3%) | |
| 3 | 8/58 (13.8%) | 1/30 (3.3%) | |
| 2 | 0/58 (0.0%) | 0/30 (0.0%) | |
| 1 | 1/58 (1.7%) | 0/30 (0.0%) | |
| 0 | 0/58 (0.0%) | 0/30 (0.0%) | |
| **Naming (Max score 3)** | **3.0 (3.0 - 3.0)** | **3.0 (3.0 - 3.0)** | ***0.30*** |
| 3 | 54/58 (93.1%) | 30/30 (100%) | *0.70* |
| 2 | 3/58 (5.2%) | 0/30 (0.0%) | |
| 1 | 0/58 (0.0%) | 0/30 (0.0%) | |
| 0 | 1/58 (1.7%) | 0/30 (0.0%) | |
| **Attention (Max score 6)** | **6.0 (4.8 - 6.0)** | **6.0 (5.0 - 6.0)** | ***0.53*** |
| 6 | 35/58 (60.3%) | 20/30 (66.7%) | *0.99* |
| 5 | 9/58 (15.5%) | 4/30 (13.3%) | |
| 4 | 8/58 (13.8%) | 4/30 (13.3%) | |
| 3 | 3/58 (5.2%) | 2/30 (6.7%) | |
| 2 | 2/58 (3.4%) | 0/30 (0.0%) | |
| 1 | 1/58 (1.7%) | 0/30 (0.0%) | |
| 0 | 0/58 (0.0%) | 0/30 (0.0%) | |
| **Language (Max score 3)** | **3.0 (2.0 - 3.0)** | **3.0 (2.0 - 3.0)** | ***0.38*** |
| 3 | 32/58 (55.2%) | 20/30 (66.7%) | *0.60* |
| 2 | 17/58 (29.3%) | 6/30 (20.0%) | |
| 1 | 9/58 (15.5%) | 4/30 (13.3%) | |
| 0 | 0/58 (0.0%) | 0/30 (0.0%) | |
| **Abstraction (Max score 2)** | **2.0 (2.0 - 2.0)** | **2.0 (2.0 - 2.0)** | ***0.45*** |
| 2 | 50/58 (86.2%) | 28/30 (93.3%) | *0.81* |
| 1 | 7/58 (12.1%) | 2/30 (6.7%) | |
| 0 | 1/58 (1.7%) | 0/30 (0.0%) | |
| **Delayed Recall (Max score 5)** | **4.0 (3.0 - 5.0)** | **4.0 (3.0 - 5.0)** | ***0.43*** |
| 5 | 19/58 (32.8%) | 12/30 (40.0%) | *0.29* |
| 4 | 12/58 (20.7%) | 6/30 (20.0%) | |
| 3 | 14/58 (24.1%) | 6/30 (20.0%) | |
| 2 | 5/58 (8.6%) | 4/30 (13.3%) | |
| 1 | 1/58 (1.7%) | 2/30 (6.7%) | |
| 0 | 7/58 (12.1%) | 0/30 (0.0%) | |
| **Orientation (Max score 6)** | **6.0 (6.0 - 6.0)** | **6.0 (6.0 - 6.0)** | ***0.55*** |
| 6 | 56/58 (96.6%) | 30/30 (100%) | *1.00* |
| 5 | 1/58 (1.7%) | 0/30 (0.0%) | |
| 4 | 1/58 (1.7%) | 0/30 (0.0%) | |
| 3 | 0/58 (0.0%) | 0/30 (0.0%) | |
| 2 | 0/58 (0.0%) | 0/30 (0.0%) | |
| 1 | 0/58 (0.0%) | 0/30 (0.0%) | |
| 0 | 0/58 (0.0%) | 0/30 (0.0%) | |
| **Total Score (Max 30)** | **27.0 (25.0 - 29.0)** | **28.0 (26.8 - 29.3)** | ***0.15*** |
| Normal cognition (≥26) | 42/58 (72.4%) | 25/30 (83.3%) | *0.42* |
| Mild Impairment (18-25) | 14/58 (24.1%) | 5/30 (16.7%) | |
| Moderate Impairment (10-17) | 2/58 (3.4%) | 0/30 (0.0%) | |
| Severe Impairment (<10) | 0/58 (0.0%) | 0/30 (0.0%) | |

Data are n/N (%), where N is the total number of participants with available data. Italicised P-values are from non-parametric tests.

Table 21: MoCA scores in COVID-19 participants 2-3 months and 6 months post-infection (paired) and controls.

| | COVID-19, 2-3m (N=45) | COVID-19, 6m (N=45) | Controls (N=30) | *P*-values | |
|---|---|---|---|---|---|
| | | | | 2-3m vs 6m | 6m vs Controls |
| **Visuospatial (Max score 5)** | **5.0 (4.0 - 5.0)** | **5.0 (5.0 - 5.0)** | **5.0 (5.0 - 5.0)** | ***0.03*** | ***0.65*** |
| 5 | 26/45 (57.8%) | 36/45 (80.0%) | 25/30 (83.3%) | *0.03* | 0.94 |
| 4 | 13/45 (28.9%) | 5/45 (11.1%) | 4/30 (13.3%) | | |
| 3 | 5/45 (13.3) | 3/45 (6.7%) | 1/30 (3.3%) | | |
| 2 | 0/45 (0.0%) | 1/45 (2.2%) | 0/30 (0.0%) | | |
| 1 | 0/45 (0.0%) | 0/45 (0.0%) | 0/30 (0.0%) | | |
| 0 | 0/45 (0.0%) | 0/45 (0.0%) | 0/30 (0.0%) | | |
| **Naming (Max score 3)** | **3.0 (3.0 - 3.0)** | **3.0 (3.0 - 3.0)** | **3.0 (3.0 - 3.0)** | ***0.75*** | ***1.00*** |
| 3 | 43/35 (95.6%) | 44/45 (97.8%) | 30/30 (100%) | *0.75* | 1.00 |
| 2 | 1/45 (2.2%) | 1/45 (2.2%) | 0/30 (0.0%) | | |
| 1 | 0/45 (0.0%) | 0/45 (0.0%) | 0/30 (0.0%) | | |
| 0 | 1/45 (2.2%) | 0/45 (0.0%) | 0/30 (0.0%) | | |
| **Attention (Max score 6)** | **6.0 (5.0 - 6.0)** | **6.0 (6.0 - 6.0)** | **6.0 (5.0 - 6.0)** | ***0.09*** | ***0.27*** |
| 6 | 29/45 (64.4%) | 35/45 (77.8%) | 20/30 (66.7%) | *0.09* | 0.67 |
| 5 | 8/45 (17.8%) | 5/45 (11.1) | 4/30 (13.3%) | | |
| 4 | 6/45 (13.3%) | 4/45 (8.9%) | 4/30 (13.3%) | | |
| 3 | 1/45 (2.2%) | 1/45 (2.2%) | 2/30 (6.7%) | | |
| 2 | 0/45 (0.0%) | 0/45 (0.0%) | 0/30 (0.0%) | | |
| 1 | 1/45 (2.2%) | 0/45 (0.0%) | 0/30 (0.0%) | | |
| 0 | 0/45 (0.0%) | 0/45 (0.0%) | 0/30 (0.0%) | | |
| **Language (Max score 3)** | **3.0 (2.0 - 3.0)** | **3.0 (2.5 - 3.0)** | **3.0 (2.0 - 3.0)** | **0.002** | **0.34** |
| 3 | 26/45 (57.8%) | 34/45 (75.6%) | 20/30 (66.7%) | *0.002* | 0.39 |
| 2 | 11/45 (24.4%) | 9/45 (20.0%) | 6/30 (20.0%) | | |
| 1 | 8/45 (17.8%) | 2/45 (4.4%) | 4/30 (13.3%) | | |
| 0 | 0/45 (0.0%) | 0/45 (0.0%) | 0/30 (0.0%) | | |
| **Abstraction (Max score 2)** | **2.0 (2.0 - 2.0)** | **2.0 (2.0 - 2.0)** | **2.0 (2.0 - 2.0)** | **0.77** | **0.79** |
| 2 | 39/45 (86.7%) | 42/45 (93.3%) | 28/30 (93.3%) | *0.77* | 0.49 |
| 1 | 5/45 (11.1%) | 1/45 (2.2%) | 2/30 (6.7%) | | |
| 0 | 1/45 (0.0%) | 2/45 (4.4%) | 0/30 (0.0%) | | |
| **Delayed Recall (Max score 5)** | **4.0 (3.0 - 5.0)** | **5.0 (3.0 - 5.0)** | **4.0 (3.0 - 5.0)** | ***0.008*** | **0.26** |
| 5 | 14/45 (31.1%) | 24/45 (53.3%) | 12/30 (40.0%) | *0.008* | 0.45 |
| 4 | 11/45 (24.4%) | 6/45 (13.3%) | 6/30 (20.0%) | | |
| 3 | 12/45 (26.7%) | 11/45 (24.4%) | 6/30 (20.0%) | | |
| 2 | 4/45 (8.9%) | 2/45 (4.4%) | 4/30 (13.3%) | | |
| 1 | 0/45 (0.0%) | 1/45 (2.2%) | 2/30 (6.7%) | | |
| 0 | 4/45 (8.9%) | 1/45 (2.2%) | 0/30 (0.0%) | | |
| **Orientation (Max score 6)** | **6.0 (6.0 - 6.0)** | **6.0 (6.0 - 6.0)** | **6.0 (6.0 - 6.0)** | ***1.00*** | **1.00** |
| 6 | 44/45 (97.8%) | 44/45 (97.8%) | 30/30 (100%) | *1.00* | 1.00 |
| 5 | 0/45 (0.0%) | 1/45 (2.2%) | 0/30 (0.0%) | | |
| 4 | 1/45 (2.2%) | 0/45 (0.0%) | 0/30 (0.0%) | | |
| 3 | 0/45 (0.0%) | 0/45 (0.0%) | 0/30 (0.0%) | | |
| 2 | 0/45 (0.0%) | 0/45 (0.0%) | 0/30 (0.0%) | | |
| 1 | 0/45 (0.0%) | 0/45 (0.0%) | 0/30 (0.0%) | | |
| 0 | 0/45 (0.0%) | 0/45 (0.0%) | 0/30 (0.0%) | | |
| **Total Score (Max 30)** | **27.0 (26.0 - 29.0)** | **29.0 (27.5 - 30.0)** | **28.0 (26.8 - 29.3)** | ***<0.001*** | ***0.10*** |
| Normal cognition (≥26) | 35/45 (77.8%) | 41/45 (91.1%) | 25/30 (83.3%) | *0.016* | 0.47 |
| Mild Impairment (18-25) | 9/45 (20.0%) | 4/45 (8.9%) | 5/30 (16.7%) | | |
| Moderate Impairment (10-17) | 1/45 (2.2%) | 0/45 (0.0%) | 0/30 (0.0%) | | |
| Severe Impairment (<10) | 0/45 (0.0%) | 0/45 (0.0%) | 0/30 (0.0%) | | |

Data are n/N (%), where N is the total number of participants with available data. Italicised P-values are from non-parametric tests. MoCA was not assessed at 18 months as they had normalised by 6 months.

## Mental health

At 2-3 months post-infection, participants had higher cumulative self-reported symptom scores for depression (median PHQ-9 score 3 vs 1.5 in controls, *P*=0.008, Table 22). Symptom scores for anxiety also tended to be higher (GAD-7 median score 2.0 vs 0.5 in controls, *P*=0.067). 11/58 COVID-19 participants (19%) reported symptoms of moderate to severe depression, and 8/58 (14%) reported symptoms compatible with moderate to severe anxiety. While no associations between disease severity and cumulative scores for depression and anxiety were seen (ρ[disease severity x PHQ-9 score] = 0.19, *P*=0.16; ρ[disease severity x GAD-7 score]=0.05, *P*=0.73), a weak association between admission time (in days) and depression scores was observed (ρ=0.37, *P*=0.005).

By 6 months post-infection, cumulative self-reported symptom scores for both depression and anxiety improved (median PHQ-9 2.0 vs 4.0, *P*=0.030, median GAD7 1.0 vs 2.0, *P*=0.020), with more participants reporting no significant symptoms of anxiety or depression (Table 23, Figures 24 and 25). COVID-19 participants had comparable cumulative scores with controls (*P*=0.51 and *P*=0.66 for PHQ-9 and GAD-7 scores versus controls, respectively).

By 18 months, COVID-19 participants achieved similar PHQ-9 and GAD-7 scores, with no significant changes seen (Table 24, Figures 24 and 25).

| Table 22: PHQ-9 and GAD-7 scores in COVID-19 participants 2-3 months post-infection and controls. | | | |
|---|---|---|---|
| | COVID-19, 2-3m (N=57) | Controls (N=30) | *P*-value |
| PHQ-9 Score | 3.0 (1.0 - 7.5) | 1.5 (0.0 - 5.0) | *0·008* |
| 0 - 4 (None) | 33/57 (57.9%) | 21/30 (70.0%) | *0.28* |
| 5-9 (Mild) | 13/57 (22.8%) | 8/30 (26.7%) | |
| 10 - 14 (Moderate) | 7/57 (12.3%) | 1/30 (3.3%) | |
| 15-19 (Moderately severe) | 4/57 (7.0%) | 0/30 (0.0%) | |
| 20-27 (Severe) | 0/57 (0.0%) | 0/30 (0.0%) | |
| GAD-7 Score | 2.0 (0.0 - 7.5) | 0.5 (0.0 - 4.3) | *0.067* |
| 0 - 4 (Minimal) | 35/57 (61.4%) | 23/30 (76.7%) | *0.34* |
| 5-9 (Mild) | 14/57 (24.6%) | 6/30 (20.0%) | |
| 10 - 14 (Moderate) | 3/57 (5.3%) | 1/30 (3.3%) | |
| ≥15 (Severe) | 5/57 (8.8%) | 0/30 (0.0%) | |
| Data are median (IQR) and n/N (%), where N is the total number of participants with available data. Italicised P-values are from non-parametric tests. PHQ-9 = Patient Health Questionnaire-9. GAD-7 = Generalised Anxiety Disorder-7 item scale. | | | |

| Table 23: Paired PHQ-9 and GAD-7 scores in COVID-19 participants 2-3 and 6 months post-infection. | | | |
|---|---|---|---|
| | COVID-19, 2-3m (N=44) | COVID-19, 6m (N=44) | *P*-value |
| PHQ-9 Score | 4.0 (2.0 - 7.8) | 2.0 (0.0 - 7.0) | *0.030* |
| 0 - 4 (None) | 24/44 (54.5%) | 30/44 (68.2%) | *0.061* |
| 5-9 (Mild) | 11/44 (25.0%) | 8/44 (18.2%) | |
| 10 - 14 (Moderate) | 5/44 (11.4%) | 2/44 (4.5%) | |
| 15-19 (Moderately severe) | 4/44 (9.1%) | 4/44 (9.1%) | |
| 20-27 (Severe) | 0/44 (0.0%) | 0/44 (0.0%) | |
| GAD-7 Score | 2.0 (0.0 - 7.8) | 1.0 (0.0 - 6.0) | *0.020* |
| 0 - 4 (Minimal) | 28/44 (63.6%) | 31/44 (70.5%) | *0.14* |
| 5-9 (Mild) | 9/44 (20.5%) | 7/44 (15.9%) | |
| 10 - 14 (Moderate) | 2/44 (4.5%) | 6/44 (13.6%) | |
| ≥15 (Severe) | 5/44 (11.4%) | 0/44 (0.0%) | |
| Data are median (IQR) and n/N (%), where N is the total number of participants with available data. Italicised P-values are from non-parametric tests. PHQ-9 = Patient Health Questionnaire-9. GAD-7 = Generalised Anxiety Disorder-7 item scale. | | | |

| Table 24: Paired PHQ-9 and GAD-7 scores in COVID-19 participants 6 and 18 months post-infection. | | | |
|---|---|---|---|
| | COVID-19, 6m (N=34) | COVID-19, 18m (N=34) | *P*-value |
| PHQ-9 Score | 2.0 (0.0 - 5.5) | 1.0 (0.0 - 7.3) | *0.32* |
| 0 - 4 (None) | 24/34 (70.6%) | 24/34 (70.6%) | *1.00* |
| 5-9 (Mild) | 6/34 (17.6%) | 5/34 (14.7%) | |
| 10 - 14 (Moderate) | 1/34 (2.9%) | 2/34 (5.9%) | |
| 15-19 (Moderately severe) | 3/34 (8.8%) | 3/34 (8.8%) | |
| 20-27 (Severe) | 0/34 (0.0%) | 0/34 (0.0%) | |
| GAD-7 Score | 1.0 (0.0 - 6.3) | 0.5 (0.0 - 4.8) | *0.98* |
| 0 - 4 (Minimal) | 24/34 (70.6%) | 26/34 (76.5%) | *1.00* |
| 5-9 (Mild) | 6/34 (17.6%) | 4/34 (11.8%) | |
| 10 - 14 (Moderate) | 4/34 (11/8%) | 3/34 (8.8%) | |
| ≥15 (Severe) | 0/34 (0.0%) | 1/34 (2.9%) | |

Data are median (IQR) and n/N (%), where N is the total number of participants with available data. Italicised P-values are from non-parametric tests. PHQ-9 = Patient Health Questionnaire-9. GAD-7 = Generalised Anxiety Disorder-7 item scale.

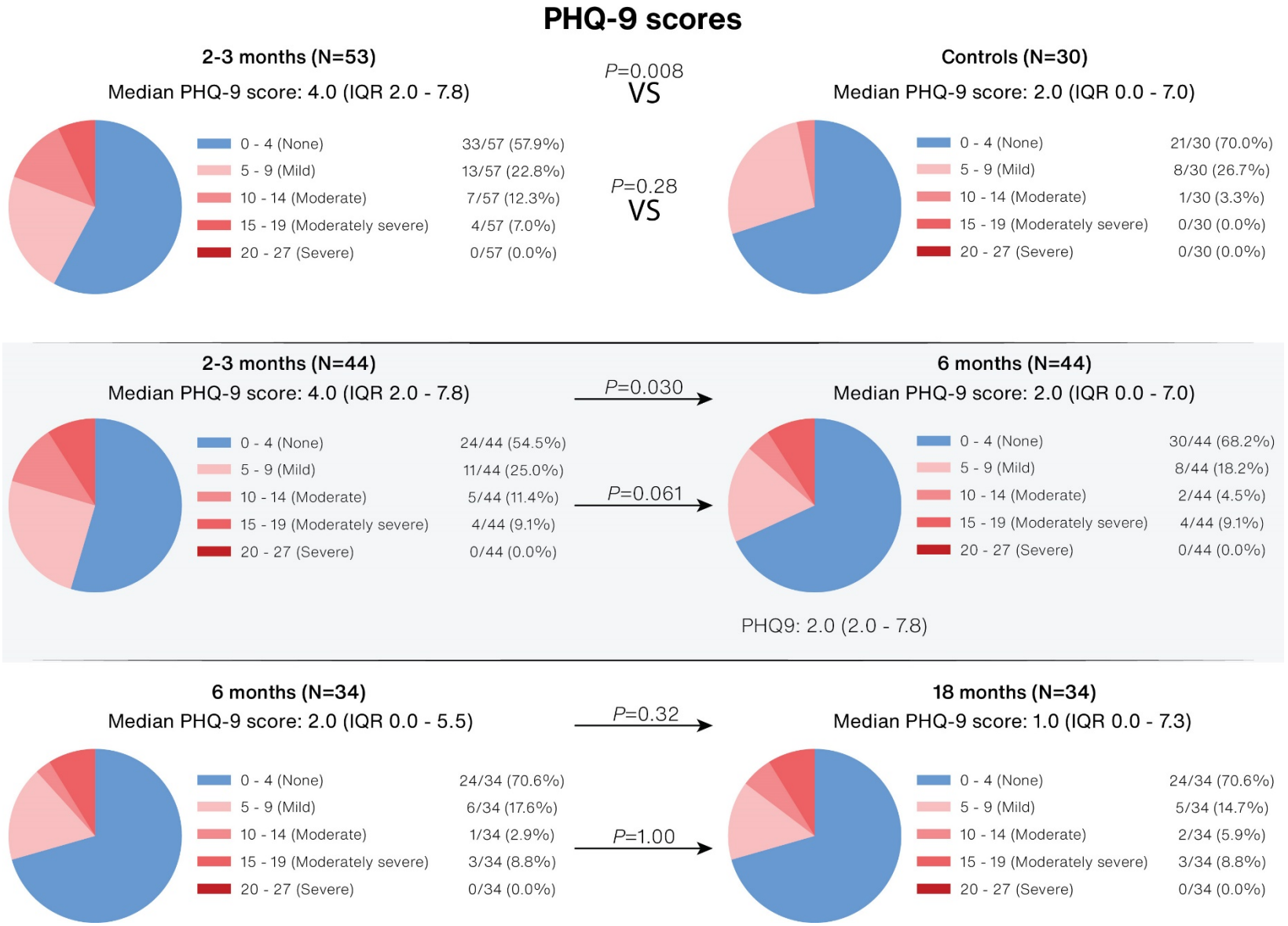


**Figure 24. PHQ-9 scores in patients 2-3 months post infection versus controls (1st row), change in PHQ-9 scores from 2-3 months to 6 months post-infection (2nd row), and change in PHQ-9 scores from 6 months to 18 months post infection (3rd row).**

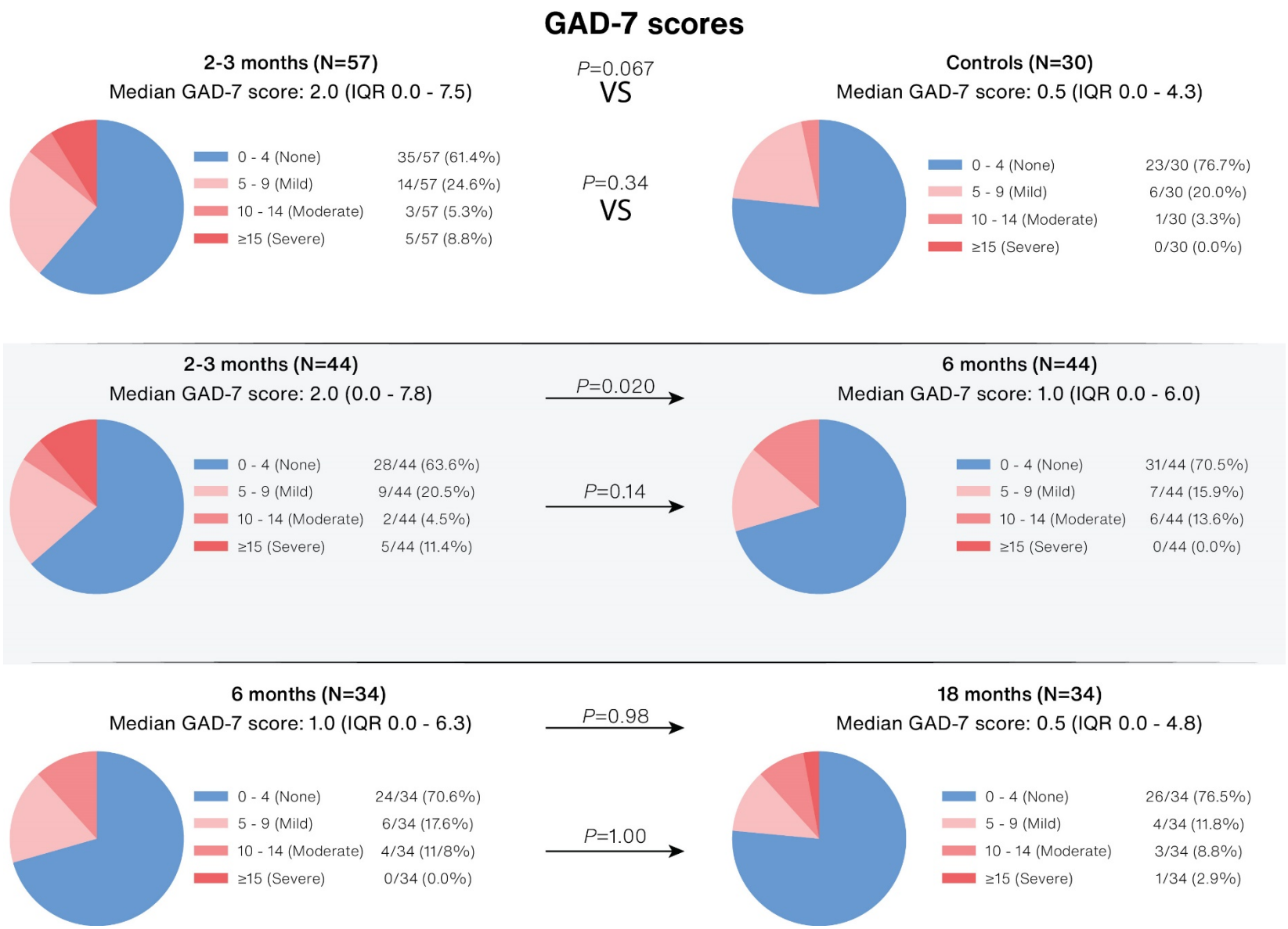


**Figure 25. GAD-7 scores in patients 2-3 months post infection versus controls (1st row), change in PHQ-9 scores from 2-3 months to 6 months post-infection (2nd row), and change in PHQ-9 scores from 6 months to 18 months post infection (3rd row).**

### Quality of life

2-3 months post infection, participants reported significantly reduced quality of life measures as assessed using the SF-36 questionnaire when compared with controls (Figure 26). Role limitations due to physical health and emotional problems, as well as reduced energy were the life-domains most severely impacted. No relationship was seen between quality of life measures and age or sex. While a weak correlation was seen between disease severity and physical functioning ($\rho$=-0.38, *P*=0.004), such a relationship was not seen with the other quality of life domains (all *P*-values >0.15).

By 6 months post infection, participants underwent a statistically significant improvement in all quality of life measures except general health (Figure 26). Despite this, role limitations due to physical health and emotional problems and reduced physical functioning continued to be more prevalent in COVID-19 participants compared to controls. Further, less dramatic improvements were seen from 6-to-18 months post-infection. COVID-19 participants differed most from controls in role limitations due to physical health, with 13 COVID-19 participants (28.9%) achieving the lowest score possible (zero) compared to only 1 control (2.2%, Figure 27). Of interest, there was no difference in disease severity (*P*=0.77), age (*P*=0.25) or sex (*P*=0.74) between the 13 COVID-19 participants with the lowest score compared to those with higher scores.

a) COVID-19, 2-3 months vs Controls

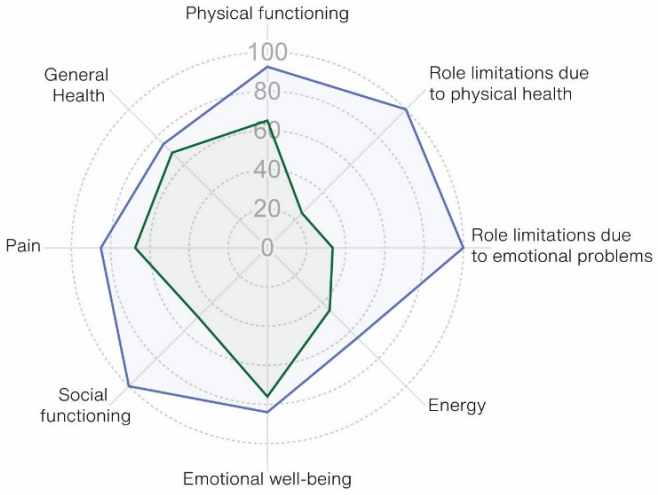


| | COVID-19,2-3m (N=58) | Controls (N=30) | P-value |
|---|---|---|---|
| Physical Functioning | 65.0 (45.0 -90.0) | 92.5 (83.8 - 100.0) | <0.001 |
| Role limitations due to physical health | 25.0 (0.0 -75.0) | 100.0 (100.0 - 100.0) | <0.001 |
| Role limitations due to emotional problems | 33.3 (0.0 -100.0) | 100.0 (100.0 - 100.0) | <0.001 |
| Energy | 45.0 (25.0 - 70.0) | 65.0 (55.0 - 80.0) | <0.001 |
| Emotional well-being | 76.0 (62.0 - 88.0) | 84.0 (72.0 - 92.0) | 0.044 |
| Social functioning | 50.0 (37.5 - 87.5) | 100.0 (62.5 - 100.0) | <0.001 |
| Pain | 67.5 (35.0 - 90.0 | 85.0 (67.5 - 100.0) | 0.003 |
| General Health | 68.8 (43.8 - 81.3) | 75.0 (60.9 - 87.5) | 0.035 |

COVID-19, 2-3 months
Controls

b) COVID-19, 2-3 months to 6 months post-infection

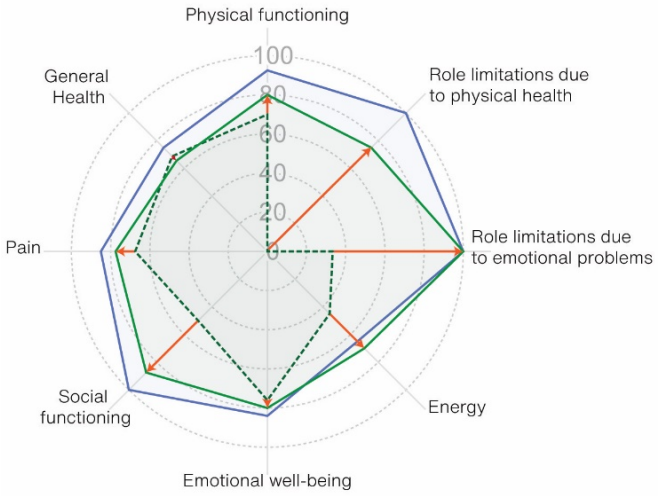


| | COVID-19,2-3m (N=44) | COVID-19,6m (N=44) | P-values 2-3 vs 6m | P-values 6m vs Controls |
|---|---|---|---|---|
| Physical Functioning | 70.0 (41.3 - 90.0) | 80.0 (60.0 - 95.0) | <0.001 | 0.009 |
| Role limitations due to physical health | 0.0 (0.0 - 75.0) | 75.0 (25.0 - 100.0) | <0.001 | 0.001 |
| Role limitations due to emotional problems | 33.3 (0.0 - 100.0) | 100.0 (33.3 - 100.0) | <0.001 | 0.034 |
| Energy | 45.0 (26.3 - 70.0) | 70.0 (38.8 - 78.8) | <0.001 | 0.31 |
| Emotional well-being | 76.0 (65.0 - 87.0) | 80.0 (68.0 - 92.0) | 0.083 | 0.57 |
| Social functioning | 50.0 (37.5 - 87.5) | 87.5 (53.1 - 100.0) | <0.001 | 0.29 |
| Pain | 67.5 (33.1 - 89.4) | 77.5 (45.0 - 100.0) | 0.036 | 0.17 |
| General Health | 68.8 (37.5 - 79.7) | 65.5 (43.8 - 87.5) | 0.16 | 0.22 |

COVID-19, 2-3 months
COVID-19, 6 months
Controls

c) COVID-19, 6 months to 18 months post-infection

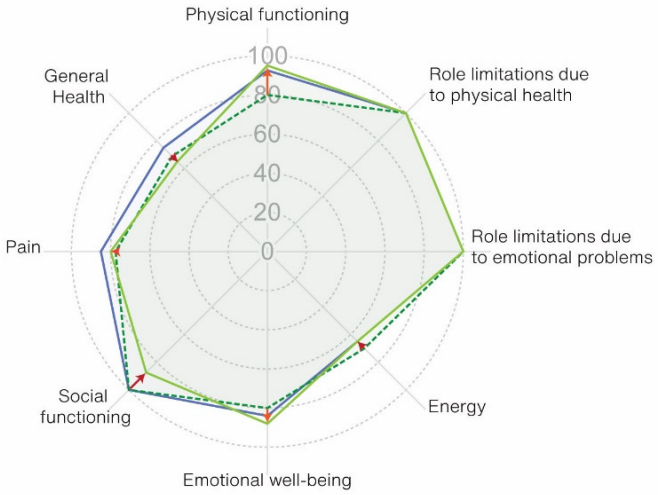


| | COVID-19,6m (N=39) | COVID-19,18m (N=39) | P-values 6m vs 18m | P-values 18m vs Controls |
|---|---|---|---|---|
| Physical Functioning | 80.0 (60.0 - 95.0) | 95.0 (75.0 - 100.0) | 0.034 | 0.35 |
| Role limitations due to physical health | 100.0 (25.0 - 100.0) | 100.0 (0.00 - 100.0) | 0.72 | 0.008 |
| Role limitations due to emotional problems | 100.0 (33.3 - 100.0) | 100.0 (100.0 - 100.0) | 0.068 | 0.82 |
| Energy | 70.0 (50.0 - 75.0) | 65.0 (25.0 - 80.0) | 0.054 | 0.049 |
| Emotional well-being | 80.0 (68.0 - 92.0) | 88.0 (72.0 - 92.0) | 0.041 | 0.67 |
| Social functioning | 100.0 (62.5 - 100.0) | 87.5 (50.0 - 100.0) | 0.45 | 0.085 |
| Pain | 77.5 (57.5 - 100.0) | 80.0 (45.0 - 100.0) | 0.64 | 0.24 |
| General Health | 68.8 (43.8 - 87.5) | 65.0 (45.0 - 85.0) | 0.96 | 0.03 |

COVID-19, 6 months
COVID-19, 18 months
Controls

**Figure 26. Quality of life (Short Form-36) radar plots, showing median scores for a) COVID-19 participants 2-3 months post-infection and controls, b) Paired changes for COVID-19 participants from 2-3 to 6 months post-infection and c) paired changes for COVID-19 participants from 6 to 18 months post-infection. Orange arrows indicate improvement, while red arrows indicate deterioration. Accompanying tables show median and IQR for each domain. *P*-values from non-parametric tests.**

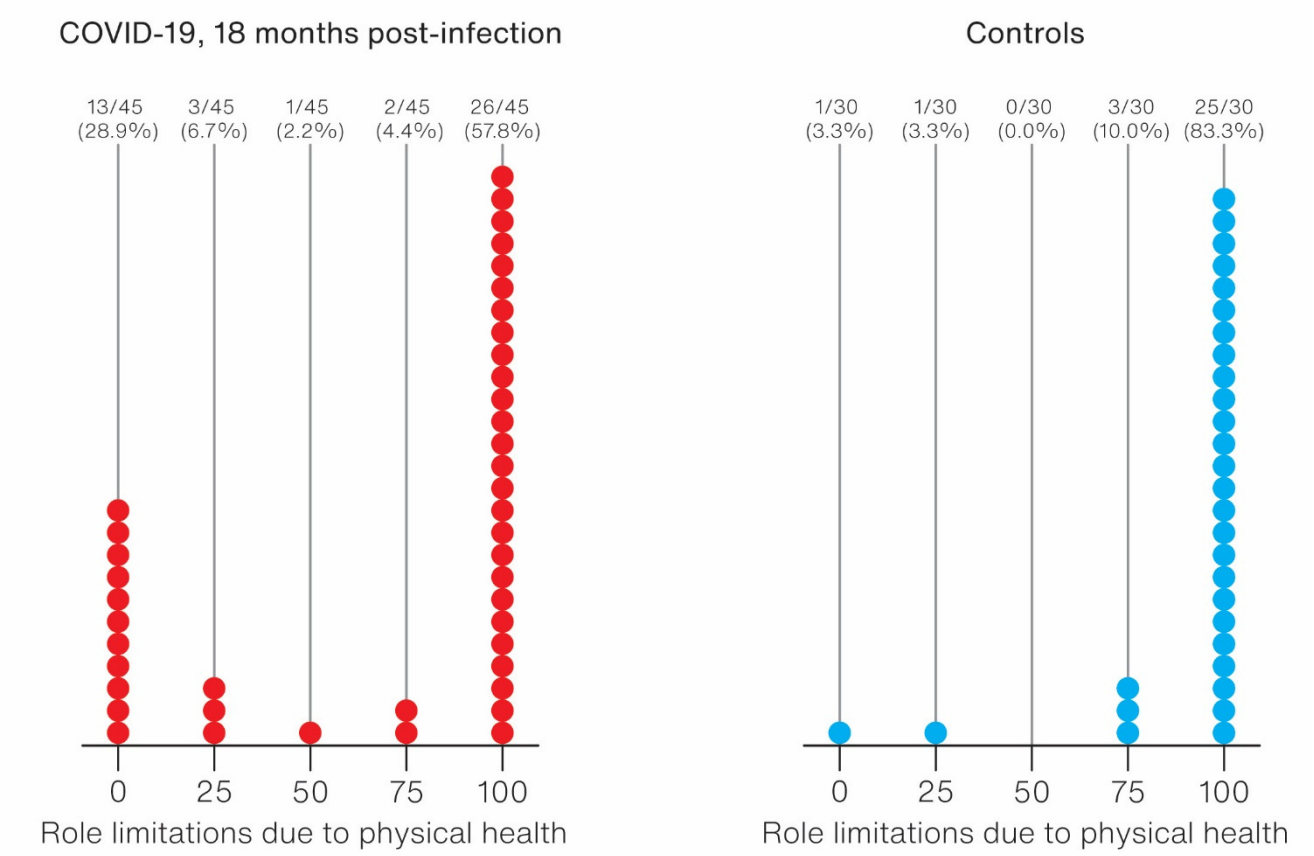


**Figure 27. Abacus-style bar charts showing the distribution of "Role limitations due to physical health" scores achieved by COVID-19 participants 18 months post infection and controls. Despite identical medians in both groups, a significant number of COVID-19 participants continued to have impaired quality of life due to their physical health.**

### Symptoms

At 2-3 months post infection, COVID-19 participants experienced a vast range of symptoms (Figure 28A), with breathlessness and limb/joint pain (assessed using the PHQ-15 questionnaire) being the most frequently reported. In comparison to the control group, the presence of breathlessness was the most distinctive difference observed, with 79% of participants reporting this symptom compared to only 10% of controls ($P<0.001$).

By 6 months post-infection, sleep disturbance became the most frequently reported symptom (experienced by 63%, Figure 28B), although its burden did not differ significantly from controls (53%, $P=0.35$). Encouragingly, a significant improvement in breathlessness was observed, with a near 50% reduction in the frequency of COVID-19 participants reporting shortness of breath ($P<0.0001$).

At 18 months post-infection, no significant change in symptom burden was observed (Figure 28C). The burden of breathlessness remained higher among COVID-19 participants compared to controls (47% vs 10%; $P=0.001$), whereas all other symptoms were similar across COVID-19 participants and controls.

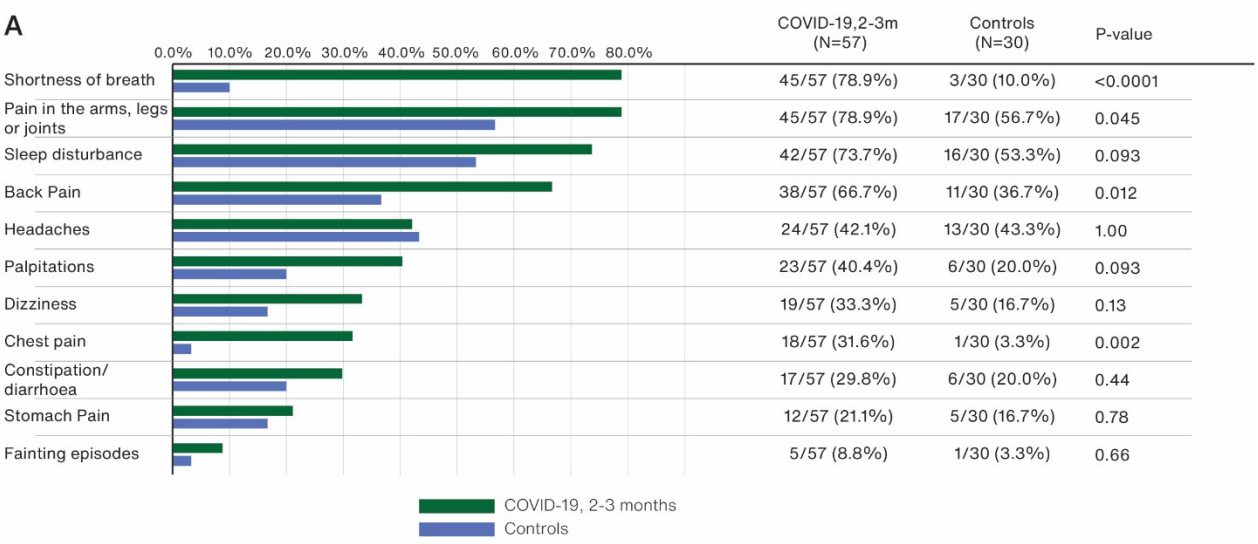


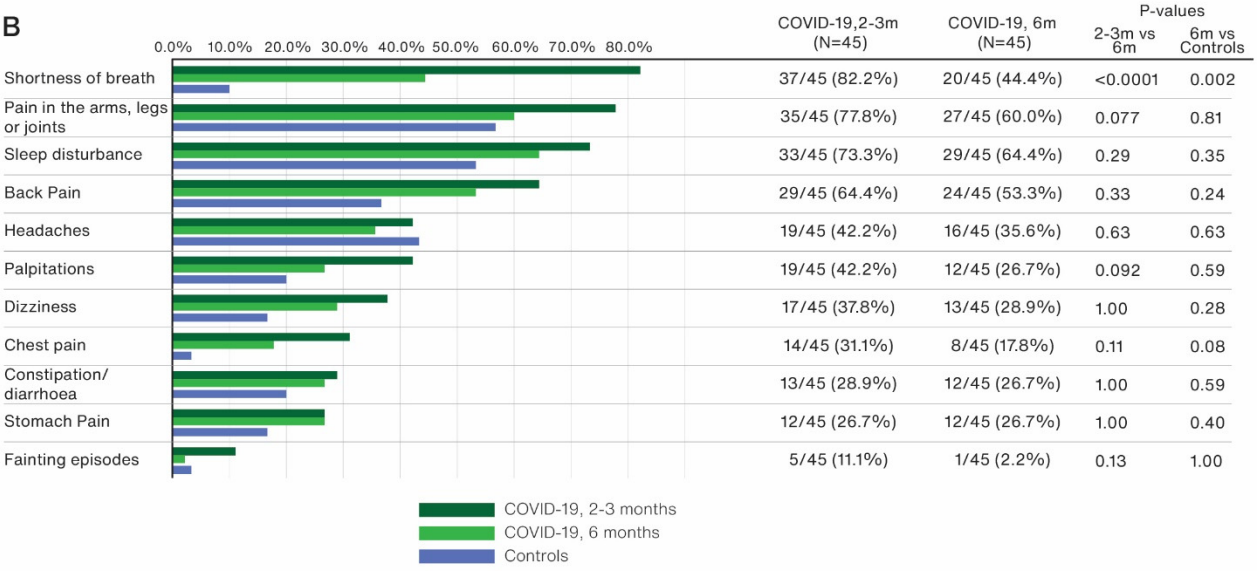


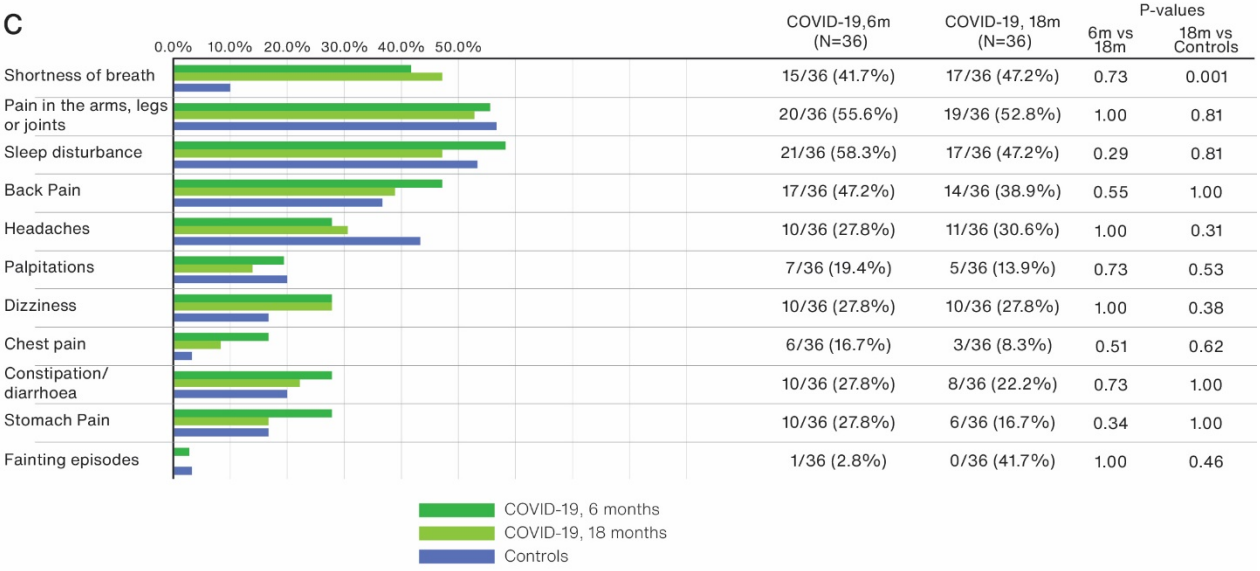


**Figure 28. Symptom bar charts showing symptom prevalence for A) COVID-19 participants 2-3 months post-infection and controls, B) paired changes for patients from 2-3 to 6 months post-infection and C) paired changes for COVID-19 participants from 6 to 18 months post-infection.**

Using the MRC Dyspnoea Scale, COVID-19 participants' and controls' impact of breathless on physical activity was assessed. At 2-3 months post-infection, a significant proportion of participants (64%) reported breathlessness that caused reductions in their physical activity, with 13% having to stop to catch their breath after walking 100 metres, and 1 participant experiencing breathlessness whilst dressing (Figure 29A). By 6 months, participants were less impacted by breathlessness (*P*=0.008); 17/44 (39%) reported less limitation due to shortness of breath, 22/44 (50%) experienced no change, and a minority (5 participants) reported breathlessness when hurrying on the level or walking up a hill (MRC grade 2), having previously reported no limitation. By 18 months post-infection, although there was no statistically significant change in the distribution of MRC dyspnoea scores from 6 months (*P*=1.00), a higher proportion of participants reported freedom from limiting breathlessness (61% vs 42% at 6 months). Despite this, some (6 participants, 15%) reported worsening breathlessness. Across all the timepoints assessed, physical limitations secondary to shortness of breath were more prevalent in COVID-19 participants compared to controls (Figure 29B).

Significant fatigue (as assessed using the FSS) was seen in the majority of participants (55%) at 2-3 months post-infection (Figure 29C). Longitudinal assessment revealed incremental improvements in the prevalence of fatigue, with 42% of participants at 6 months and 36% of participants at 18 months achieving scores compatible with significant fatigue on the FSS, respectively.

A)

MRC Dyspnoea Scale
- 1: Breathless with strenuous exercise
- 2: Breathless when hurrying on the level or walking up a hill
- 3: Walks slower than peers due to breathlessness
- 4: Stops for breath after 100 metres
- 5: Too breathless to leave the house/breathless when dressing

| MRC Dyspnoea Grade | COVID-19,2-3m (N=56) | Controls (N=30) |
|---|---|---|
| 1 | 20/56 (35.7%) | 27/30 (90.0%) |
| 2 | 17/56 (30.4%) | 1/30 (3.3%) |
| 3 | 11/56 (19.6%) | 2/30 (6.7%) |
| 4 | 7/56 (12.5%) | 0/30 (0.0%) |
| 5 | 1/56 (1.8%) | 0/30 (0.0%) |

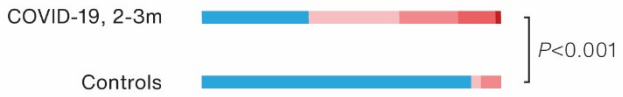


| MRC Dyspnoea Grade | COVID-19,2-3m (N=44) | COVID-19, 6m (N=44) |
|---|---|---|
| 1 | 16/44 (36.4%) | 20/44 (45.5%) |
| 2 | 14/44 (31.8%) | 15/44 (34.1%) |
| 3 | 7/44 (15.9%) | 9/44 (20.5%) |
| 4 | 6/44 (13.6%) | 0/44 (0.0%) |
| 5 | 1/44 (2.3%) | 0/44 (0.0%) |

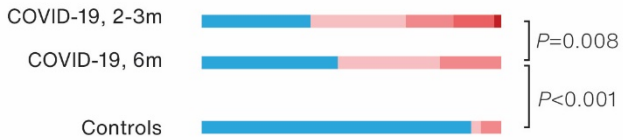


| MRC Dyspnoea Grade | COVID-19,6m (N=38) | COVID-19, 18m (N=38) |
|---|---|---|
| 1 | 16/38 (42.1%) | 23/38 (60.5%) |
| 2 | 15/38 (39.5%) | 8/38 (21.1%) |
| 3 | 7/38 (18.4%) | 2/38 (5.3%) |
| 4 | 0/38 (0.0%) | 4/38 (10.5%) |
| 5 | 0/38 (0.0%) | 1/38 (2.6%) |

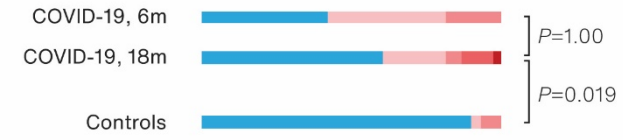


B)

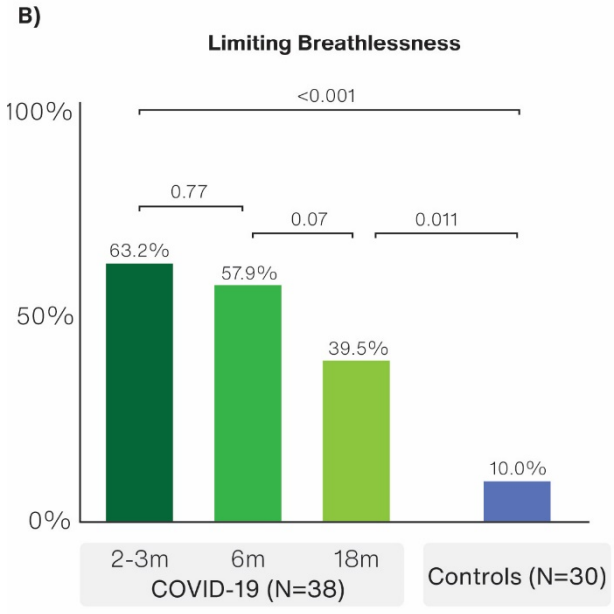


C)

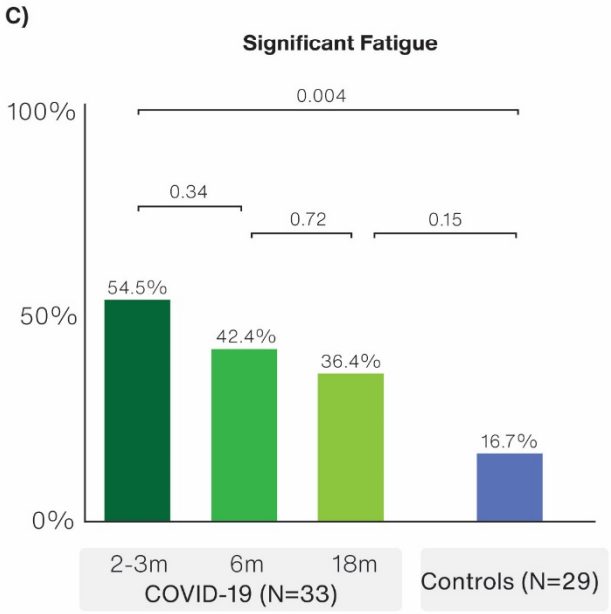


**Figure 29. A) Tables showing the distribution of MRC Dyspnoea scores for COVID-19 participants 2-3 months post-infection and controls, together with paired changes from 2-3 months to 6 months and 6 months to 18 months post-infection. B) Bar graph depicting limiting breathless in COVID-19 participants at all time points and controls. C) Bar graph depicting significant fatigue in COVID-19 participants at all time points and controls.**

In view of the persistent higher rates of intrusive breathlessness between COVID-19 participants and controls at all time-points, binomial logistic regression was utilised to assess whether parameters frequently used in clinical practice could stratify those COVID-19 participants with or without breathlessness. Apart from $\dot{V}E/\dot{V}CO_2$ slope at 2-3 months post infection ($X^2$=5.1, *P*=0.024, with only 13.5% (Nagelski $R^2$) of the variation being explained), none of the parameters nor multivariate models were useful in correctly predicting COVID-19 participants with intrusive breathlessness 18 months post-infection (**Figure 30**);

- 2-3 months multivariate model: $X_2(11)$=15.2, *P*=0.13. Nagelski $R^2$=42%.
- 6 months multivariate model: $X_2(12)$=9.0, *P*=0.70. Nagelski $R^2$=29.5%.
- 18 months multivariate model:$X_2(10)$=7.86, *P*=0.55. Nagelski $R^2$=42.1%.

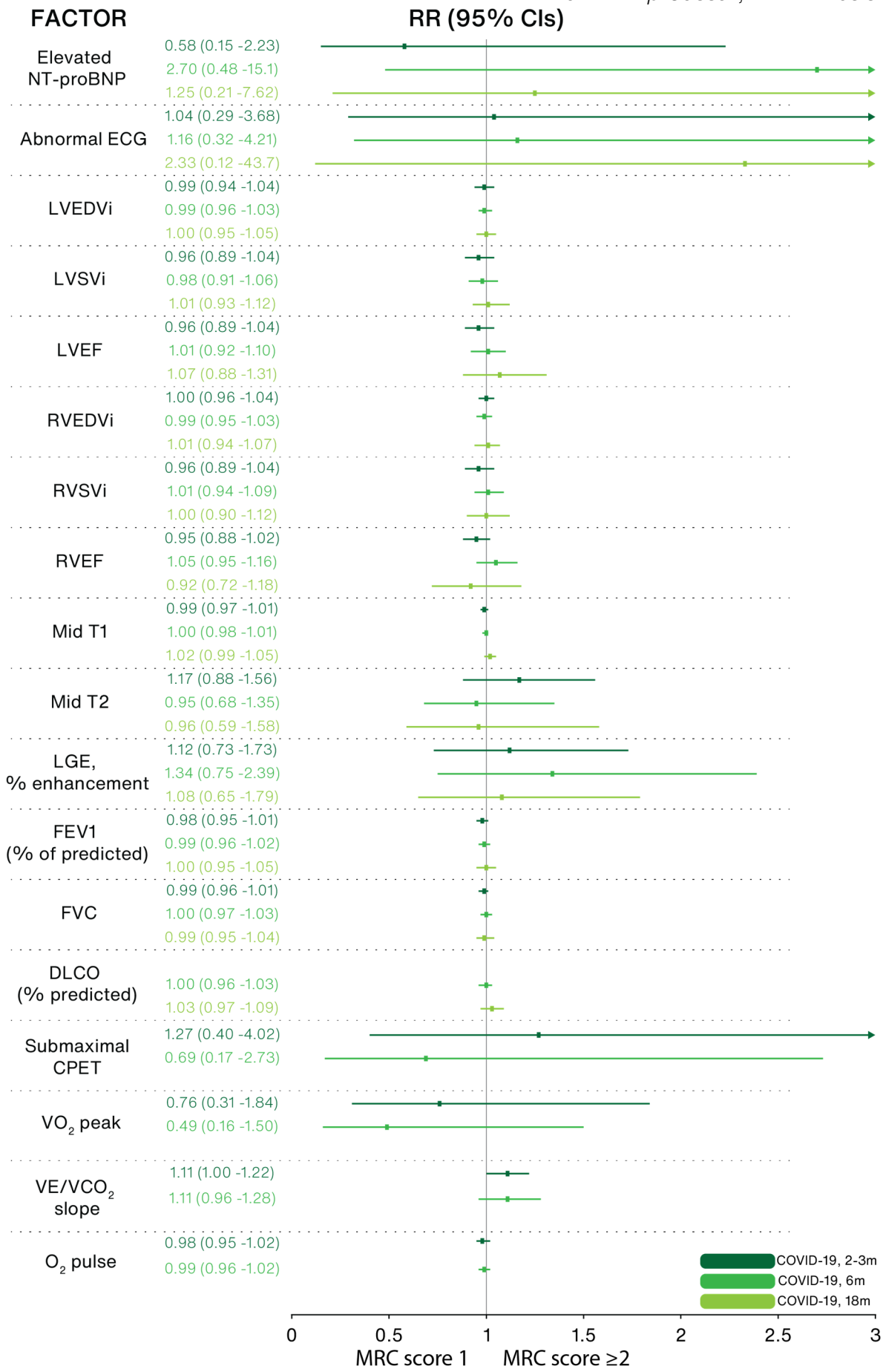


**Figure 30. Forest plot depicting the odds of having intrusive breathlessness 18 months post-infection using any of the ECG, CMR, PFT, and CPET measures obtained throughout the study.**

## Discussion

The main findings of the present study are as follows:

1) Findings from qualitative brain imaging in participants following COVID-19 were comparable to controls. A high prevalence of mild cognitive impairment was observed shorty after infection, which resolved over time.
2) Shortly following infection, participants demonstrated significant impairments in their quality of life. Although this improved with time, reduced energy, poorer overall general health and limitations due to physical health persisted.
3) By 18 months post infection, breathlessness was not only more frequently reported by participants, but also continued to have an impact on physical activity when compared with controls. Overall, univariate and multivariate models failed to show a relationship between frequently utilized clinical parameters and limiting breathlessness.

Early in the pandemic, reports of a relatively high frequency of non-haemorrhagic cerebrovascular events associated with moderate to severe COVID-19 started to surface; only one month after the World Health Organisation declared COVID-19 a pandemic, Mao and colleagues provided an insightful report describing the neurologic manifestations of 214 patients hospitalised with COVID-19 in Wuhan, China.[187] Of the patients studied, 6 suffered a cerebrovascular event during admission (2.8%), with 5 occurring in patients who fulfilled criteria of severe disease (an older, more co-morbid population compared to patients with non-severe disease). Several studies have also reported on the incidence of ischaemic stroke in hospitalised patients, albeit at different rates (ranging from 0.9% in a cohort from New York to 4.6% in a cohort from China).[7,193,194] Common to all reports is the association of stroke with more severe disease, increased age and co-morbidities (as described by Mao and colleagues). The increased incidence of stroke during illness is not unique to COVID-19; it is well-

established that infectious diseases are known to be associated with stroke, with platelet activation, inflammation, dehydration and impaired endothelial function postulated to play a role.[195,196] Separate to these mechanisms, the downregulation of ACE2 receptors and consequent increased circulating concentrations of angiotensin-II, together with endotheliitis (features which are particularly unique to COVID-19) may further contribute to the occurrence of cerebrovascular events in patients with acute COVID-19.[197] In the largest multi-centre multi-national study to date investigating the risk of stroke in patients with acute COVID-19, Shahjouei and colleagues analysed data from over 26,000 hospitalised patients.[8] The overall risk of stroke was found to be 0.5%, with the need for mechanical ventilation and a prior history of ischaemic heart disease determined to be significant predictors. Of importance, the risk of stroke was comparable to the stroke incidence following influenza. In the present study, one participant with severe COVID-19 and requiring mechanical ventilation developed an ischaemic stroke, in keeping with the overall low incidence of stroke and association with more severe disease.

In contrast to the imaging findings of the present study, a significant proportion of COVID-19 participants achieved MOCA scores compatible with some degree of cognitive impairment shortly following infection. In addition, COVID-19 participants had higher PHQ-9 (depression assessment) and GAD-7 (anxiety assessment) scores versus controls. Reassuringly, by 6 months post-infection, cognitive, depression and anxiety scores improved, with all becoming comparable with controls. Few longitudinal studies evaluating cognitive function following COVID-19 exist; Alemanno and colleagues report results from 87 patients admitted to a rehabilitation unit following hospital discharge.[198] On admission to the unit, median MoCA scores ranged from 15.9 – 21.7 (depending on the oxygen requirement during admission). The disparity with the present study's results is likely secondary to inclusion of patients requiring

rehabilitation (versus none requiring rehabilitation in the present study), proximity of assessment to infection (immediately after discharge vs 2-3 months post-infection), the presence of co-morbidities and older age (mean 67 vs 55 years). Despite this, reassessment one month following discharge showed an improvement in cognitive function. Data from the national multi-centre PHOSP-COVID study revealed a more modest prevalence of cognitive impairment following infection; 5 months following hospital discharge, 14% had evidence of cognitive impairment, improving to 10% ($P$=0.0013) by 13 months post-discharge.[199] Similar to the previously described report, patients were older and comorbidities were common. Additionally, 28% received invasive ventilation (vs 12% in the present study). Interestingly, the authors note an association between inflammatory mediators (IL-6 and CD70) and cognitive impairment, suggesting that not all cognitive impairment is pre-existing and that neuroinflammation could play a role. Regarding the prevalence of anxiety and depression post COVID-19, Bourmistrova and colleagues, in a systematic review using data from 6743 participants (both hospitalised and treated in the community) approximately 1 to 6 months following infection found that rates of anxiety and depression were comparable to the general population, in contrast to the higher rates observed 1 month following hospital treatment. [200,201] Overall, these findings suggest that any impact on mental health is short lived and may be due to psychosocial factors, given the psychological impact of quarantine and lockdown measures.[202]

Across the globe, several studies have reported on the persistence of symptoms long after resolution of the acute illness; defined as the persistence of symptoms lasting over 12 weeks following infection, an estimated 1.8 million individuals are estimated to be suffering from long-COVID in the United Kingdom alone.[203,204] While over 200 symptoms have been described by patients inflicted with long-COVID, fatigue and dyspnoea are the two most common (and debilitating) features of the disease.[205,206] In

the present study, 47% of COVID-19 participants experienced shortness of breath 18 months post-infection, with 40% reporting limitations in exercise capacity due to dypsnoea. Fatigue was seen in 36%. Importantly, neither CMR, CPET, pulmonary function or gas transfer parameters were associated with persistent breathlessness 18 months post-infection, in keeping with the often normal results of tests offered as standard care.[205] Immune dysregulation, microbiome dysregulation, microvascular clots, autoimmunity, dysfunctional neurological signalling and mitochondrial dysfunction have all been postulated to play a role.[205,207] In the first therapeutic clinical trial in long-COVID, a metabolic modulator was shown to improve fatigue in patients with long-COVID, suggesting that mitochondrial dysfunction may very well be a promising therapeutic target in patients suffering from fatigue-predominant long-COVID.[208]

## Clinical Implications

Findings from this study suggest that cerebrovascular insults during acute COVID-19 are rare and occur in those with severe disease. Shortly after acute infection, COVID-19 participants demonstrated a reduction in cognitive function which improves over time. No association between cognitive performance and qualitative brain imaging was seen. A high proportion of fatigue and breathlessness persisted long after resolution of the acute infection, and did not associate with CMR, CPET, lung function or gas transfer parameters. This suggests that, in a low-risk population with no significant past medical co-morbidities, such clinical investigations are unlikely to be of use in characterizing persistent breathless post-COVID-19.

## Study limitations

This was a single-centre study limited by a relatively small sample size. While not all COVID-19 participants returned for repeat assessment, the paired results provided show that the characteristics of the participants who returned were representative of the originally recruited cohort. COVID-19 participants and controls with significant co-morbidities were excluded from recruitment, which may limit the external validity of the study findings. Quantitative brain imaging findings were not included in this thesis, and therefore the neurophysiological impact of COVID-19 may have been underestimated. However, the exclusive use of qualitative parameters that form part of clinical standard practice makes the study more relevant to a clinical audience.

## Conclusion

In this chapter, moderate to severe COVID-19 was not associated with long term cognitive impairment or psychological illness. A significant burden of breathlessness and fatigue continued to be observed 18 months following acute infection. There was no association between breathlessness and frequently used clinical parameters, highlighting the need for further research into the driving mechanisms of persistent symptoms post-COVID-19.

## Chapter 6: General Conclusions

Early in the pandemic, it became clear that dysregulated inflammation and immunity played a pivotal role in the pathophysiology of COVID-19.[209] Together with the expression of ACE2 receptors (the main gateway through which SARS-CoV-2 enters cells) in numerous extra-pulmonary organs, concerns about the potential for long term pulmonary and extra-pulmonary effects were appropriately raised.[210]

In this thesis, I showed that multi-organ tissue abnormalities on MR imaging were common 2-3 months following moderate to severe COVID-19, with COVID-19 participants having abnormal imaging markers in the heart (elevated native myocardial T1), lungs (hyperintensities on lung HASTE imaging), liver (elevated iron-corrected hepatic T1) and kidneys (elevated renal cortical T1 and reduced corticomedullary differentiation).

In chapter 3 of this thesis, the longitudinal impact of COVID-19 on the heart, lungs and exercise capacity was explored. Whilst native myocardial T1 was elevated at 2-3 months, none of the COVID-19 participants fulfilled criteria for acute myocarditis.[125] Native myocardial T1 normalised by 6 months, extracellular volume (a measure of diffuse myocardial fibrosis) was comparable with controls throughout the study, and none of the COVID-19 participants had impairments of left or right ventricular systolic function. These findings are reassuring and in keeping with numerous studies that suggest that long-term myocardial injury, especially myocarditis, are not as common as initially thought early in the pandemic.[211] Given that the lungs are the primary target of SARS-CoV-2, it is not surprising that, despite reductions in the extent of lung involvement over time, pulmonary abnormalities continued to be observed in 70% of COVID-19 participants by the end of the study, as were reductions in diffusion capacity (DLco) on gas transfer testing. On CPET, reduced peak oxygen consumption was common in COVID-19 participants shortly following infection (55%), which improved

by 6 months (31%) but remained alarmingly high. Whilst one cannot fault the assumption that persistent impairments of lung function are responsible for the observed impairments in exercise capacity, in this study, none of the COVID-19 participants with reduced peak oxygen consumption had significant reductions in respiratory reserve (i.e respiratory limitation causing cessation of exercise). In other words, impairments of lung function did not explain reductions in exercise capacity. In depth analysis revealed that, besides intrusive symptoms resulting in premature termination of exercise, reduced tissue oxygen extraction (which could be due to numerous mechanisms and unable to be accurately determined in the absence of level 3 CPET) likely plays a role in the observed limitations of exercise capacity.

In chapter 4, the relationship between moderate to severe COVID-19 and hepatic and renal function was discussed. The initial elevations in hepatic iron-corrected T1 and renal cortical T1 normalised by 6 months. In contrast to the hepatic findings, resolution of renal tissue abnormalities was not accompanied by improvement in renal function. On the contrary, renal function declined in most COVID-19 participants over time, even in those who did not suffer an acute kidney injury during admission. Of concern was the fact that a validated CKD risk prediction score failed to highlight the COVID-19 participants who experienced the most significant reductions in their renal function. This has potential long-term implications in survivors of moderate to severe COVID-19, and further research is required to clarify the long-term trajectory of renal function in the years to come.

Finally, in chapter 5, the relationship between COVID-19, the brain, cognition, mood, quality of life and persistent symptoms was explored. Reassuringly, no group differences in qualitative MRI imaging of the brain were seen between COVID-19 participants and controls throughout the study. Persistent impairments in cognition were not observed. COVID-19 participants had severely reduced quality of life shortly

after infection, with impairments in all the quality-of-life domains assessed. Significant improvement was seen on repeat assessment, although role limitations due to physical health and poorer general health persisted (compared to controls). Throughout the study, COVID-19 participants reported a high prevalence of shortness of breath, with 40% reporting breathlessness when hurrying or walking up a hill 18 months post infection. Of importance is the fact that none of the devised multivariate models (consisting of ECG, spirometry, gas transfer, MRI and CPET parameters) were successful in identifying COVID-19 participants with limiting breathlessness, suggesting that, in patients with no significant past medical history, such clinical investigations are of little use in characterizing persistent breathless post-COVID-19.

In summary, the longitudinal assessment of multiorgan health, exercise capacity, cognition and quality of life revealed that resolution of tissue organ abnormalities on MR imaging is not necessarily accompanied by restoration of organ function; the long-term trajectory and impact of reduced lung and renal function in survivors of moderate to severe COVID-19 warrants further research. Frequently used clinical parameters failed to predict persistent breathlessness, suggesting that the mechanisms driving such breathlessness remain unclear and warrants further investigation.

## References


1. Wang C, Horby PW, Hayden FG, Gao GF. A novel coronavirus outbreak of global health concern. Lancet. 2020;395(10223):470-3.
2. Huang C, Wang Y, Li X, Ren L, et al. Clinical features of patients infected with 2019 novel coronavirus in Wuhan, China. Lancet. 2020;395(10223):497-506.
3. World Health Organisation. WHO Director-General's opening remarks at the media briefing on COVID-19 - 11 March 2020. Accessed 01/10/2021. https://www.who.int/director-general/speeches/detail/who-director-general-s-opening-remarks-at-the-media-briefing-on-covid-19---11-march-2020.
4. Zhou F, Yu T, Du R, Fan G, et al. Clinical course and risk factors for mortality of adult inpatients with COVID-19 in Wuhan, China: a retrospective cohort study. Lancet. 2020;395(10229):1054-62.
5. Wang D, Hu B, Hu C, Zhu F, et al. Clinical Characteristics of 138 Hospitalized Patients With 2019 Novel Coronavirus-Infected Pneumonia in Wuhan, China. JAMA. 2020;323(11):1061-9.
6. Yang X, Yu Y, Xu J, Shu H, et al. Clinical course and outcomes of critically ill patients with SARS-CoV-2 pneumonia in Wuhan, China: a single-centered, retrospective, observational study. Lancet Respir Med. 2020;8(5):475-81.
7. Li Y, Li M, Wang M, Zhou Y, et al. Acute cerebrovascular disease following COVID-19: a single center, retrospective, observational study. Stroke Vasc Neurol. 2020;5(3):279-84.
8. Shahjouei S, Naderi S, Li J, Khan A, et al. Risk of stroke in hospitalized SARS-CoV-2 infected patients: A multinational study. EBioMedicine. 2020;59:102939.
9. Wang MY, Zhao R, Gao LJ, Gao XF, et al. SARS-CoV-2: Structure, Biology, and Structure-Based Therapeutics Development. Front Cell Infect Microbiol. 2020;10:587269.
10. Javorsky A, Humbert PO, Kvansakul M. Structural basis of coronavirus E protein interactions with human PALS1 PDZ domain. Commun Biol. 2021;4(1):724.
11. Zhang Z, Nomura N, Muramoto Y, Ekimoto T, et al. Structure of SARS-CoV-2 membrane protein essential for virus assembly. Nat Commun. 2022;13(1):4399.
12. Jackson CB, Farzan M, Chen B, Choe H. Mechanisms of SARS-CoV-2 entry into cells. Nat Rev Mol Cell Biol. 2022;23(1):3-20.
13. Jayaweera M, Perera H, Gunawardana B, Manatunge J. Transmission of COVID-19 virus by droplets and aerosols: A critical review on the unresolved dichotomy. Environ Res. 2020;188:109819.
14. van Doremalen N, Bushmaker T, Morris DH, Holbrook MG, et al. Aerosol and Surface Stability of SARS-CoV-2 as Compared with SARS-CoV-1. N Engl J Med. 2020;382(16):1564-7.
15. World Health Organisation. Report of the WHO-China Joint Mission on Coronavirus Disease 2019 (COVID-19). Accessed 20/12/2022. https://www.who.int/publications/i/item/report-of-the-who-china-joint-mission-on-coronavirus-disease-2019-(covid-19).
16. Xin H, Li Y, Wu P, Li Z, et al. Estimating the Latent Period of Coronavirus Disease 2019 (COVID-19). Clin Infect Dis. 2021;74(9):1678-81.
17. Johansson MA, Quandelacy TM, Kada S, Prasad PV, et al. SARS-CoV-2 Transmission From People Without COVID-19 Symptoms. JAMA Netw Open. 2021;4(1):e2035057.

18. Casas-Rojo JM, Anton-Santos JM, Millan-Nunez-Cortes J, Lumbreras-Bermejo C, et al. [Clinical characteristics of patients hospitalized with COVID-19 in Spain: Results from the SEMI-COVID-19 Registry]. Rev Clin Esp. 2020;220(8):480-94.
19. Zhang R, Ouyang H, Fu L, Wang S, et al. CT features of SARS-CoV-2 pneumonia according to clinical presentation: a retrospective analysis of 120 consecutive patients from Wuhan city. Eur Radiol. 2020;30(8):4417-26.
20. Bajracharya S, Shrestha A, Rajbhandari B. Symptoms of COVID-19 Confirmed Cases Presenting to Emergency Department in a Tertiary Care Centre: A Descriptive Cross-sectional Study. JNMA J Nepal Med Assoc. 2020;58(232):1041-5.
21. Umakanthan S, Sahu P, Ranade AV, Bukelo MM, et al. Origin, transmission, diagnosis and management of coronavirus disease 2019 (COVID-19). Postgrad Med J. 2020;96(1142):753-8.
22. National Institutes of Health. COVID-19 Treatment Guidelines Panel. Coronavirus Disease 2019 (COVID-19) Treatment Guidelines.
23. Ma Q, Liu J, Liu Q, Kang L, et al. Global Percentage of Asymptomatic SARS-CoV-2 Infections Among the Tested Population and Individuals With Confirmed COVID-19 Diagnosis: A Systematic Review and Meta-analysis. JAMA Netw Open. 2021;4(12):e2137257.
24. Kwok S, Adam S, Ho JH, Iqbal Z, et al. Obesity: A critical risk factor in the COVID-19 pandemic. Clin Obes. 2020;10(6):e12403.
25. Gao YD, Ding M, Dong X, Zhang JJ, et al. Risk factors for severe and critically ill COVID-19 patients: A review. Allergy. 2021;76(2):428-55.
26. Garg S, Kim L, Whitaker M, O'Halloran A, et al. Hospitalization Rates and Characteristics of Patients Hospitalized with Laboratory-Confirmed Coronavirus Disease 2019 - COVID-NET, 14 States, March 1-30, 2020. MMWR Morb Mortal Wkly Rep. 2020;69(15):458-64.
27. Bager P, Wohlfahrt J, Bhatt S, Stegger M, et al. Risk of hospitalisation associated with infection with SARS-CoV-2 omicron variant versus delta variant in Denmark: an observational cohort study. Lancet Infect Dis. 2022;22(7):967-76.
28. Watson OJ, Barnsley G, Toor J, Hogan AB, et al. Global impact of the first year of COVID-19 vaccination: a mathematical modelling study. Lancet Infect Dis. 2022;22(9):1293-302.
29. Verity R, Okell LC, Dorigatti I, Winskill P, et al. Estimates of the severity of coronavirus disease 2019: a model-based analysis. Lancet Infect Dis. 2020;20(6):669-77.
30. Kuba K, Imai Y, Ohto-Nakanishi T, Penninger JM. Trilogy of ACE2: a peptidase in the renin-angiotensin system, a SARS receptor, and a partner for amino acid transporters. Pharmacol Ther. 2010;128(1):119-28.
31. Trifiro G, Massari M, Da Cas R, Menniti Ippolito F, et al. Renin-Angiotensin-Aldosterone System Inhibitors and Risk of Death in Patients Hospitalised with COVID-19: A Retrospective Italian Cohort Study of 43,000 Patients. Drug Saf. 2020;43(12):1297-308.
32. Hou YJ, Okuda K, Edwards CE, Martinez DR, et al. SARS-CoV-2 Reverse Genetics Reveals a Variable Infection Gradient in the Respiratory Tract. Cell. 2020;182(2):429-46 e14.
33. Wang Y, Wang Y, Luo W, Huang L, et al. A comprehensive investigation of the mRNA and protein level of ACE2, the putative receptor of SARS-CoV-2, in human tissues and blood cells. Int J Med Sci. 2020;17(11):1522-31.

34. V'Kovski P, Kratzel A, Steiner S, Stalder H, Thiel V. Coronavirus biology and replication: implications for SARS-CoV-2. Nat Rev Microbiol. 2021;19(3):155-70.
35. Varga Z, Flammer AJ, Steiger P, Haberecker M, et al. Endothelial cell infection and endotheliitis in COVID-19. Lancet. 2020;395(10234):1417-8.
36. Merad M, Martin JC. Pathological inflammation in patients with COVID-19: a key role for monocytes and macrophages. Nat Rev Immunol. 2020;20(6):355-62.
37. Acharya D, Liu G, Gack MU. Dysregulation of type I interferon responses in COVID-19. Nat Rev Immunol. 2020;20(7):397-8.
38. Hu X, Li J, Fu M, Zhao X, Wang W. The JAK/STAT signaling pathway: from bench to clinic. Signal Transduct Target Ther. 2021;6(1):402.
39. Huang KJ, Su IJ, Theron M, Wu YC, et al. An interferon-gamma-related cytokine storm in SARS patients. J Med Virol. 2005;75(2):185-94.
40. Ragab D, Salah Eldin H, Taeimah M, Khattab R, Salem R. The COVID-19 Cytokine Storm; What We Know So Far. Front Immunol. 2020;11:1446.
41. National Institute for Health and Care Excellence. COVID-19 rapid guideline: managing COVID-19. Accessed 08/12/2022.
42. Xu Z, Shi L, Wang Y, Zhang J, et al. Pathological findings of COVID-19 associated with acute respiratory distress syndrome. Lancet Respir Med. 2020;8(4):420-2.
43. Barnes BJ, Adrover JM, Baxter-Stoltzfus A, Borczuk A, et al. Targeting potential drivers of COVID-19: Neutrophil extracellular traps. J Exp Med. 2020;217(6).
44. Menter T, Haslbauer JD, Nienhold R, Savic S, et al. Postmortem examination of COVID-19 patients reveals diffuse alveolar damage with severe capillary congestion and variegated findings in lungs and other organs suggesting vascular dysfunction. Histopathology. 2020;77(2):198-209.
45. Wichmann D, Sperhake JP, Lutgehetmann M, Steurer S, et al. Autopsy Findings and Venous Thromboembolism in Patients With COVID-19: A Prospective Cohort Study. Ann Intern Med. 2020;173(4):268-77.
46. Kawakami R, Sakamoto A, Kawai K, Gianatti A, et al. Pathological Evidence for SARS-CoV-2 as a Cause of Myocarditis: JACC Review Topic of the Week. J Am Coll Cardiol. 2021;77(3):314-25.
47. Basso C, Calabrese F, Angelini A, Carturan E, Thiene G. Classification and histological, immunohistochemical, and molecular diagnosis of inflammatory myocardial disease. Heart Fail Rev. 2013;18(6):673-81.
48. Halushka MK, Vander Heide RS. Myocarditis is rare in COVID-19 autopsies: cardiovascular findings across 277 postmortem examinations. Cardiovasc Pathol. 2021;50:107300.
49. Su H, Yang M, Wan C, Yi LX, et al. Renal histopathological analysis of 26 postmortem findings of patients with COVID-19 in China. Kidney Int. 2020;98(1):219-27.
50. Mizuiri S, Ohashi Y. ACE and ACE2 in kidney disease. World J Nephrol. 2015;4(1):74-82.
51. Fassan M, Mescoli C, Sbaraglia M, Guzzardo V, et al. Liver histopathology in COVID-19 patients: A mono-Institutional series of liver biopsies and autopsy specimens. Pathol Res Pract. 2021;221:153451.
52. Nardo AD, Schneeweiss-Gleixner M, Bakail M, Dixon ED, et al. Pathophysiological mechanisms of liver injury in COVID-19. Liver Int. 2021;41(1):20-32.

53. Leowattana W. Angiotensin-converting enzyme 2 receptors, chronic liver diseases, common medications, and clinical outcomes in coronavirus disease 2019 patients. World J Virol. 2021;10(3):86-96.
54. Solomon IH, Normandin E, Bhattacharyya S, Mukerji SS, et al. Neuropathological Features of Covid-19. N Engl J Med. 2020;383(10):989-92.
55. Matschke J, Lutgehetmann M, Hagel C, Sperhake JP, et al. Neuropathology of patients with COVID-19 in Germany: a post-mortem case series. Lancet Neurol. 2020;19(11):919-29.
56. Martini M, Gazzaniga V, Bragazzi NL, Barberis I. The Spanish Influenza Pandemic: a lesson from history 100 years after 1918. J Prev Med Hyg. 2019;60(1):E64-E7.
57. Centers for Disease Control and Prevention. 2009 H1N1 Pandemic (H1N1pdm09 virus). Accessed 13/12/2022. https://www.cdc.gov/flu/pandemic-resources/2009-h1n1-pandemic.html.
58. Viboud C, Grais RF, Lafont BA, Miller MA, et al. Multinational impact of the 1968 Hong Kong influenza pandemic: evidence for a smoldering pandemic. J Infect Dis. 2005;192(2):233-48.
59. Glezen WP. Emerging infections: pandemic influenza. Epidemiol Rev. 1996;18(1):64-76.
60. Peiris JS, Yuen KY, Osterhaus AD, Stohr K. The severe acute respiratory syndrome. N Engl J Med. 2003;349(25):2431-41.
61. Zumla A, Hui DS, Perlman S. Middle East respiratory syndrome. Lancet. 2015;386(9997):995-1007.
62. World Health Organisation. Middle East respiratory syndrome. Accessed 27/11/2023. https://www.emro.who.int/health-topics/mers-cov/mers-outbreaks.html.
63. Liu DX, Liang JQ, Fung TS. Human Coronavirus-229E, -OC43, -NL63, and -HKU1 (Coronaviridae). Encyclopedia of Virology. 2021:428-40.
64. Kaur N, Singh R, Dar Z, Bijarnia RK, et al. Genetic comparison among various coronavirus strains for the identification of potential vaccine targets of SARS-CoV2. Infect Genet Evol. 2021;89:104490.
65. Su MC, Hsieh YT, Wang YH, Lin AS, et al. Exercise capacity and pulmonary function in hospital workers recovered from severe acute respiratory syndrome. Respiration. 2007;74(5):511-6.
66. Hui DS, Wong KT, Antonio GE, Tong M, et al. Long-term sequelae of SARS: physical, neuropsychiatric, and quality-of-life assessment. Hong Kong Med J. 2009;15 Suppl 8:21-3.
67. Moldofsky H, Patcai J. Chronic widespread musculoskeletal pain, fatigue, depression and disordered sleep in chronic post-SARS syndrome; a case-controlled study. BMC Neurol. 2011;11:37.
68. Lam MH, Wing YK, Yu MW, Leung CM, et al. Mental morbidities and chronic fatigue in severe acute respiratory syndrome survivors: long-term follow-up. Arch Intern Med. 2009;169(22):2142-7.
69. Lee SH, Shin HS, Park HY, Kim JL, et al. Depression as a Mediator of Chronic Fatigue and Post-Traumatic Stress Symptoms in Middle East Respiratory Syndrome Survivors. Psychiatry Investig. 2019;16(1):59-64.
70. Lyons D, Frampton M, Naqvi S, Donohoe D, et al. Fallout from the COVID-19 pandemic - should we prepare for a tsunami of post viral depression? Ir J Psychol Med. 2020;37(4):295-300.

71. Luyt CE, Combes A, Becquemin MH, Beigelman-Aubry C, et al. Long-term outcomes of pandemic 2009 influenza A(H1N1)-associated severe ARDS. Chest. 2012;142(3):583-92.
72. Chen J, Wu J, Hao S, Yang M, et al. Long term outcomes in survivors of epidemic Influenza A (H7N9) virus infection. Sci Rep. 2017;7(1):17275.
73. Asthma: diagnosis and monitoring of asthma in adults, children and young people. National Institute for Health and Care Excellence: Guidelines. London2017.
74. Chronic obstructive pulmonary disease in over 16s: diagnosis and management. National Institute for Health and Care Excellence: Guidelines. London2019.
75. Prineas RJ, Crow RS, Zhang Z-M. The Minnesota code manual of electrocardiographic findings : including measurement and comparison with the Novacode ; standards and procedures for ECG measurement in epidemiologic and clinical trials. 2nd ed. / Ronald J. Prineas, Richard S. Crow, Zhu-Ming Zhang. ed. London: Springer; 2010.
76. Henzler T, Dietrich O, Krissak R, Wichmann T, et al. Half-fourier-acquisition single-shot turbo spin-echo (HASTE) MRI of the lung at 3 Tesla using parallel imaging with 32-receiver channel technology. Journal of Magnetic Resonance Imaging: An Official Journal of the International Society for Magnetic Resonance in Medicine. 2009;30(3):541-6.
77. Romei C, Turturici L, Tavanti L, Miedema J, et al. The use of chest magnetic resonance imaging in interstitial lung disease: a systematic review. Eur Respir Rev. 2018;27(150).
78. Piechnik SK, Ferreira VM, Dall'Armellina E, Cochlin LE, et al. Shortened modified look-locker inversion recovery (ShMOLLI) for clinical myocardial T1-mapping at 1.5 And 3 T within a 9 heartbeat breathhold. J Cardiovasc Magn Reson. 2010;12.
79. Ferreira VM, Piechnik SK, Dall'Armellina E, Karamitsos TD, et al. Non-contrast T1-mapping detects acute myocardial edema with high diagnostic accuracy: a comparison to T2-weighted cardiovascular magnetic resonance. Journal of cardiovascular magnetic resonance. 2012;14(1):42.
80. Reeder SB, McKenzie CA, Pineda AR, Yu H, et al. Water–fat separation with IDEAL gradient-echo imaging. Journal of Magnetic Resonance Imaging: An Official Journal of the International Society for Magnetic Resonance in Medicine. 2007;25(3):644-52.
81. Tunnicliffe EM, Banerjee R, Pavlides M, Neubauer S, Robson MD. A model for hepatic fibrosis: the competing effects of cell loss and iron on shortened modified Look-Locker inversion recovery T1 (shMOLLI-T1) in the liver. Journal of Magnetic Resonance Imaging. 2017;45(2):450-62.
82. Cox EF, Buchanan CE, Bradley CR, Prestwich B, et al. Multiparametric renal magnetic resonance imaging: validation, interventions, and alterations in chronic kidney disease. Frontiers in physiology. 2017;8:696.
83. Graham BL, Steenbruggen I, Miller MR, Barjaktarevic IZ, et al. Standardization of Spirometry 2019 Update. An Official American Thoracic Society and European Respiratory Society Technical Statement. Am J Respir Crit Care Med. 2019;200(8):e70-e88.
84. Graham BL, Brusasco V, Burgos F, Cooper BG, et al. 2017 ERS/ATS standards for single-breath carbon monoxide uptake in the lung. Eur Respir J. 2017;49(1).
85. Mezzani A. Cardiopulmonary Exercise Testing: Basics of Methodology and Measurements. Ann Am Thorac Soc. 2017;14(Supplement_1):S3-S11.

86. Kroenke K, Spitzer RL, Williams JB. The PHQ-15: validity of a new measure for evaluating the severity of somatic symptoms. Psychosom Med. 2002;64(2):258-66.
87. Bestall J, Paul E, Garrod R, Garnham R, et al. Usefulness of the Medical Research Council (MRC) dyspnoea scale as a measure of disability in patients with chronic obstructive pulmonary disease. Thorax. 1999;54(7):581-6.
88. Krupp LB, LaRocca NG, Muir-Nash J, Steinberg AD. The fatigue severity scale: application to patients with multiple sclerosis and systemic lupus erythematosus. Archives of neurology. 1989;46(10):1121-3.
89. Spitzer RL, Kroenke K, Williams JB, Löwe B. A brief measure for assessing generalized anxiety disorder: the GAD-7. Archives of internal medicine. 2006;166(10):1092-7.
90. Kroenke K, Spitzer RL, Williams JB. The PHQ-9: validity of a brief depression severity measure. Journal of general internal medicine. 2001;16(9):606-13.
91. Ware Jr JE, Sherbourne CD. The MOS 36-item short-form health survey (SF-36): I. Conceptual framework and item selection. Medical care. 1992:473-83.
92. Nasreddine ZS, Phillips NA, Bédirian V, Charbonneau S, et al. The Montreal Cognitive Assessment, MoCA: a brief screening tool for mild cognitive impairment. Journal of the American Geriatrics Society. 2005;53(4):695-9.
93. Ghayda RA, Lee KH, Kim JS, Lee S, et al. Chest CT abnormalities in COVID-19: a systematic review. Int J Med Sci. 2021;18(15):3395-402.
94. Shi H, Han X, Jiang N, Cao Y, et al. Radiological findings from 81 patients with COVID-19 pneumonia in Wuhan, China: a descriptive study. Lancet Infect Dis. 2020;20(4):425-34.
95. Wu C, Chen X, Cai Y, Xia J, et al. Risk Factors Associated With Acute Respiratory Distress Syndrome and Death in Patients With Coronavirus Disease 2019 Pneumonia in Wuhan, China. JAMA Intern Med. 2020;180(7):934-43.
96. Marshall R, Bellingan G, Laurent G. The acute respiratory distress syndrome: fibrosis in the fast lane. Thorax. 1998;53(10):815-7.
97. Dos Santos CC. Advances in mechanisms of repair and remodelling in acute lung injury. Intensive Care Med. 2008;34(4):619-30.
98. Sandoval Y, Januzzi JL, Jr., Jaffe AS. Cardiac Troponin for Assessment of Myocardial Injury in COVID-19: JACC Review Topic of the Week. J Am Coll Cardiol. 2020;76(10):1244-58.
99. Ahmed H, Patel K, Greenwood DC, Halpin S, et al. Long-term clinical outcomes in survivors of severe acute respiratory syndrome and Middle East respiratory syndrome coronavirus outbreaks after hospitalisation or ICU admission: A systematic review and meta-analysis. J Rehabil Med. 2020;52(5):jrm00063.
100. Schulz-Menger J, Bluemke DA, Bremerich J, Flamm SD, et al. Standardized image interpretation and post-processing in cardiovascular magnetic resonance - 2020 update : Society for Cardiovascular Magnetic Resonance (SCMR): Board of Trustees Task Force on Standardized Post-Processing. J Cardiovasc Magn Reson. 2020;22(1):19.
101. Yang EY, Ghosn MG, Khan MA, Gramze NL, et al. Myocardial Extracellular Volume Fraction Adds Prognostic Information Beyond Myocardial Replacement Fibrosis. Circ Cardiovasc Imaging. 2019;12(12):e009535.
102. Liu D, Ma X, Liu J, Zhao L, et al. Quantitative analysis of late gadolinium enhancement in hypertrophic cardiomyopathy: comparison of diagnostic performance in myocardial fibrosis between gadobutrol and gadopentetate dimeglumine. Int J Cardiovasc Imaging. 2017;33(8):1191-200.

103. Miller MR, Hankinson J, Brusasco V, Burgos F, et al. Standardisation of spirometry. European respiratory journal. 2005;26(2):319-38.
104. Quanjer PH, Stanojevic S, Cole TJ, Baur X, et al. Multi-ethnic reference values for spirometry for the 3-95-yr age range: the global lung function 2012 equations. Eur Respir J. 2012;40(6):1324-43.
105. Stanojevic S, Graham BL, Cooper BG, Thompson BR, et al. Official ERS technical standards: Global Lung Function Initiative reference values for the carbon monoxide transfer factor for Caucasians. Eur Respir J. 2017;50(3).
106. Wanger J, Clausen JL, Coates A, Pedersen OF, et al. Standardisation of the measurement of lung volumes. Eur Respir J. 2005;26(3):511-22.
107. Pellegrino R, Viegi G, Brusasco V, Crapo RO, et al. Interpretative strategies for lung function tests. Eur Respir J. 2005;26(5):948-68.
108. Radtke T, Crook S, Kaltsakas G, Louvaris Z, et al. ERS statement on standardisation of cardiopulmonary exercise testing in chronic lung diseases. Eur Respir Rev. 2019;28(154).
109. Stickland MK, Neder JA, Guenette JA, O'Donnell DE, Jensen D. Using Cardiopulmonary Exercise Testing to Understand Dyspnea and Exercise Intolerance in Respiratory Disease. Chest. 2022;161(6):1505-16.
110. Wasserman K. Principles of exercise testing and interpretation : including pathophysiology and clinical applications. 5th ed. Philadelphia: Wolters Kluwer Health/Lippincott Williams & Wilkins; 2012. xiii, 572 p. p.
111. Yousuf R, Danielle L Cardiopulmonary Exercise Testing. Accessed 01/03/2023. https://www.ncbi.nlm.nih.gov/books/NBK557886/.
112. Levett DZH, Jack S, Swart M, Carlisle J, et al. Perioperative cardiopulmonary exercise testing (CPET): consensus clinical guidelines on indications, organization, conduct, and physiological interpretation. Br J Anaesth. 2018;120(3):484-500.
113. Jones NL. Clinical exercise testing. 3rd ed. Philadelphia: Saunders; 1988. x, 325 p. p.
114. Ghosh AK. Anaerobic threshold: its concept and role in endurance sport. Malays J Med Sci. 2004;11(1):24-36.
115. Luijnenburg SE, Robbers-Visser D, Moelker A, Vliegen HW, et al. Intra-observer and interobserver variability of biventricular function, volumes and mass in patients with congenital heart disease measured by CMR imaging. Int J Cardiovasc Imaging. 2010;26(1):57-64.
116. Thygesen K, Alpert JS, Jaffe AS, Chaitman BR, et al. Fourth Universal Definition of Myocardial Infarction (2018). Circulation. 2018;138(20):e618-e51.
117. National Institute for Health and Care Excellence. Chronic heart failure in adults: diagnosis and management. Accessed 10/01/2023. https://www.nice.org.uk/guidance/ng106.
118. Petersen SE, Aung N, Sanghvi MM, Zemrak F, et al. Reference ranges for cardiac structure and function using cardiovascular magnetic resonance (CMR) in Caucasians from the UK Biobank population cohort. J Cardiovasc Magn Reson. 2017;19(1):18.
119. Wasserman K. Principles of exercise testing and interpretation : including pathophysiology and clinical applications. 6th ed. ed. Philadelphia, Pa. ; London: Lippincott Williams & Wilkins; 2020.
120. Robson A. Dyspnoea, hyperventilation and functional cough: a guide to which tests help sort them out. Breathe (Sheff). 2017;13(1):45-50.

121. Puntmann VO, Carerj ML, Wieters I, Fahim M, et al. Outcomes of Cardiovascular Magnetic Resonance Imaging in Patients Recently Recovered From Coronavirus Disease 2019 (COVID-19). JAMA Cardiology. 2020.
122. Starekova J, Bluemke DA, Bradham WS, Eckhardt LL, et al. Evaluation for Myocarditis in Competitive Student Athletes Recovering From Coronavirus Disease 2019 With Cardiac Magnetic Resonance Imaging. JAMA Cardiol. 2021;6(8):945-50.
123. Kotecha T, Knight DS, Razvi Y, Kumar K, et al. Patterns of myocardial injury in recovered troponin-positive COVID-19 patients assessed by cardiovascular magnetic resonance. Eur Heart J. 2021;42(19):1866-78.
124. Ammirati E, Moslehi JJ. Diagnosis and Treatment of Acute Myocarditis: A Review. JAMA. 2023;329(13):1098-113.
125. Ferreira VM, Schulz-Menger J, Holmvang G, Kramer CM, et al. Cardiovascular Magnetic Resonance in Nonischemic Myocardial Inflammation: Expert Recommendations. J Am Coll Cardiol. 2018;72(24):3158-76.
126. Mahmod M, Piechnik SK, Levelt E, Ferreira VM, et al. Adenosine stress native T1 mapping in severe aortic stenosis: evidence for a role of the intravascular compartment on myocardial T1 values. Journal of Cardiovascular Magnetic Resonance. 2014;16(1):1-8.
127. Huang C, Wang Y, Li X, Ren L, et al. Clinical features of patients infected with 2019 novel coronavirus in Wuhan, China. The lancet. 2020;395(10223):497-506.
128. Talla A, Vasaikar SV, Lemos MP, Moodie Z, et al. Longitudinal immune dynamics of mild COVID-19 define signatures of recovery and persistence. bioRxiv. 2021.
129. de Graaf MA, Antoni ML, Ter Kuile MM, Arbous MS, et al. Short-term outpatient follow-up of COVID-19 patients: A multidisciplinary approach. EClinicalMedicine. 2021;32:100731.
130. Sonnweber T, Sahanic S, Pizzini A, Luger A, et al. Cardiopulmonary recovery after COVID-19: an observational prospective multicentre trial. Eur Respir J. 2021;57(4).
131. Evans RA, McAuley H, Harrison EM, Shikotra A, et al. Physical, cognitive and mental health impacts of COVID-19 following hospitalisation – a multi-centre prospective cohort study. medRxiv. 2021:2021.03.22.21254057.
132. Wu X, Liu X, Zhou Y, Yu H, et al. 3-month, 6-month, 9-month, and 12-month respiratory outcomes in patients following COVID-19-related hospitalisation: a prospective study. Lancet Respir Med. 2021;9(7):747-54.
133. Mo X, Jian W, Su Z, Chen M, et al. Abnormal pulmonary function in COVID-19 patients at time of hospital discharge. Eur Respir J. 2020;55(6).
134. Magor-Elliott SRM, Alamoudi A, Chamley RR, Xu H, et al. Altered lung physiology in two cohorts after COVID-19 infection as assessed by computed cardiopulmonography. J Appl Physiol (1985). 2022;133(5):1175-91.
135. Nusair S. Abnormal carbon monoxide diffusion capacity in COVID-19 patients at time of hospital discharge. Eur Respir J. 2020;56(1).
136. Neder JA, Marillier M, Bernard AC, O'Donnell DE. Transfer coefficient of the lung for carbon monoxide and the accessible alveolar volume: clinically useful if used wisely. Breathe (Sheff). 2019;15(1):69-76.
137. Johnson DC. Importance of adjusting carbon monoxide diffusing capacity (DLCO) and carbon monoxide transfer coefficient (KCO) for alveolar volume. Respir Med. 2000;94(1):28-37.

138. Weatherley ND, Stewart NJ, Chan HF, Austin M, et al. Hyperpolarised xenon magnetic resonance spectroscopy for the longitudinal assessment of changes in gas diffusion in IPF. Thorax. 2019;74(5):500-2.
139. Grist JT, Collier GJ, Walters H, Kim M, et al. Lung Abnormalities Detected with Hyperpolarized (129)Xe MRI in Patients with Long COVID. Radiology. 2022;305(3):709-17.
140. Brat K, Stastna N, Merta Z, Olson LJ, et al. Cardiopulmonary exercise testing for identification of patients with hyperventilation syndrome. PLoS One. 2019;14(4):e0215997.
141. Jack S, Rossiter HB, Pearson MG, Ward SA, et al. Ventilatory responses to inhaled carbon dioxide, hypoxia, and exercise in idiopathic hyperventilation. Am J Respir Crit Care Med. 2004;170(2):118-25.
142. Hall JE, Hall ME. Guyton and Hall textbook of medical physiology. 14th edition. ed. Philadelphia, PA: Elsevier; 2021. p. xix, 1132 pages.
143. Lewis RA, Durrington C, Condliffe R, Kiely DG. BNP/NT-proBNP in pulmonary arterial hypertension: time for point-of-care testing? Eur Respir Rev. 2020;29(156).
144. Tschope C, Kasner M, Westermann D, Gaub R, et al. The role of NT-proBNP in the diagnostics of isolated diastolic dysfunction: correlation with echocardiographic and invasive measurements. Eur Heart J. 2005;26(21):2277-84.
145. Hansen JE, Ulubay G, Chow BF, Sun XG, Wasserman K. Mixed-expired and end-tidal CO2 distinguish between ventilation and perfusion defects during exercise testing in patients with lung and heart diseases. Chest. 2007;132(3):977-83.
146. Baratto C, Caravita S, Faini A, Perego GB, et al. Impact of COVID-19 on exercise pathophysiology. A combined cardiopulmonary and echocardiographic exercise study. J Appl Physiol (1985). 2021.
147. Singh I, Joseph P, Heerdt PM, Cullinan M, et al. Persistent Exertional Intolerance After COVID-19: Insights From Invasive Cardiopulmonary Exercise Testing. Chest. 2021.
148. Germain A, Ruppert D, Levine SM, Hanson MR. Prospective Biomarkers from Plasma Metabolomics of Myalgic Encephalomyelitis/Chronic Fatigue Syndrome Implicate Redox Imbalance in Disease Symptomatology. Metabolites. 2018;8(4).
149. Gassen NC, Papies J, Bajaj T, Emanuel J, et al. SARS-CoV-2-mediated dysregulation of metabolism and autophagy uncovers host-targeting antivirals. Nat Commun. 2021;12(1):3818.
150. Shang C, Liu Z, Zhu Y, Lu J, et al. SARS-CoV-2 Causes Mitochondrial Dysfunction and Mitophagy Impairment. Front Microbiol. 2021;12:780768.
151. Carney EF. The impact of chronic kidney disease on global health. Nat Rev Nephrol. 2020;16(5):251.
152. Cheemerla S, Balakrishnan M. Global Epidemiology of Chronic Liver Disease. Clin Liver Dis (Hoboken). 2021;17(5):365-70.
153. Mojtahed A, Kelly CJ, Herlihy AH, Kin S, et al. Reference range of liver corrected T1 values in a population at low risk for fatty liver disease-a UK Biobank sub-study, with an appendix of interesting cases. Abdom Radiol (NY). 2019;44(1):72-84.
154. Gillis KA, McComb C, Patel RK, Stevens KK, et al. Non-Contrast Renal Magnetic Resonance Imaging to Assess Perfusion and Corticomedullary Differentiation in Health and Chronic Kidney Disease. Nephron. 2016;133(3):183-92.
155. Dekkers IA, de Boer A, Sharma K, Cox EF, et al. Consensus-based technical recommendations for clinical translation of renal T1 and T2 mapping MRI. Magnetic Resonance Materials in Physics, Biology and Medicine. 2020:1-14.

156. Cai Q, Huang D, Yu H, Zhu Z, et al. COVID-19: Abnormal liver function tests. J Hepatol. 2020;73(3):566-74.
157. Levin A, Stevens PE. Summary of KDIGO 2012 CKD Guideline: behind the scenes, need for guidance, and a framework for moving forward. Kidney Int. 2014;85(1):49-61.
158. Labranche R, Gilbert G, Cerny M, Vu KN, et al. Liver Iron Quantification with MR Imaging: A Primer for Radiologists. Radiographics. 2018;38(2):392-412.
159. Mao R, Qiu Y, He JS, Tan JY, et al. Manifestations and prognosis of gastrointestinal and liver involvement in patients with COVID-19: a systematic review and meta-analysis. Lancet Gastroenterol Hepatol. 2020;5(7):667-78.
160. Fan Z, Chen L, Li J, Cheng X, et al. Clinical Features of COVID-19-Related Liver Functional Abnormality. Clin Gastroenterol Hepatol. 2020;18(7):1561-6.
161. Sivandzadeh GR, Askari H, Safarpour AR, Ejtehadi F, et al. COVID-19 infection and liver injury: Clinical features, biomarkers, potential mechanisms, treatment, and management challenges. World J Clin Cases. 2021;9(22):6178-200.
162. Liu T, Wu D, Yan W, Wang X, et al. Twelve-Month Systemic Consequences of Coronavirus Disease 2019 (COVID-19) in Patients Discharged From Hospital: A Prospective Cohort Study in Wuhan, China. Clin Infect Dis. 2022;74(11):1953-65.
163. Liao X, Li D, Ma Z, Zhang L, et al. 12-Month Post-Discharge Liver Function Test Abnormalities Among Patients With COVID-19: A Single-Center Prospective Cohort Study. Front Cell Infect Microbiol. 2022;12:864933.
164. Jones DL, Baluja MQ, Graham DW, Corbishley A, et al. Shedding of SARS-CoV-2 in feces and urine and its potential role in person-to-person transmission and the environment-based spread of COVID-19. Sci Total Environ. 2020;749:141364.
165. Puelles VG, Lütgehetmann M, Lindenmeyer MT, Sperhake JP, et al. Multiorgan and Renal Tropism of SARS-CoV-2. New England Journal of Medicine. 2020.
166. Chen N, Zhou M, Dong X, Qu J, et al. Epidemiological and clinical characteristics of 99 cases of 2019 novel coronavirus pneumonia in Wuhan, China: a descriptive study. Lancet. 2020;395(10223):507-13.
167. Shafran N, Issachar A, Shochat T, Shafran IH, et al. Abnormal liver tests in patients with SARS-CoV-2 or influenza - prognostic similarities and temporal disparities. JHEP Rep. 2021;3(3):100258.
168. Zhao SW, Li YM, Li YL, Su C. Liver injury in COVID-19: Clinical features, potential mechanisms, risk factors and clinical treatments. World J Gastroenterol. 2023;29(2):241-56.
169. Radzina M, Putrins DS, Micena A, Vanaga I, et al. Post-COVID-19 Liver Injury: Comprehensive Imaging With Multiparametric Ultrasound. J Ultrasound Med. 2022;41(4):935-49.
170. Medeiros AK, Barbisan CC, Cruz IR, de Araujo EM, et al. Higher frequency of hepatic steatosis at CT among COVID-19-positive patients. Abdom Radiol (NY). 2020;45(9):2748-54.
171. Milic J, Barbieri S, Gozzi L, Brigo A, et al. Metabolic-Associated Fatty Liver Disease Is Highly Prevalent in the Postacute COVID Syndrome. Open Forum Infect Dis. 2022;9(3):ofac003.
172. Boeckmans J, Rombaut M, Demuyser T, Declerck B, et al. Infections at the nexus of metabolic-associated fatty liver disease. Arch Toxicol. 2021;95(7):2235-53.
173. Zheng KI, Gao F, Wang XB, Sun QF, et al. Letter to the Editor: Obesity as a risk factor for greater severity of COVID-19 in patients with metabolic associated fatty liver disease. Metabolism. 2020;108:154244.

174. Mahamid M, Nseir W, Khoury T, Mahamid B, et al. Nonalcoholic fatty liver disease is associated with COVID-19 severity independently of metabolic syndrome: a retrospective case-control study. Eur J Gastroenterol Hepatol. 2021;33(12):1578-81.
175. Gao F, Zheng KI, Yan HD, Sun QF, et al. Association and Interaction Between Serum Interleukin-6 Levels and Metabolic Dysfunction-Associated Fatty Liver Disease in Patients With Severe Coronavirus Disease 2019. Front Endocrinol (Lausanne). 2021;12:604100.
176. Chan L, Chaudhary K, Saha A, Chauhan K, et al. AKI in Hospitalized Patients with COVID-19. J Am Soc Nephrol. 2021;32(1):151-60.
177. Gu X, Huang L, Cui D, Wang Y, et al. Association of acute kidney injury with 1-year outcome of kidney function in hospital survivors with COVID-19: A cohort study. EBioMedicine. 2022;76:103817.
178. Nugent J, Aklilu A, Yamamoto Y, Simonov M, et al. Assessment of Acute Kidney Injury and Longitudinal Kidney Function After Hospital Discharge Among Patients With and Without COVID-19. JAMA Netw Open. 2021;4(3):e211095.
179. Strohbehn IA, Zhao S, Seethapathy H, Lee M, et al. Acute Kidney Injury Incidence, Recovery, and Long-term Kidney Outcomes Among Hospitalized Patients With COVID-19 and Influenza. Kidney Int Rep. 2021;6(10):2565-74.
180. Puelles VG, Lutgehetmann M, Lindenmeyer MT, Sperhake JP, et al. Multiorgan and Renal Tropism of SARS-CoV-2. N Engl J Med. 2020;383(6):590-2.
181. Arnold DM, Patriquin CJ, Nazy I. Thrombotic microangiopathies: a general approach to diagnosis and management. CMAJ. 2017;189(4):E153-E9.
182. Bowe B, Xie Y, Xu E, Al-Aly Z. Kidney Outcomes in Long COVID. J Am Soc Nephrol. 2021;32(11):2851-62.
183. Black LM, Lever JM, Agarwal A. Renal Inflammation and Fibrosis: A Double-edged Sword. J Histochem Cytochem. 2019;67(9):663-81.
184. Zeisberg M, Neilson EG. Mechanisms of tubulointerstitial fibrosis. J Am Soc Nephrol. 2010;21(11):1819-34.
185. Jansen J, Reimer KC, Nagai JS, Varghese FS, et al. SARS-CoV-2 infects the human kidney and drives fibrosis in kidney organoids. Cell Stem Cell. 2022;29(2):217-31 e8.
186. Lee VS, Kaur M, Bokacheva L, Chen Q, et al. What causes diminished corticomedullary differentiation in renal insufficiency? J Magn Reson Imaging. 2007;25(4):790-5.
187. Mao L, Jin H, Wang M, Hu Y, et al. Neurologic Manifestations of Hospitalized Patients With Coronavirus Disease 2019 in Wuhan, China. JAMA Neurol. 2020;77(6):683-90.
188. Shah SMA, Mohammad D, Qureshi MFH, Abbas MZ, Aleem S. Prevalence, Psychological Responses and Associated Correlates of Depression, Anxiety and Stress in a Global Population, During the Coronavirus Disease (COVID-19) Pandemic. Community Ment Health J. 2021;57(1):101-10.
189. Taquet M, Luciano S, Geddes JR, Harrison PJ. Bidirectional associations between COVID-19 and psychiatric disorder: retrospective cohort studies of 62 354 COVID-19 cases in the USA. Lancet Psychiatry. 2021;8(2):130-40.
190. Wang B, Li X, Li H, Xiao L, et al. Clinical, Radiological and Pathological Characteristics Between Cerebral Small Vessel Disease and Multiple Sclerosis: A Review. Front Neurol. 2022;13:841521.
191. Tillema JM, Pirko I. Neuroradiological evaluation of demyelinating disease. Ther Adv Neurol Disord. 2013;6(4):249-68.

192. van Everdingen KJ, van der Grond J, Kappelle LJ, Ramos LM, Mali WP. Diffusion-weighted magnetic resonance imaging in acute stroke. Stroke. 1998;29(9):1783-90.
193. Lodigiani C, Iapichino G, Carenzo L, Cecconi M, et al. Venous and arterial thromboembolic complications in COVID-19 patients admitted to an academic hospital in Milan, Italy. Thromb Res. 2020;191:9-14.
194. Yaghi S, Ishida K, Torres J, Mac Grory B, et al. SARS-CoV-2 and Stroke in a New York Healthcare System. Stroke. 2020;51(7):2002-11.
195. Cowan LT, Alonso A, Pankow JS, Folsom AR, et al. Hospitalized Infection as a Trigger for Acute Ischemic Stroke: The Atherosclerosis Risk in Communities Study. Stroke. 2016;47(6):1612-7.
196. Elkind MS, Carty CL, O'Meara ES, Lumley T, et al. Hospitalization for infection and risk of acute ischemic stroke: the Cardiovascular Health Study. Stroke. 2011;42(7):1851-6.
197. Sagris D, Papanikolaou A, Kvernland A, Korompoki E, et al. COVID-19 and ischemic stroke. Eur J Neurol. 2021;28(11):3826-36.
198. Alemanno F, Houdayer E, Parma A, Spina A, et al. COVID-19 cognitive deficits after respiratory assistance in the subacute phase: A COVID-rehabilitation unit experience. PLoS One. 2021;16(2):e0246590.
199. Group P-CC. Clinical characteristics with inflammation profiling of long COVID and association with 1-year recovery following hospitalisation in the UK: a prospective observational study. Lancet Respir Med. 2022;10(8):761-75.
200. Bourmistrova NW, Solomon T, Braude P, Strawbridge R, Carter B. Long-term effects of COVID-19 on mental health: A systematic review. J Affect Disord. 2022;299:118-25.
201. Mazza MG, De Lorenzo R, Conte C, Poletti S, et al. Anxiety and depression in COVID-19 survivors: Role of inflammatory and clinical predictors. Brain Behav Immun. 2020;89:594-600.
202. Brooks SK, Webster RK, Smith LE, Woodland L, et al. The psychological impact of quarantine and how to reduce it: rapid review of the evidence. Lancet. 2020;395(10227):912-20.
203. British Medical Journal. Why we need to keep using the patient made term "Long Covid". Accessed 10/10/2022. https://blogs.bmj.com/bmj/2020/10/01/why-we-need-to-keep-using-the-patient-made-term-long-covid/.
204. Office for National Statistics. Prevalence of ongoing symptoms following coronavirus (COVID-19) infection in the UK: 2 February 2023. https://www.ons.gov.uk/peoplepopulationandcommunity/healthandsocialcare/conditionsanddiseases/bulletins/prevalenceofongoingsymptomsfollowingcoronaviruscovid19infectionintheuk/2february2023.
205. Davis HE, McCorkell L, Vogel JM, Topol EJ. Long COVID: major findings, mechanisms and recommendations. Nat Rev Microbiol. 2023;21(3):133-46.
206. Healey Q, Sheikh A, Daines L, Vasileiou E. Symptoms and signs of long COVID: A rapid review and meta-analysis. J Glob Health. 2022;12:05014.
207. Nunn AVW, Guy GW, Brysch W, Bell JD. Understanding Long COVID; Mitochondrial Health and Adaptation-Old Pathways, New Problems. Biomedicines. 2022;10(12).
208. Finnigan LEM, Cassar MP, Koziel MJ, Pradines J, et al. Efficacy and tolerability of an endogenous metabolic modulator (AXA1125) in fatigue-predominant long

COVID: a single-centre, double-blind, randomised controlled phase 2a pilot study. EClinicalMedicine. 2023;59:101946.
209. Davitt E, Davitt C, Mazer MB, Areti SS, et al. COVID-19 disease and immune dysregulation. Best Pract Res Clin Haematol. 2022;35(3):101401.
210. Nalbandian A, Sehgal K, Gupta A, Madhavan MV, et al. Post-acute COVID-19 syndrome. Nat Med. 2021;27(4):601-15.
211. Zuin M, Rigatelli G, Bilato C, Porcari A, et al. One-Year Risk of Myocarditis After COVID-19 Infection: A Systematic Review and Meta-analysis. Can J Cardiol. 2023;39(6):839-44.

## Scientific Papers


1. Brightling CE, Evans RA, Singapuri A, Smith N, Wain LV, Group P-CC. Long COVID research: an update from the PHOSP-COVID Scientific Summit. *Lancet Respir Med* 2023; **11**(11): e93-e4.
2. Group CMP-CC. Multiorgan MRI findings after hospitalisation with COVID-19 in the UK (C-MORE): a prospective, multicentre, observational cohort study. *Lancet Respir Med* 2023; **11**(11): 1003-19.
3. Zheng B, Vivaldi G, Daines L, et al. Determinants of recovery from post-COVID-19 dyspnoea: analysis of UK prospective cohorts of hospitalised COVID-19 patients and community-based controls. *Lancet Reg Health Eur* 2023; **29**: 100635.
4. Finnigan LEM, Cassar MP, Koziel MJ, et al. Efficacy and tolerability of an endogenous metabolic modulator (AXA1125) in fatigue-predominant long COVID: a single-centre, double-blind, randomised controlled phase 2a pilot study. *EClinicalMedicine* 2023; **59**: 101946.
5. Vidula MK, Rajewska-Tabor J, Cao JJ, et al. Myocardial Injury on CMR in Patients With COVID-19 and Suspected Cardiac Involvement. *JACC Cardiovasc Imaging* 2023; **16**(5): 609-24.
6. Melhorn J, Alamoudi A, Mentzer AJ, et al. Persistence of inflammatory and vascular mediators 5 months after hospitalization with COVID-19 infection. *Front Med (Lausanne)* 2023; **10**: 1056506.
7. Liew F, Talwar S, Cross A, et al. SARS-CoV-2-specific nasal IgA wanes 9 months after hospitalisation with COVID-19 and is not induced by subsequent vaccination. *EBioMedicine* 2023; **87**: 104402.
8. Magor-Elliott SRM, Alamoudi A, Chamley RR, et al. Altered lung physiology in two cohorts after COVID-19 infection as assessed by computed cardiopulmonography. *J Appl Physiol (1985)* 2022; **133**(5): 1175-91.
9. Group P-CC. Clinical characteristics with inflammation profiling of long COVID and association with 1-year recovery following hospitalisation in the UK: a prospective observational study. *Lancet Respir Med* 2022; **10**(8): 761-75.
10. Jackson C, Stewart ID, Plekhanova T, et al. Effects of sleep disturbance on dyspnoea and impaired lung function following hospital admission due to COVID-19 in the UK: a prospective multicentre cohort study. *Lancet Respir Med* 2023; **11**(8): 673-84.
11. Tomic A, Skelly DT, Ogbe A, et al. Divergent trajectories of antiviral memory after SARS-CoV-2 infection. *Nat Commun* 2022; **13**(1): 1251.
12. Cassar MP, Tunnicliffe EM, Petousi N, et al. Symptom Persistence Despite Improvement in Cardiopulmonary Health - Insights from longitudinal CMR, CPET and lung function testing post-COVID-19. *EClinicalMedicine* 2021; **41**: 101159.
13. Griffanti L, Raman B, Alfaro-Almagro F, et al. Adapting the UK Biobank Brain Imaging Protocol and Analysis Pipeline for the C-MORE Multi-Organ Study of COVID-19 Survivors. *Front Neurol* 2021; **12**: 753284.
14. Skelly DT, Harding AC, Gilbert-Jaramillo J, et al. Two doses of SARS-CoV-2 vaccination induce robust immune responses to emerging SARS-CoV-2 variants of concern. *Nat Commun* 2021; **12**(1): 5061.

15. Raman B*, Cassar MP*, Tunnicliffe EM, et al. Medium-term effects of SARS-CoV-2 infection on multiple vital organs, exercise capacity, cognition, quality of life and mental health, post-hospital discharge. *EClinicalMedicine* 2021; **31**: 100683. *Joint first authors.

## Conference Abstracts

1. Finnigan L, Azer K, Koziel M, et al. AXA1125, an Endogenous Metabolic Modulator Composition, Improves Long COVID Fatigue, Vascular Biology and Mitochondrial Energetics: Findings from a Phase 2a Placebo-Controlled Clinical Trial. European Congress of Clinical Microbiology & Infectious Diseases 2023.
2. Finnigan L, Cassar MP, Koziel M, et al. Efficacy and Tolerability of an Endogenous Metabolic Modulator (AXA1125) in Fatigue-Predominant Long COVID: a Single-Centre, Double-Blind, Randomised Controlled Phase 2a Pilot Study. European Congress of Clinical Microbiology & Infectious Diseases 2023.
3. Cassar MP, Finnigan L, Ashkir Z, et al. Abnormal skeletal metabolism but not cardiac dysfunction as a cause for fatigue post covid-19. J Am Coll Cardiol. 2023 Mar 7;81(8):1397.
4. Melhorn J, Alamoudi a, Mentzer AJ, et al. Persistence of inflammatory and vascular mediators five months after hospitalisation with COVID-19 infection. N. *Eur Respir J 2022; 60: Suppl. 66, 4475.*
5. Cassar MP, Lewandowski A, Mahmod M, et al. Longitudinal assessment of cardiopulmonary health and symptoms in moderate to severe COVID-19. Oxford BHF Centre of Research Excellence Research Symposium. 19/11/2021. Short-listed for best poster.
6. Cassar MP, Lewandowski AJ, Mahmod M, et al. Longitudinal trajectory of cardiac magnetic resonance and cardiopulmonary exercise testing findings in moderate to severe COVID-19 and association with symptoms. European Heart Journal, Volume 42, Issue Supplement_1, October 2021, ehab724.0238, https://doi.org/10.1093/eurheartj/ehab724.0238
7. Cassar MP, Petousi N, Ho LP, et al. Breathlessness post COVID-19 despite improvement in cardiopulmonary health. European Respiratory Journal Sep 2021, 58 (suppl 65) PA3890; DOI: 10.1183/13993003.congress-2021.PA3890
8. Griffanti L, Cassar MP, Raman B, et al. Adapting the UK Biobank brain MRI protocol and analysis pipeline to multi-organ imaging of COVID-19 survivors. European Congress of Radiology, 2021
9. Raman B*, Cassar MP*, Tunnicliffe EM, et al. Holistic study of medium term effects of SARS-CoV-2 infection on multiple vital organs, exercise capacity, physical, cognitive and psychological health. *Joint first authors. Society for Cardiovascular Magnetic Resonance Conference, 2021